MASSACHUSETTS INSTITUTE OF TECHNOLOGY

ARTIFICIAL INTELLIGENCE LABORATORY

A.I. Memo No. 617

February, 1981

Control of a Tendon Arm

Kok Huang Lim

ABSTRACT. The dynamics and control of a tendon driven three degree of freedom shoulder joint are studied. A control scheme consisting of two phases has been developed. In the first phase, approximation of the time optimal control trajectory was applied open loop to the system. In the second phase a closed loop linear feedback law was employed to bring the system to the desired final state and to maintain it there.

Acknowledgements. This report describes research done at the Artificial Intelligence Laboratory and at the Laboratory for Information and Decision Systems of the Massachusetts Institute of Technology. Support for the Artificial Intelligence Laboratory's research is provided in part by the Office of Naval Research under Office of Naval Research contract N00014-77C-0389.

Table of Contents

Chapter 1. Introduction

1.1 Problem Descriptrion

This thesis deals with the time-optimal control of a tendon arm system. The tendon arm system consists of a rigid link attached to a base plate through a three degree-of-freedom joint thus affording the arm rotational freedom in three axes. Movement of the arm is made possible by four tendons: one end of each tendon is attached to the top of the arm and the other end is wound on a motor shaft located under the base plate. The design of the tendon attachments is such that through the interaction of the four motors and tendons, and by controlling the current input (or torque output) of the motors, control of the movement of the arm in three axes is possible. Section 2.1 contains a more detailed description of the tendon arm system, and figure 2-1 shows a schematic diagram of it. The tendon arm system is designed by John Hollerbach and Danny Hillis of the M.I.T. Artificial Intelligence Laboratory.

We are interested in designing a controller to move the arm from an initial position to any specified final position. Time-optimal control is chosen because

1. it achieves the desired motion in minimum time — this is desirable because the faster it can move, the more motion tasks per unit time could be completed this way, and
2. it requires few words of computer memory to represent the optimal solution — traditionally, time-optimal solution is associated with bang-bang control, hence the optimal solution is completely specified by the switching times.

These are the motivations for choosing time-optimal control, namely, it yields a rapid-moving system which is implementable.

The second point mentioned in the last paragraph is only valid if the problem is nonsingular. In the presence of singularity, the time-optimal solution need not be bang-bang. Our problem is, in fact, singular, but the form of the singular arcs is such that the control signals can be approximated very closely

by straight line segments, hence the storage requirements for such a control is quite low also (about 5 integer words per trajectory).

Since our system equations are highly nonlinear and complicated, it is not possible to express the optimal solution in feedback form. Thus, in addition to this open-loop control, some sort of closed-loop control law is required to correct for any disturbances. The overall control scheme will consist of two phases : an initial phase during which open-loop time-optimal control is applied, and a second phase which is feedback regulation at the final position.

Although time-optimal control has been applied to manipulators (Kahn[1]), it does not shed much light on our problem because the tendon arm is different from conventional manipulator design. The only reference that is available on tendon arm dynamics is Riemenschneider *et al* [2] but the paper deals with a one degree-of-freedom arm which is much simpler than the three degree-of- freedom arm studied herein.

1.2 Thesis Outline

This thesis is organized into seven Chapters:

Chapter 1 provides an introduction to the problem under study.

Chapter 2 describes the physical tendon arm system and develops a mathematical model describing the system. A simplified reduced-order model is also obtained, and the responses of the two are compared.

Chapter 3 first states the time-optimal control problem and presents necessary conditions for the optimal solution from Pontryagin's Minimum Principle. These are then applied to the reduced-order model of the tendon arm system.

Chapter 4 presents the conjugate gradient method and describes an iterative procedure for solving our time-optimal problem. Approximation for the time-optimal solution is also proposed.

Chapter 5 motivates the need for a closed-loop feedback control law at the final position, and presents the linear regulator approach for designing the feedback law.

Chapter 6 describes the implementation of the overall control scheme.

Chapter 7 is a summary of the results of the thesis and describes areas of further work.

Chapter 2. Modeling of the Tendon Arm System

In order to study and develop a control strategy for the tendon arm system, we must have a mathematical model of it. In this Chapter, the physical system is first described, equations describing the system dynamics are then developed, and a reduced-order model is obtained by ignoring the third degree-of-freedom of the arm.

2.1 A Description of the Tendon Arm System

The schematic diagram of the tendon arm system is shown in figure 2-1. It is a cylindrical rod, known as the arm, attached at one end to a base plate via a three degree-of-freedom "joint". Figure 2-2 shows the "joint" in greater detail. The outer rectangular block, together with the inner member, can be rotated about the $Y - Y$ axis. The inner member can be independently rotated about the $X - X$ axis. The cylindrical part of the inner member can be rotated about the $Z - Z$ axis, *i.e.* the longitudinal axis of the cylinder. Potentiometers are mounted as shown in the diagram to measure the three angles of rotation. This construction of the "joint" lends itself to a very natural way of defining the position of the arm in terms of the three angles θ, ϕ, and ψ, which are measured directly by the potentiometers, as shown in figure 2-3. This coordinate system will be used throughout this thesis to describe the arm. Another coordinate system, described by the angles α, β, and ψ, is sometimes used. This is shown in figure 2-4.

At the upper half of the cylindrical rod, there are points of "insertion" (attachment) for four tendons, two at one height, and the other two at another. Each tendon is wrapped around the arm through a certain angle before it breaks off from the surface of the arm (see figure 2-5). The other end of the tendon passes through a pulley on the base plate and is wrapped round a threaded cylinder mounted on the shaft of a motor under the base plate. As the motor rotates, the tendon will be wrapped or unwrapped from the motor shaft thereby causing a shortening or lengthening of the tendon between the motor and the arm. Through the interaction of the four motors and tendons, the arm can be moved from one position to

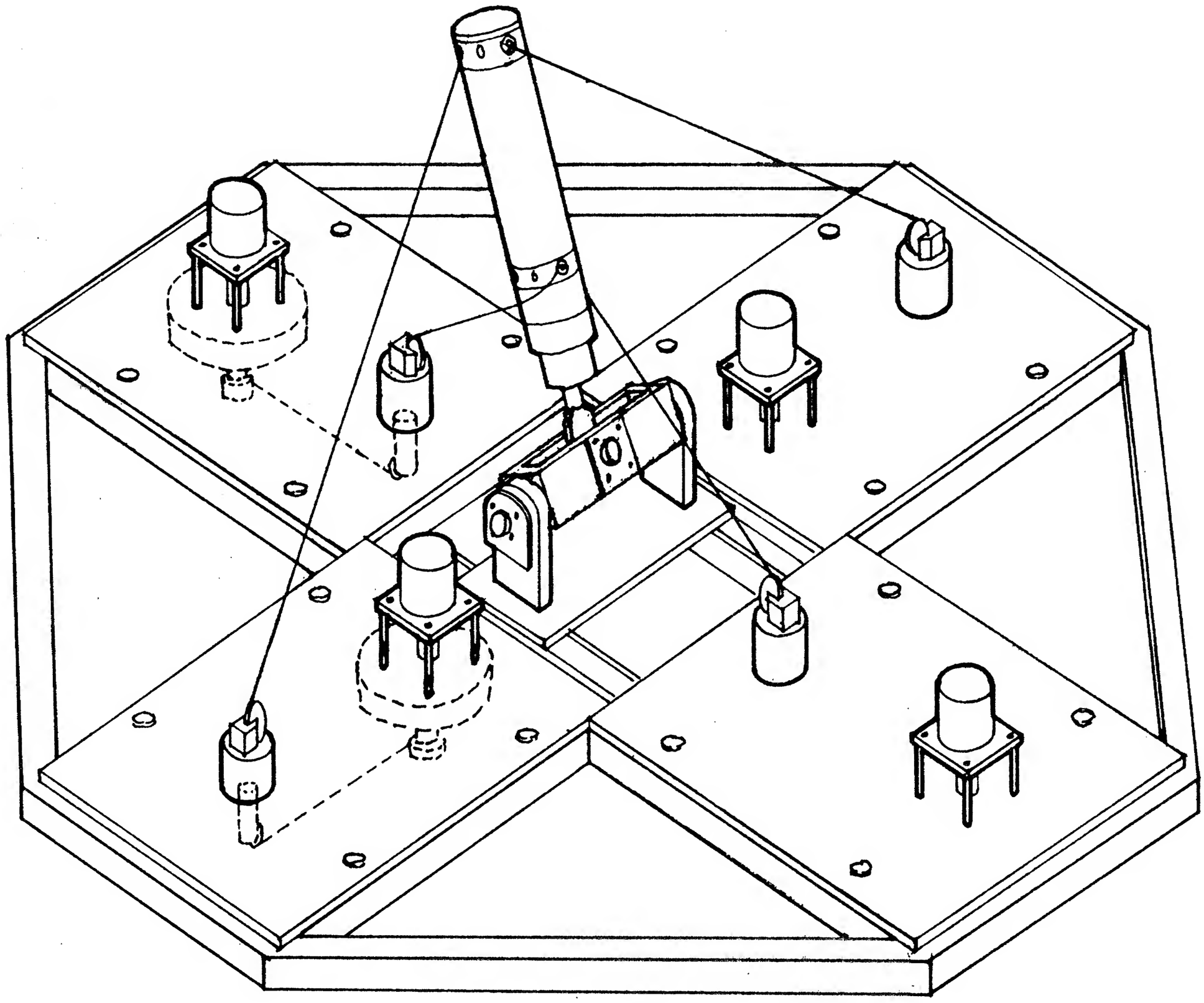

Figure 2-1. Schematic diagram of the tendon arm system

another.

2.2 Equations of Motion

2.2.1 Coordinate Systems and Coordinate Transformation

We choose as our fixed coordinate system one that has its origin at the "joint" with the x-axis along

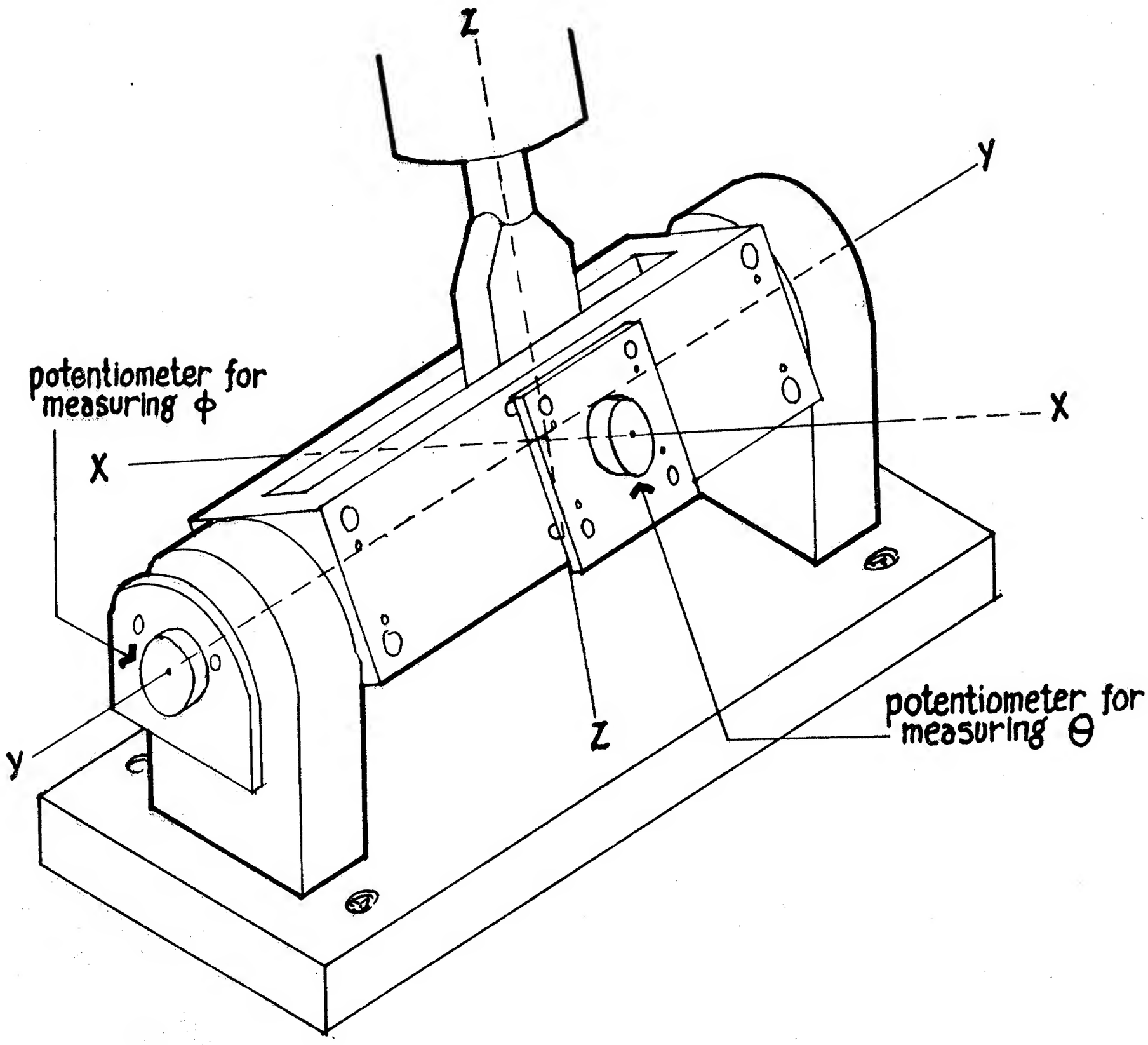

Figure 2-2. A more detailed diagram of the three degree-of-freedom "joint"

P_3, P_4 and the y-axis along P_2, P_1. P_1, P_2, P_3, and P_4 are the points on the base plate through which the tendons pass (refer to figure 2-5).

In computing the dynamics of the arm, we refer all quantities to a moving coordinate system which is fixed to the arm and with the three axes coinciding with those of the fixed coordinate system when $\theta = \phi = \psi = 0$. These three axes are the principal axes of the arm.

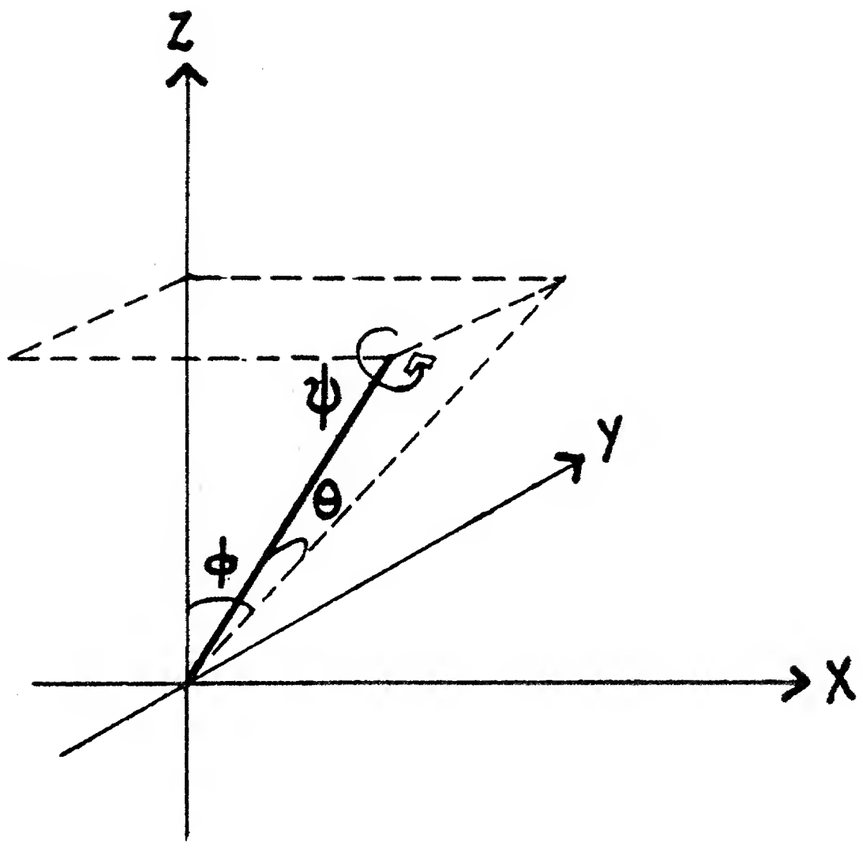

Figure 2-3. Angles defining the position of the arm

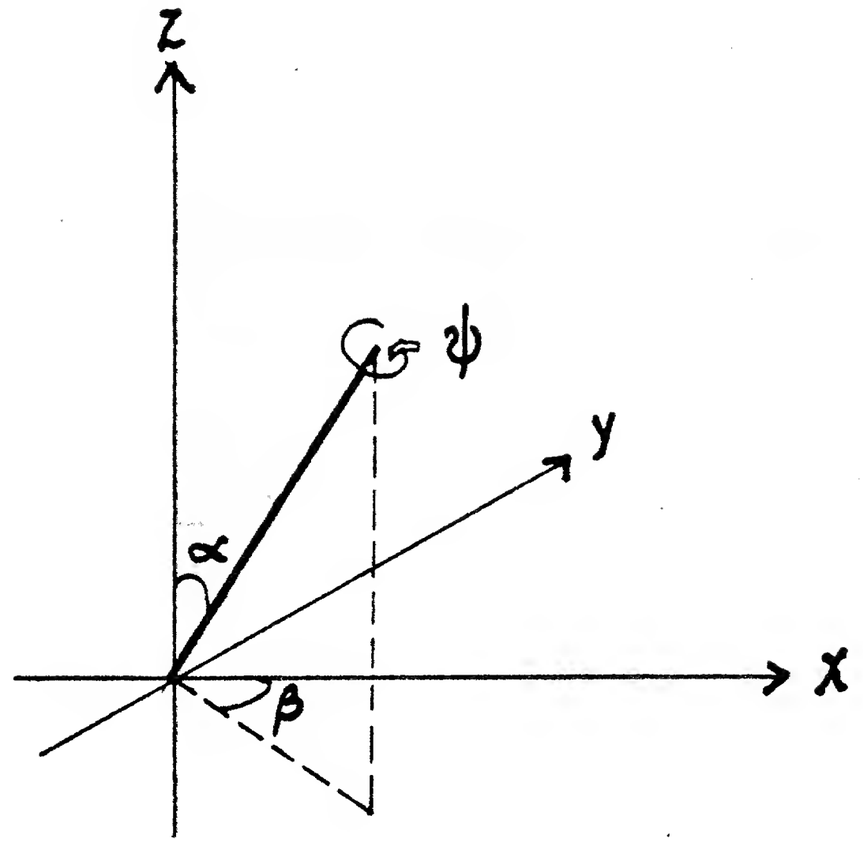

Figure 2-4. Another set of angles that defines the position of the arm

If P denotes the coordinates of a point in the fixed coordinate system, to refer it to the moving coordinate system, we need to perform the following transformations:

1. a rotation through an angle ϕ about the y-axis, and
2. a rotation through an angle θ about the new x-axis, and
3. a rotation through an angle ψ about the new z-axis.

i.e.

$$P' = S_z(\psi)\, S_x(\theta)\, S_y(\phi)\, P \tag{2.1}$$

where P' denotes the coordinates of the point referred to the moving (primed) coordinate system, and

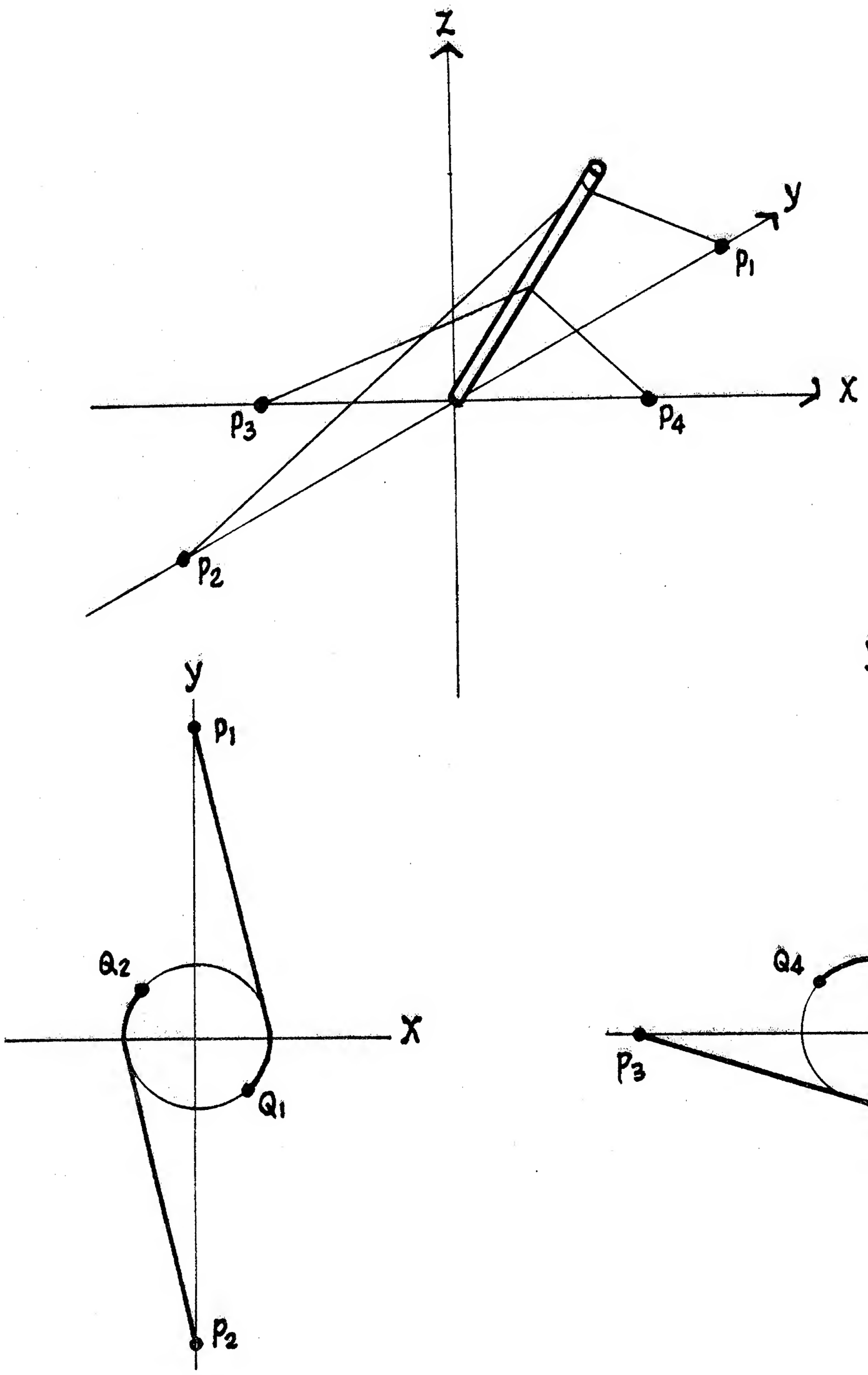

Figure 2-5. Schematic diagram of the arm showing the tendon wrapping geometry.

$$S_x(\theta) = \begin{bmatrix} 1 & 0 & 0 \\ 0 & \cos\theta & \sin\theta \\ 0 & -\sin\theta & \cos\theta \end{bmatrix}, \quad S_y(\phi) = \begin{bmatrix} \cos\phi & 0 & -\sin\phi \\ 0 & 1 & 0 \\ \sin\phi & 0 & \cos\phi \end{bmatrix}, \quad S_z(\psi) = \begin{bmatrix} \cos\psi & \sin\psi & 0 \\ -\sin\psi & \cos\psi & 0 \\ 0 & 0 & 1 \end{bmatrix} \tag{2.2}$$

or

$$P' = W(\theta, \phi, \psi)\, P \tag{2.3}$$

where

$$W(\theta, \phi, \psi) = \begin{bmatrix} \cos\phi\cos\psi + \sin\theta\sin\phi\sin\psi & \cos\theta\sin\psi & -\sin\phi\cos\psi + \sin\theta\cos\phi\sin\psi \\ -\cos\phi\sin\psi + \sin\theta\sin\phi\cos\psi & \cos\theta\cos\psi & \sin\phi\sin\psi + \sin\theta\cos\phi\cos\psi \\ \cos\theta\sin\phi & -\sin\theta & \cos\theta\cos\phi \end{bmatrix} \tag{2.4}$$

2.2.2 Some Geometric Calculations

Referring to figure 2-6 which shows some parameters of the arm,

$$P_1 = \begin{bmatrix} 0 \\ a \\ 0 \end{bmatrix}, \quad P_2 = \begin{bmatrix} 0 \\ -a \\ 0 \end{bmatrix}, \quad P_3 = \begin{bmatrix} -s \\ 0 \\ 0 \end{bmatrix}, \quad P_4 = \begin{bmatrix} s \\ 0 \\ 0 \end{bmatrix}. \tag{2.5}$$

Using equation (2.3),

$$P'_1 = -P'_2 = \begin{bmatrix} a\cos\theta\sin\psi \\ a\cos\theta\cos\psi \\ -a\sin\theta \end{bmatrix}, \quad P'_3 = -P'_4 = \begin{bmatrix} -s\cos\phi\cos\psi - s\sin\theta\sin\phi\sin\psi \\ s\cos\phi\sin\psi - s\sin\theta\sin\phi\cos\psi \\ -s\cos\theta\sin\phi \end{bmatrix}. \tag{2.6}$$

From now onwards, we will refer all quantities to the moving coordinate system.

Let Q_i be the point at which tendon i is attached to the arm, and R_i be the point at which tendon i leaves the surface of the arm. Then in order to calculate the directions in which the tendons pull on the arm, we need the coordinates of the R_i's.

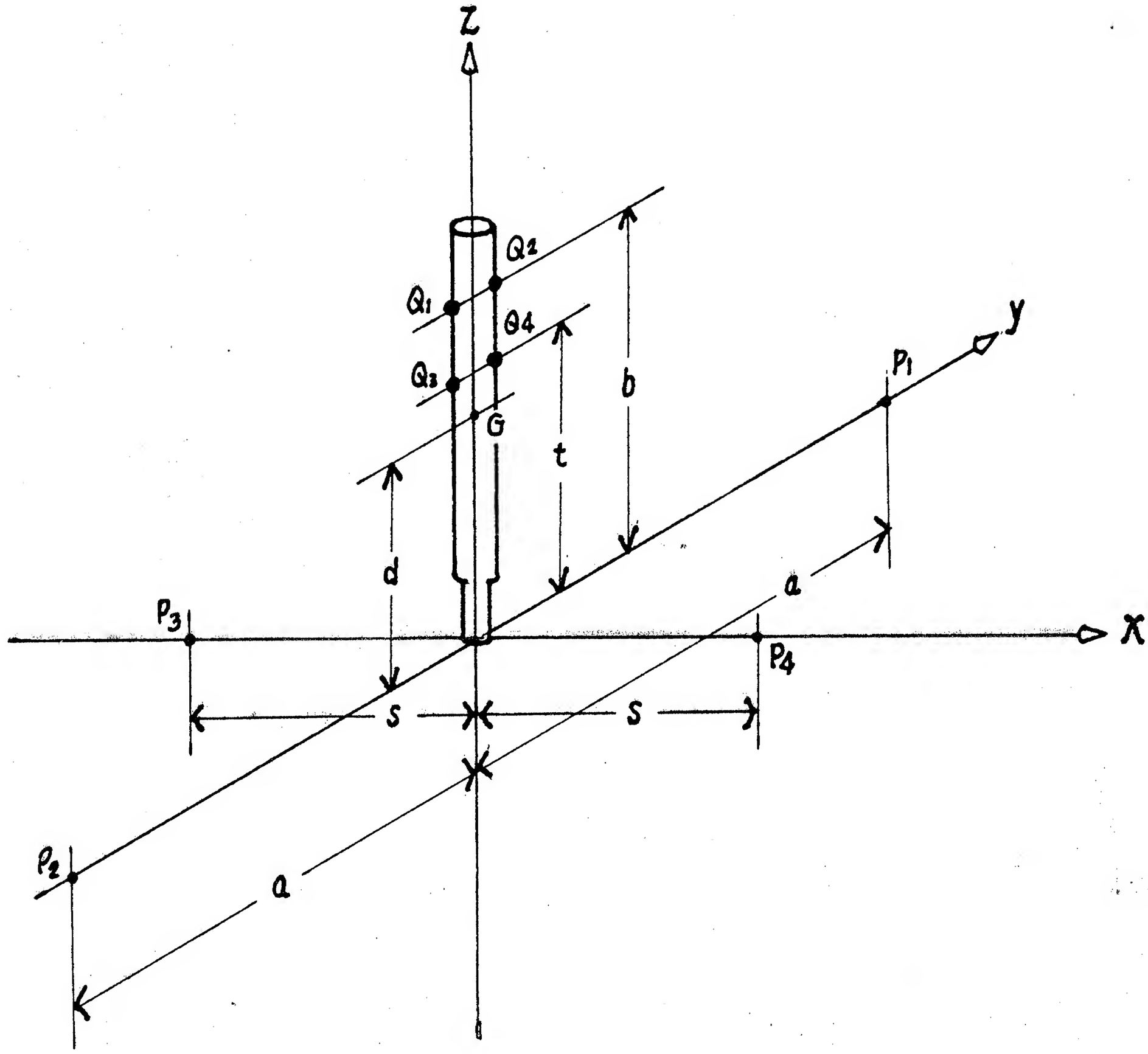

Figure 2-6. Schematic diagram showing some parameters of the arm.

Coordinates of R_1 *and* R_2

Let (x_1, y_1, z_1) denote the coordinates of R_1 with respect to the primed coordinate system.

From figure 2-7(a) and equation (2.6),

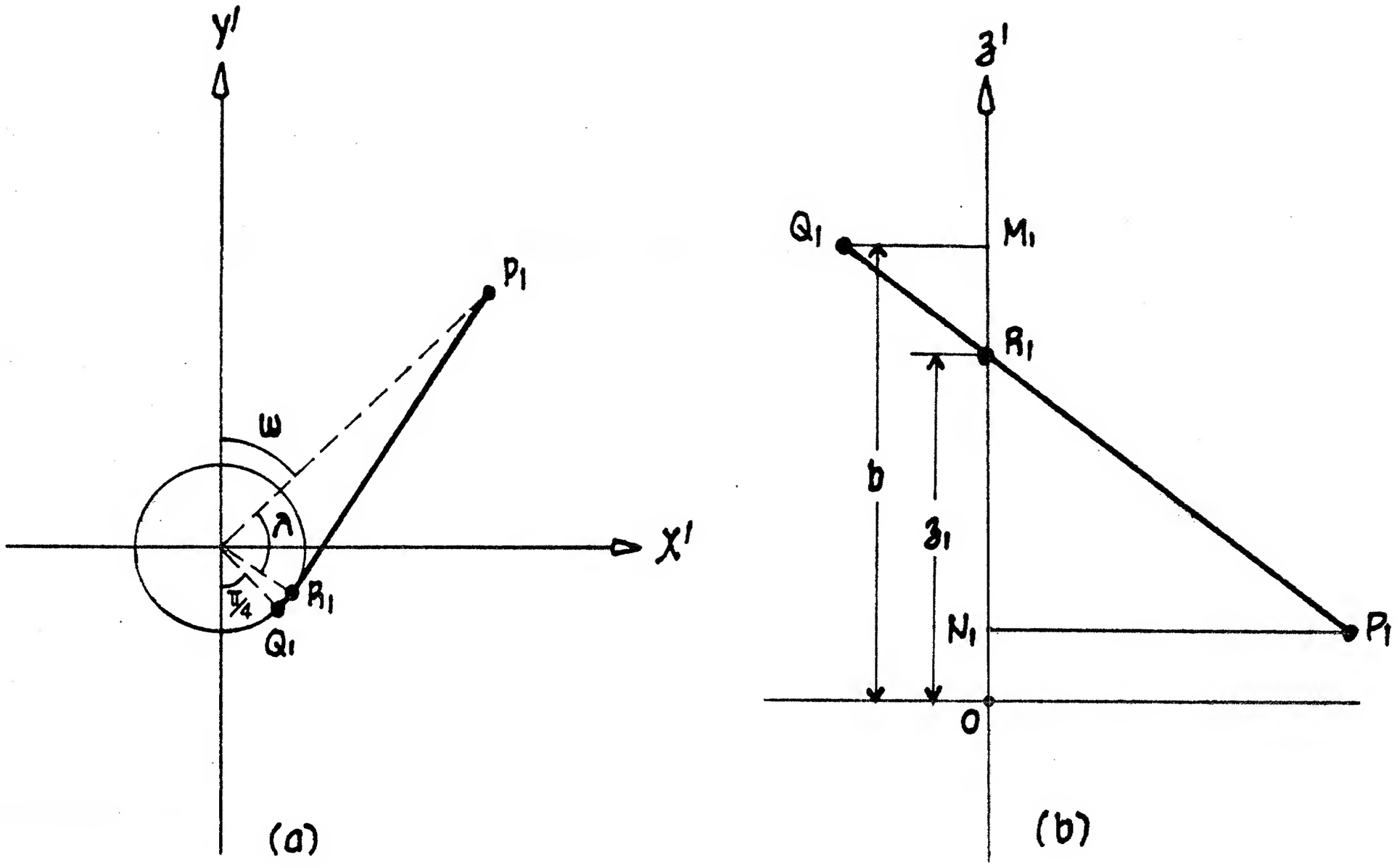

Figure 2-7. (a) Schematic of the arm looking down the z'-axis showing only tendon 1. (b) Unwrapping tendon 1 onto a plane.

$$\omega = tan^{-1}\left(\frac{a\cos\theta\sin\psi}{a\cos\theta\cos\psi}\right) = \psi \tag{2.7}$$

$$\lambda = \cos^{-1}\left(\frac{\rho}{a\cos\theta}\right) \tag{2.8}$$

where ρ is the radius of the cylindrical arm.

$$x_1 = +\rho\sin(\pi - \lambda - \omega) = \rho\sin(\omega + \lambda) \tag{2.9}$$

$$y_1 = -\rho\cos(\pi - \lambda - \omega) = \rho\cos(\omega + \lambda) \tag{2.10}$$

Referring to figure 2-7(b),

$$\frac{M_1R_1}{R_1N_1} = \frac{Q_1M_1}{N_1P_1}$$

implies

$$z_1 = -a\sin\theta + \frac{b + a\sin\theta}{1 + (\frac{3\pi}{4} - \omega - \lambda)/\tan\lambda} \tag{2.11}$$

$$L_1 = R_1P_1 = \left[(z_1 + a\sin\theta)^2 + \rho^2\tan^2\lambda\right]^{\frac{1}{2}} \tag{2.12}$$

$$l_1 = Q_1P_1 = \left[(b + a\sin\theta)^2 + \rho^2(\frac{3\pi}{4} - \omega - \lambda + \tan\lambda)^2\right]^{\frac{1}{2}} \tag{2.13}$$

Similarly, the coordinates of R_2 are given by,

$$x_2 = -\rho\sin(\omega + \lambda) \tag{2.14}$$

$$y_2 = -\rho\cos(\omega + \lambda) \tag{2.15}$$

$$z_2 = a\sin\theta + \frac{b - a\sin\theta}{1 + (\frac{3\pi}{4} - \omega - \lambda)/\tan\lambda} \tag{2.16}$$

$$L_2 = R_2P_2 = \left[(z_2 - a\sin\theta)^2 + \rho^2\tan^2\lambda\right]^{\frac{1}{2}} \tag{2.17}$$

$$l_2 = Q_2P_2 = \left[(b - a\sin\theta)^2 + \rho^2(\frac{3\pi}{4} - \omega - \lambda + \tan\lambda)^2\right]^{\frac{1}{2}} \tag{2.18}$$

Coordinates of R_3 and R_4

Let (x_3, y_3, z_3) be the coordinates of R_3 in the primed coordinates.

From figure 2-8(a) and equation(2.6),

$$\begin{aligned}\omega' &= \tan^{-1}\left(\frac{-\cos\phi\sin\psi + \sin\theta\sin\phi\cos\psi}{\cos\phi\cos\psi + \sin\theta\sin\phi\sin\psi}\right)\\ &= \tan^{-1}\left(\frac{-\tan\psi + \tan\phi\sin\theta}{1 + \tan\psi\tan\phi\sin\theta}\right)\end{aligned} \tag{2.19}$$

Define

$$\tan\mu' = \tan\phi\sin\theta \tag{2.20}$$

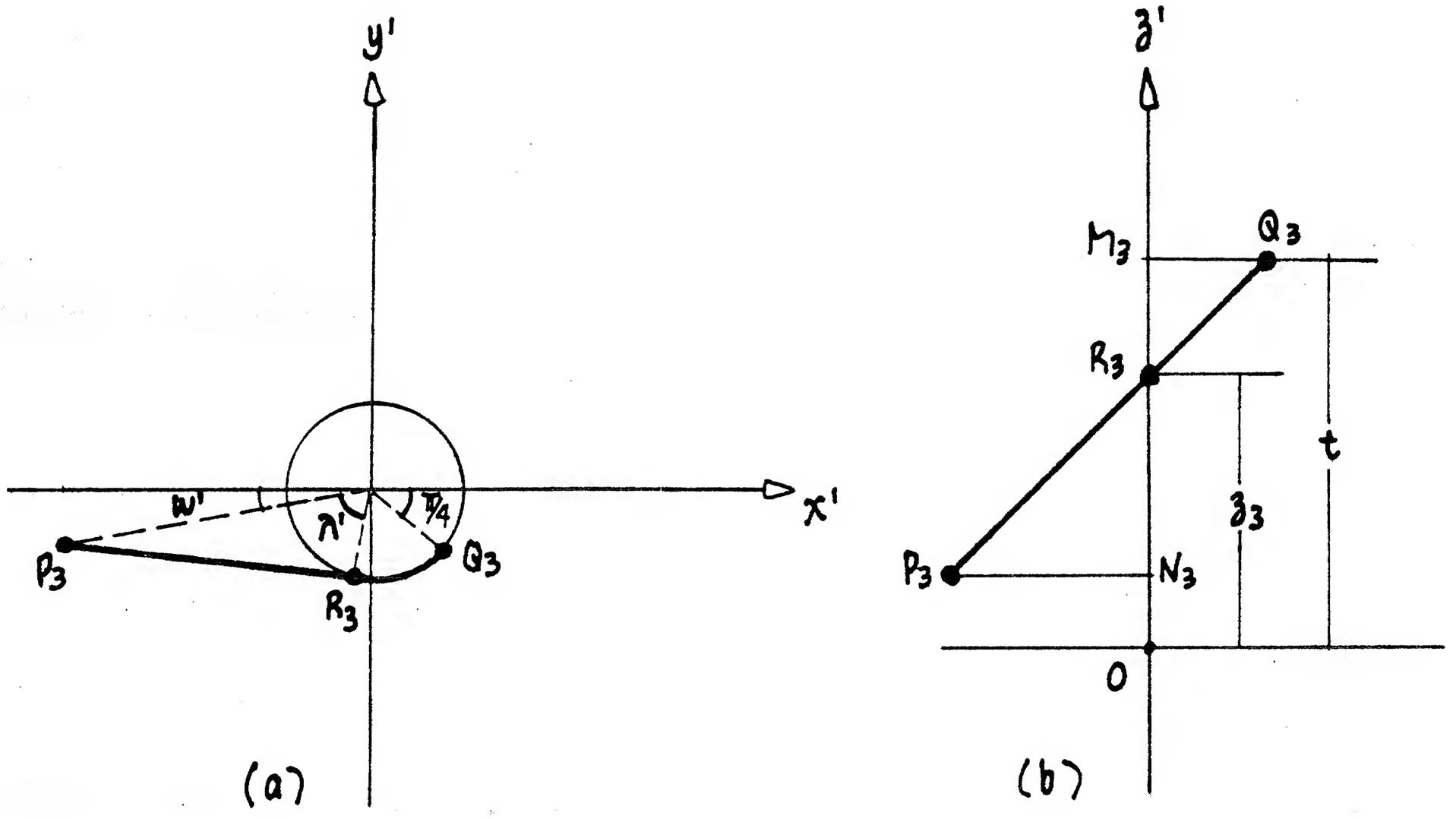

Figure 2-8. (a) Schematic of the arm looking down the z'-axis showing only tendon 3. (b) Unwrapping tendon 3 onto a plane.

Then from equations (2.19) and (2.20),

$$\omega' = \mu' - \psi \tag{2.21}$$

$$\lambda' = \cos^{-1}\left(\frac{\rho}{s(\cos^2\phi + \sin^2\phi\sin^2\theta)^{\frac{1}{2}}}\right) \tag{2.22}$$

$$x_3 = -\rho\cos(\omega' + \lambda') \tag{2.23}$$

$$y_3 = -\rho\sin(\omega' + \lambda') \tag{2.24}$$

Referring to figure 2-8(b),

$$\frac{M_3R_3}{R_3N_3} = \frac{M_3Q_3}{N_3P_3}$$

implies

$$z_3 = -s\sin\phi\cos\theta + \frac{t + s\sin\phi\cos\theta}{1 + (\frac{3\pi}{4} - \omega' - \lambda')/\tan\lambda'} \tag{2.25}$$

$$L_3 = R_3P_3 = \left[(z_3 + s\sin\phi\cos\theta)^2 + \rho^2\tan^2\lambda'\right]^{\frac{1}{2}} \tag{2.26}$$

$$l_3 = Q_3P_3 = \left[(t + s\sin\phi\cos\theta)^2 + \rho^2(\frac{3\pi}{4} - \omega' - \lambda' + \tan\lambda')^2\right]^{\frac{1}{2}} \tag{2.27}$$

Similarly, for R_4,

$$x_4 = \rho\cos(\omega' + \lambda') \tag{2.28}$$

$$y_4 = \rho\sin(\omega' + \lambda') \tag{2.29}$$

$$z_4 = s\sin\phi\cos\theta + \frac{t - s\sin\phi\cos\theta}{1 + (\frac{3\pi}{4} - \omega' - \lambda')/\tan\lambda'} \tag{2.30}$$

$$L_4 = R_4P_4 = \left[(z_4 - s\sin\phi\cos\theta)^2 + \rho^2\tan^2\lambda'\right]^{\frac{1}{2}} \tag{2.31}$$

$$l_4 = Q_4P_4 = \left[(t - s\sin\phi\cos\theta)^2 + \rho^2(\frac{3\pi}{4} - \omega' - \lambda' + \tan\lambda')^2\right]^{\frac{1}{2}} \tag{2.32}$$

Coordinates of the center of gravity

Let G be the center of gravity of the arm (see figure 2-6), and let GD be the unit vector along the direction of the gravitation field which will be assumed to be vertically down.

Expressed in the primed coordinate system,

$$G = \begin{bmatrix} 0 \\ 0 \\ d \end{bmatrix} \tag{2.33}$$

$$GD = \begin{bmatrix} \sin\phi\cos\psi - \sin\theta\cos\phi\sin\psi \\ -\sin\phi\sin\psi - \sin\theta\cos\phi\cos\psi \\ -\cos\theta\cos\phi \end{bmatrix} \tag{2.34}$$

2.2.3 Resultant Torque exerted by the four Tendons about the point of rotation O

Let F_i, $i = 1, \ldots, 4$, be the tension in tendon i, the direction of F_i will be in the direction of R_iP_i.

Resultant torque acting on the arm about O

$$\begin{aligned}
&= O\vec{R}_1 \times \vec{F}_1 + O\vec{R}_2 \times \vec{F}_2 + O\vec{R}_3 \times \vec{F}_3 + O\vec{R}_4 \times \vec{F}_4 + O\vec{G} \times m\vec{g} \\
&= \frac{F_1}{|R_1P_1|} O\vec{R}_1 \times R_1\vec{P}_1 + \frac{F_2}{|R_2P_2|} O\vec{R}_2 \times R_2\vec{P}_2 + \frac{F_3}{|R_3P_3|} O\vec{R}_3 \times R_3\vec{P}_3 \\
&\quad + \frac{F_4}{|R_4P_4|} O\vec{R}_4 \times R_4\vec{P}_4 + mgO\vec{G} \times \vec{GD} \\
&= iT_1 + jT_2 + kT_3 \qquad (2.35)
\end{aligned}$$

where

$$\begin{aligned}
T_1 = {} & \frac{F_1}{L_1}[-\rho a \sin\theta \cos(\omega + \lambda) - z_1 a \cos\theta \cos\psi] + \frac{F_2}{L_2}[-\rho a \sin\theta \cos(\omega + \lambda) + z_2 a \cos\theta \cos\psi] \\
& + \frac{F_3}{L_3}[\rho s \sin\phi \cos\theta \sin(\omega' + \lambda') - z_3 s(\cos\phi \sin\psi - \sin\theta \sin\phi \cos\psi)] \\
& + \frac{F_4}{L_4}[\rho s \sin\phi \cos\theta \sin(\omega' + \lambda') + z_4 s(\cos\phi \sin\psi - \sin\theta \sin\phi \cos\psi)] \\
& + mgd(\sin\phi \sin\psi + \cos\phi \sin\theta \cos\psi) \qquad (2.36)
\end{aligned}$$

$$\begin{aligned}
T_2 = {} & \frac{F_1}{L_1}[\rho a \sin\theta \sin(\omega + \lambda) + z_1 a \cos\theta \sin\psi] + \frac{F_2}{L_2}[\rho a \sin\theta \sin(\omega + \lambda) - z_2 a \cos\theta \sin\psi] \\
& + \frac{F_3}{L_3}[-\rho s \sin\phi \cos\theta \cos(\omega' + \lambda') - z_3 s(\cos\phi \cos\psi + \sin\phi \sin\theta \sin\psi)] \\
& + \frac{F_4}{L_4}[-\rho s \sin\phi \cos\theta \cos(\omega' + \lambda') + z_4 s(\cos\phi \cos\psi + sin\phi \sin\theta \sin\psi)] \\
& + mgd(\sin\phi \cos\psi - \cos\phi \sin\theta \sin\psi) \qquad (2.37)
\end{aligned}$$

$$T_3 = \left(\frac{F_1}{L_1} + \frac{F_2}{L_2}\right)\rho a \cos\theta \sin\lambda + \left(\frac{F_3}{L_3} + \frac{F_4}{L_4}\right)\rho s[\sin\phi \sin\theta \cos(\lambda' + \mu') - \cos\phi \sin(\lambda' + \mu')] \qquad (2.38)$$

Note: The expressions in equations (2.36)–(2.38) are derived based on the geometry of the arm as described in section 2.2.2, which assumes that all the tendons are wrapped properly on the arm. In the course of moving from one position to another, one pair of the tendons might be completely unwrapped, hence the expressions developed above will not be valid.

Referring to the notations used in section 2.2.2:

if $\omega + \lambda \geq 3\pi/4$, then tendons 1 and 2 have completely unwrapped, and

if $\omega' + \lambda' \geq 3\pi/4$, then tendons 3 and 4 have completely unwrapped.

Appendix A develops the corresponding expressions for equations (2.36)–(2.38) in the event of either pair of tendons is unwrapped. These expressions are only approximations as the tendon insertion is not ideal.

2.2.4 Arm and Motor Dynamics

Euler's dynamical equations for the rotation of a rigid body about a point O are given by,

$$\begin{aligned} J_1\frac{d\Omega_1}{dt} - (J_2 - J_3)\Omega_2\Omega_3 &= T_1 \\ J_2\frac{d\Omega_2}{dt} - (J_3 - J_1)\Omega_3\Omega_1 &= T_2 \\ J_3\frac{d\Omega_3}{dt} - (J_1 - J_2)\Omega_1\Omega_2 &= T_3 \end{aligned} \tag{2.39}$$

where the subscripts 1, 2, 3 refer to the three principal axes of the rigid body, Ω_i, J_i are the angular velocity and the moment of inertia, respectively, of the arm along the i-axis, and T_i is the external applied torque on the body.

By making the identification of the x'-, y'-, z' -axes of the arm primed coordinate system with the 1-, 2-, 3-axes of the above, we can apply equation (2.39) to the tendon arm system, with the simplifying assumption that

$$J_1 = J_2 = J. \tag{2.40}$$

This assumption is valid because the contribution of the moment of inertia of the lower rectangular block about point O, which is asymmetrical about the z'-axis, is negligible compared to that of the cylindrical rod, which is symmetrical.

Expressing the Ω_i's in terms of the three angles θ, ϕ and ψ, we obtain,

$$\Omega = \begin{bmatrix} \Omega_1 \\ \Omega_2 \\ \Omega_3 \end{bmatrix} = \begin{bmatrix} \dot{\theta}\cos\psi + \dot{\phi}\cos\theta\sin\psi \\ -\dot{\theta}\sin\psi + \dot{\phi}\cos\theta\cos\psi \\ -\dot{\phi}\sin\theta + \dot{\psi} \end{bmatrix} \tag{2.41}$$

T_1, T_2, T_3 are given by equations (2.36)–(2.38). The tensions F_1, F_2, F_3, F_4 in the tendons are related

to the input currents to the motors, I_1, I_2, I_3, I_4, through the motor dynamics

$$J_m\ddot{\gamma}_i + B_m\dot{\gamma}_i + F_i r = KI_i \qquad i = 1, \ldots, 4 \tag{2.42}$$

where

$\dot{\gamma}_i$ is the angular velocity of the motor shaft,

J_m is the moment of inertia of the motor shaft,

B_m is the velocity dependent friction coefficient,

r is the radius of the cylinder mounted on the motor shaft, and

K is the torque constant of the motor.

Because of the constraint that the tendons must be taut at all time, and the assumption that the tendons are inelastic, the angular rotation of each motor is related to that of the arm. Specifically,

$$r\gamma_i = l_0 - l_i(\theta, \phi, \psi) \tag{2.43}$$

where $l_i(\theta, \phi, \psi)$ is the length of tendon i (from point Q_i to point P_i) when the arm is at the position defined by θ, ϕ, ψ, and $l_0 = l_i(0, 0, 0)$, which implies that $\gamma_i = 0$ when $\theta = \phi = \psi = 0$.

By differentiating equation (2.43) with respect to time once, we obtain

$$r\dot{\gamma}_i = -\left[\frac{\partial l_i}{\partial \theta}\dot{\theta} + \frac{\partial l_i}{\partial \phi}\dot{\phi} + \frac{\partial l_i}{\partial \psi}\dot{\psi}\right] \tag{2.44}$$

By differentiating once more,

$$\begin{aligned} r\ddot{\gamma}_i = -\Bigg[&\frac{\partial l_i}{\partial \theta}\ddot{\theta} + \frac{\partial l_i}{\partial \phi}\ddot{\phi} + \frac{\partial l_i}{\partial \psi}\ddot{\psi} + \frac{\partial^2 l_i}{\partial \theta^2}\theta^2 + \frac{\partial^2 l_i}{\partial \phi^2}\phi^2 + \frac{\partial^2 l_i}{\partial \psi^2}\dot{\psi}^2 \\ &+ 2\frac{\partial^2 l_i}{\partial \theta \partial \phi}\dot{\theta}\dot{\phi} + 2\frac{\partial^2 l_i}{\partial \phi \partial \psi}\dot{\phi}\dot{\psi} + 2\frac{\partial^2 l_i}{\partial \psi \partial \theta}\dot{\psi}\dot{\theta}\Bigg] \end{aligned} \tag{2.45}$$

By substituting equations (2.44)–(2.45) into equation (2.42), we can obtain expressions for the F_i's in terms of the I_i's and the three angles θ, ϕ, and ψ. By substituting these into equations (2.36)–(2.39), a set of differential equations describing the dynamics of the tendon arm system is obtained.

By defining,

$$x = [\theta \quad \phi \quad \psi \quad \dot{\theta} \quad \dot{\phi} \quad \dot{\psi}]^T \tag{2.46}$$

$$u = [I_1 \quad I_2 \quad I_3 \quad I_4]^T \tag{2.47}$$

and rearranging terms, we obtain the equations of motion of the system in the form,

$$\dot{x}(t) = F_0(x(t)) + B_0(x(t))u(t) \tag{2.48}$$

where

$F_0(x)$ is a 6-vector, and

$B_0(x)$ is a 6×4 matrix.

The full detail of equation (2.48) is given in Appendix B.

2.3 Reduced-Order Model

The equations of motion obtained in the previous section is too complicated to be useful in the design of a controller. Much of the complications arises from the geometry of the tendon arm system.

A simplified fourth order model is obtained by ignoring the tendon wrapping about the arm, thereby reducing the three degree-of-freedom arm to a two degree-of-freedom one. This is achieved by equating ρ to zero (recall that ρ is the radius of the cylindrical arm).

i.e.,

$$\rho = 0 \tag{2.49}$$

This, in effect, is to ignore the twisting movement, ψ, of the arm.

Equations (2.39) become:

$$J(\ddot{\theta} + \dot{\phi}^2 \sin\theta\cos\theta) = \left(\frac{F_2}{l_2} - \frac{F_1}{l_1}\right)ab\cos\theta - \left(\frac{F_4}{l_4} - \frac{F_3}{l_3}\right)st\sin\theta\sin\phi + mgd\sin\theta\cos\phi \tag{2.50}$$

$$J(\ddot{\phi}\cos\theta - 2\dot{\theta}\dot{\phi}\sin\theta) = \left(\frac{F_4}{l_4} - \frac{F_3}{l_3}\right)st\cos\phi + mgd\sin\phi \tag{2.51}$$

where

$$
\begin{aligned}
l_1 &= [a^2 + b^2 + 2ab\sin\theta]^{\frac{1}{2}} \\
l_2 &= [a^2 + b^2 - 2ab\sin\theta]^{\frac{1}{2}} \\
l_3 &= [s^2 + t^2 + 2st\sin\phi\cos\theta]^{\frac{1}{2}} \\
l_4 &= [s^2 + t^2 - 2st\sin\phi\cos\theta]^{\frac{1}{2}}
\end{aligned}
\tag{2.52}
$$

From equations (2.42)–(2.45),

$$
F_i = \frac{1}{r}\left[KI_i + \frac{J_m}{r}\left(\frac{\partial l_i}{\partial\theta}\ddot{\theta} + \frac{\partial l_i}{\partial\phi}\ddot{\phi} + \frac{\partial^2 l_i}{\partial\theta^2}\dot{\theta}^2 + \frac{\partial^2 l_i}{\partial\phi^2}\dot{\phi}^2 + 2\frac{\partial^2 l_i}{\partial\theta\partial\phi}\dot{\theta}\dot{\phi}\right) + \frac{B_m}{r}\left(\frac{\partial l_i}{\partial\theta}\dot{\theta} + \frac{\partial l_i}{\partial\phi}\dot{\phi}\right)\right] \tag{2.53}
$$

For $i = 1, 2$, since l_i is a function of θ only,

$$
F_i = \frac{1}{r}\left[KI_i + \frac{J_m}{r}\left(\frac{dl_i}{d\theta}\ddot{\theta} + \frac{d^2 l_i}{d\theta^2}\dot{\theta}^2\right) + \frac{B_m}{r}\frac{dl_i}{d\theta}\dot{\theta}\right] \tag{2.54}
$$

Substituting equations (2.53)–(2.54) into (2.50)–(2.51), and rearranging terms,

$$\ddot{\theta}\left[J\frac{r^2}{ab\cos\theta}+J_m\left(\frac{1}{l_1}\frac{dl_1}{d\theta}-\frac{1}{l_2}\frac{dl_2}{d\theta}\right)+\frac{st\sin\phi\sin\theta}{ab\cos\theta}J_m\left(-\frac{1}{l_3}\frac{\partial l_3}{\partial\theta}+\frac{1}{l_4}\frac{\partial l_4}{\partial\theta}\right)\right]$$
$$+\ddot{\phi}\frac{st\sin\phi\sin\theta}{ab\cos\theta}J_m\left(-\frac{1}{l_3}\frac{\partial l_3}{\partial\phi}+\frac{1}{l_4}\frac{\partial l_4}{\partial\phi}\right)$$
$$=Kr\left(\frac{I_2}{l_2}-\frac{I_1}{l_1}\right)-\frac{st\sin\phi\sin\theta}{ab\cos\theta}Kr\left(\frac{I_4}{l_4}-\frac{I_3}{l_3}\right)+mg\frac{dr^2\sin\theta\cos\phi}{ab\cos\theta}$$
$$+\dot{\phi}\frac{st\sin\phi\sin\theta}{ab\cos\theta}B_m\left(\frac{1}{l_3}\frac{\partial l_3}{\partial\phi}-\frac{1}{l_4}\frac{\partial l_4}{\partial\phi}\right)$$
$$+\dot{\theta}B_m\left[\left(-\frac{1}{l_1}\frac{dl_1}{d\theta}+\frac{1}{l_2}\frac{dl_2}{d\theta}\right)+\frac{st\sin\phi\sin\theta}{ab\cos\theta}\left(\frac{1}{l_3}\frac{\partial l_3}{\partial\theta}-\frac{1}{l_4}\frac{\partial l_4}{\partial\theta}\right)\right]$$
$$+2\dot{\theta}\dot{\phi}\frac{st\sin\phi\sin\theta}{ab\cos\theta}J_m\left(\frac{1}{l_3}\frac{\partial^2 l_3}{\partial\theta\partial\phi}-\frac{1}{l_4}\frac{\partial^2 l_4}{\partial\theta\partial\phi}\right)$$
$$+\dot{\phi}^2\left[\frac{st\sin\phi\sin\theta}{ab\cos\theta}J_m\left(\frac{1}{l_3}\frac{\partial^2 l_3}{\partial\phi^2}-\frac{1}{l_4}\frac{\partial^2 l_4}{\partial\phi^2}\right)-J\frac{r^2\sin\theta}{ab}\right]$$
$$+\dot{\theta}^2J_m\left[\left(-\frac{1}{l_1}\frac{d^2l_1}{d\theta^2}+\frac{1}{l_2}\frac{d^2l_2}{d\theta^2}\right)+\frac{st\sin\phi\sin\theta}{ab\cos\theta}\left(\frac{1}{l_3}\frac{\partial^2 l_3}{\partial\theta^2}-\frac{1}{l_4}\frac{\partial^2 l_4}{\partial\theta^2}\right)\right] \tag{2.55}$$

$$\ddot{\phi}\left[J\frac{r^2\cos\theta}{st\cos\phi}+J_m\left(\frac{1}{l_3}\frac{\partial l_3}{\partial\phi}-\frac{1}{l_4}\frac{\partial l_4}{\partial\phi}\right)\right]+\ddot{\theta}J_m\left[\frac{1}{l_3}\frac{\partial l_3}{\partial\theta}-\frac{1}{l_4}\frac{\partial l_3}{\partial\theta}\right]$$
$$=Kr\left(\frac{I_4}{l_4}-\frac{I_3}{l_3}\right)+mg\frac{dr^2}{st}\tan\phi+\dot{\phi}B_m\left(-\frac{1}{l_3}\frac{\partial l_3}{\partial\phi}+\frac{1}{l_4}\frac{\partial l_4}{\partial\phi}\right)+\dot{\theta}B_m\left(-\frac{1}{l_3}\frac{\partial l_3}{\partial\theta}+\frac{1}{l_4}\frac{\partial l_4}{\partial\theta}\right)$$
$$+2\dot{\theta}\dot{\phi}\left[J\frac{r^2\sin\theta}{st\cos\phi}+J_m\left(-\frac{1}{l_3}\frac{\partial^2 l_3}{\partial\theta\partial\phi}+\frac{1}{l_4}\frac{\partial^2 l_4}{\partial\theta\partial\phi}\right)\right]+\dot{\phi}^2J_m\left(-\frac{1}{l_3}\frac{\partial^2 l_3}{\partial\phi^2}+\frac{1}{l_4}\frac{\partial^2 l_4}{\partial\phi^2}\right)$$
$$+\dot{\theta}^2J_m\left(-\frac{1}{l_3}\frac{\partial^2 l_3}{\partial\theta^2}+\frac{1}{l_4}\frac{\partial^2 l_4}{\partial\theta^2}\right) \tag{2.56}$$

By defining,

$$
\begin{aligned}
L_{1\theta} &= \frac{1}{l_1}\frac{dl_1}{d\theta} - \frac{1}{l_2}\frac{dl_2}{d\theta} \\
L_{2\theta} &= \frac{1}{l_3}\frac{\partial l_3}{\partial\theta} - \frac{1}{l_4}\frac{\partial l_4}{\partial\theta} \\
L_{1\theta\theta} &= \frac{1}{l_1}\frac{d^2 l_1}{d\theta^2} - \frac{1}{l_2}\frac{d^2 l_2}{d\theta^2} \\
L_{2\theta\theta} &= \frac{1}{l_3}\frac{\partial^2 l_3}{\partial\theta^2} - \frac{1}{l_4}\frac{\partial^2 l_4}{\partial\theta^2} \\
L_{2\phi} &= \frac{1}{l_3}\frac{\partial l_3}{\partial\phi} - \frac{1}{l_4}\frac{\partial l_4}{\partial\phi} \\
L_{2\phi\phi} &= \frac{1}{l_3}\frac{\partial^2 l_3}{\partial\phi^2} - \frac{1}{l_4}\frac{\partial^2 l_4}{\partial\phi^2} \\
L_{2\theta\phi} &= \frac{1}{l_3}\frac{\partial^2 l_3}{\partial\theta\partial\phi} - \frac{1}{l_4}\frac{\partial^2 l_4}{\partial\theta\partial\phi} \\
e &= \frac{st\sin\phi\sin\theta}{ab\cos\theta}
\end{aligned}
\tag{2.57}
$$

and

$$
N = \begin{bmatrix} Jr^2/ab\cos\theta + J_m L_{1\theta} - J_m e L_{2\theta} & -J_m e L_{2\phi} \\ J_m L_{2\theta} & Jr^2\cos\theta/st\cos\phi + J_m L_{2\phi} \end{bmatrix} \tag{2.58}
$$

Equations (2.55)–(2.56) can be written as:

$$
\begin{aligned}
\begin{bmatrix} \ddot{\theta} \\ \ddot{\phi} \end{bmatrix} &= N^{-1}\begin{bmatrix} -Kr/l_1 & Kr/l_2 & eKr/l_3 & -eKr/l_4 \\ 0 & 0 & -Kr/l_3 & Kr/l_4 \end{bmatrix}\begin{bmatrix} I_1 \\ I_2 \\ I_3 \\ I_4 \end{bmatrix} + N^{-1}\begin{bmatrix} \tan\theta\cos\phi dr^2/ab \\ \tan\phi dr^2/st \end{bmatrix} mg \\
&\quad + N^{-1}\begin{bmatrix} eB_m L_{2\phi} \\ -B_m L_{2\phi} \end{bmatrix}\dot{\phi} + N^{-1}\begin{bmatrix} -B_m L_{1\theta} + eB_m L_{20} \\ -B_m L_{2\theta} \end{bmatrix}\dot{\theta} \\
&\quad + N^{-1}\begin{bmatrix} eJ_m L_{2\theta\phi} \\ Jr^2\sin\theta/st\cos\phi - J_m L_{20\phi} \end{bmatrix} 2\dot{\theta}\dot{\phi} \\
&\quad + N^{-1}\begin{bmatrix} eJ_m L_{2\phi\phi} - Jr^2\sin\theta/ab \\ -J_m L_{2\phi\phi} \end{bmatrix}\dot{\phi}^2 + N^{-1}\begin{bmatrix} -J_m L_{1\theta\theta} + eJ_m L_{20\theta} \\ -J_m L_{2\theta\theta} \end{bmatrix}\dot{\theta}^2 \\
&= \begin{bmatrix} f_3(\theta,\phi,\dot{\theta},\dot{\phi}) \\ \hdashline f_4(\theta,\phi,\dot{\theta},\dot{\phi}) \end{bmatrix} + \begin{bmatrix} b_3(\theta,\phi) \\ \hdashline b_4(\theta,\phi) \end{bmatrix} u
\end{aligned}
\tag{2.59}
$$

where $u = [I_1 \quad I_2 \quad I_3 \quad I_4]^T$.

Define

$$x = [\theta \quad \phi \quad \dot{\theta} \quad \dot{\phi}]^T$$

the reduced-order model can be written as:

$$\dot{x}(t) = F(x(t)) + B(x(t))u \tag{2.60}$$

where

$$F(x(t)) = \begin{bmatrix} x_3(t) \\ x_4(t) \\ f_3(x(t)) \\ f_4(x(t)) \end{bmatrix} \qquad \text{a 4-vector} \tag{2.61}$$

$$B(x(t)) = \begin{bmatrix} 0 \\ \hdashline 0 \\ \hdashline b_3(x_1(t), x_2(t)) \\ \hdashline b_4(x_1(t), x_2(t)) \end{bmatrix} \qquad \text{a } 4 \times 4 \text{ matrix} \tag{2.62}$$

Note: It can be easily shown from equation (2.58) and several simple substitutions that the determinant of N is always greater than zero for all θ, ϕ between (but not including) $-\pi/2$ and $+\pi/2$. Hence N^{-1} always exists.

2.4 Comparing the Responses of the Full and Reduced-order Models

To investigate the effect of representing a sixth-order system by a fourth-order model, a step of magnitude four is applied to both I_2 and I_4 of the full (sixth) and reduced (fourth) order models developed in sections 2.2 and 2.3 respectively.

The responses of the two models are shown in figure 2-9 and tabulated in Table 2-1. (The values of the parameters used is given in Appendix G).

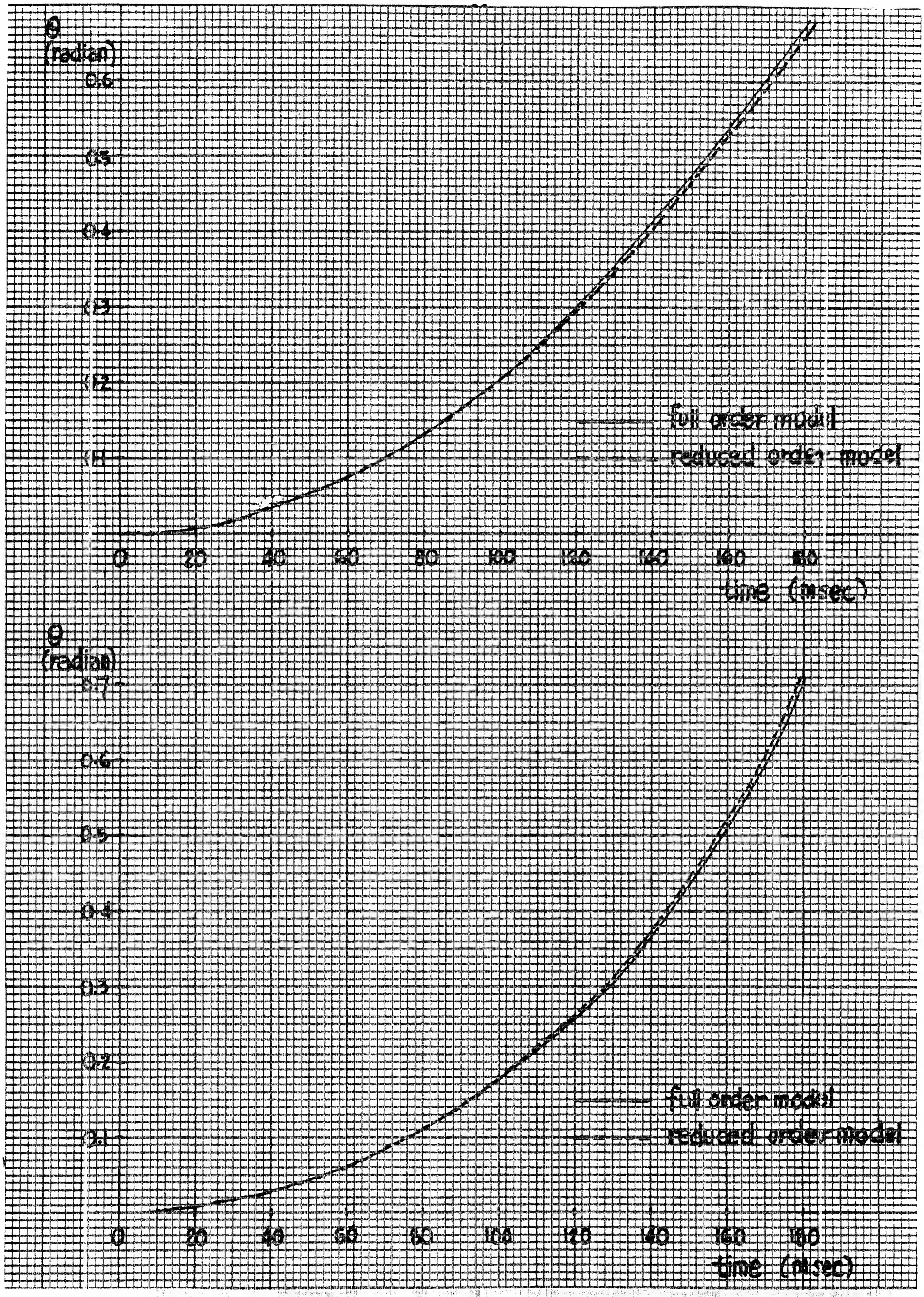

Figure 2-9. Response of the full and reduced-order model due to a step input on I_2 and I_4.

It can be seen that the difference between the two is small except for the fact that the reduced order system cannot model the angle ψ.

Table 2-1 (a) Response of the Full Order Model due to step inputs on I_2 and I_4.

Time (msec)	θ (radian)	ϕ (radian)	ψ (radian)	$\dot{\theta}$ (rad/sec)	$\dot{\phi}$ (rad/sec)	$\dot{\psi}$ (rad/sec)
0	0.0000	0.0000	0.0000	0.0000	0.0000	0.0000
10	0.0020	0.0017	-0.0004	0.4075	0.3306	-0.0877
20	0.0081	0.0066	-0.0018	0.8146	0.6619	-0.1809
30	0.0183	0.0149	-0.0041	1.2226	0.9954	-0.2856
40	0.0326	0.0265	-0.0075	1.6328	1.3329	-0.4080
50	0.0510	0.0416	-0.0123	2.0461	1.6768	-0.5543
60	0.0735	0.0601	-0.0187	2.4637	2.0301	-0.7316
70	0.1003	0.0822	-0.0271	2.8862	2.3970	-0.9469
80	0.1313	0.1081	-0.0378	3.3141	2.7828	-1.2073
90	0.1666	0.1380	-0.0514	3.7474	3.1949	-1.5214
100	0.2063	0.1721	-0.0684	4.1857	3.6431	-1.8953
110	0.2503	0.2110	-0.0895	4.6275	4.1401	-2.3384
120	0.2988	0.2551	-0.1154	5.0703	4.7040	-2.8546
130	0.3517	0.3054	-0.1469	5.5100	5.3593	-3.4496
140	0.4090	0.3628	-0.1847	5.9395	6.1405	-4.1151
150	0.4704	0.4288	-0.2294	6.3475	7.0964	-4.8444
160	0.5358	0.5055	-0.2816	6.7152	8.2984	-5.5854
170	0.6045	0.5959	-0.3409	7.0113	9.8479	-6.2504
180	0.6756	0.7041	-0.4057	7.1829	11.8885	-6.6337

Table 2-1 (b) Response of the Reduced Order Model due to Step Inputs on I_2 and I_4

Time (msec)	θ (radian)	ϕ (radian)	$\dot{\theta}$ (rad/sec)	$\dot{\phi}$ (rad/sec)
0	0.0000	0.0000	0.0000	0.0000
10	0.0020	0.0017	0.4070	0.3393
20	0.0081	0.0068	0.8134	0.6791
30	0.0183	0.0153	1.2203	1.0208
40	0.0325	0.0272	1.6288	1.3659
50	0.0509	0.0426	2.0398	1.7168
60	0.0734	0.0616	2.4540	2.0764
70	0.1000	0.0842	2.8719	2.4486
80	0.1308	0.1106	3.2936	2.8388
90	0.1659	0.1411	3.7188	3.2542
100	0.2052	0.1758	4.1466	3.7042
110	0.2488	0.2153	4.5751	4.2013
120	0.2967	0.2601	5.0014	4.7627
130	0.3488	0.3108	5.4209	5.4112
140	0.4051	0.3687	5.8265	6.1784
150	0.4653	0.4349	6.2072	7.1082
160	0.5291	0.5116	6.5462	8.2616
170	0.5960	0.6012	6.8173	9.7243
180	0.6650	0.7075	6.9785	11.6129

Chapter 3. The Time-Optimal Control Problem

As mentioned in Chapter 1, we would like to devise a control scheme to bring the arm from its initial position to any specified final position as fast as possible, *i.e.*, given any desired position x_f, we would like to find the control $u(t)$ which drives $x(t) - x_f$ to zero in minimum time, where $x(t)$ is the actual position of the arm at time t.

In this Chapter, we will first formally state the time-optimal control problem as applicable in our case, and Pontryagin's Minimum Principle will then be used to derive necessary conditions for the time-optimal solution. We will then examine the time-optimal control of the tendon arm system using the reduced-order model.

3.1 Problem Statement

Given the dynamical system with state $x(t)$ and control $u(t)$,

$$\dot{x}(t) = F(x(t)) + B(x(t))u(t) \tag{3.1}$$

where

$x(t)$	is a 4-dimensional vector
$u(t)$	is a 4-dimensional vector
$F(x(t))$	is a 4-vector-valued function
$B(x(t))$	is a (4×4)-matrix-valued function

Find an admissible control $u(t)$ which takes the system from the initial state x_0 to the final state x_f in minimum time, *i.e.* find $u(\cdot)$ to minimize the following cost function:

$$J(u(\cdot)) = \int_{t_0}^{t_f} dt \tag{3.2}$$

where an admissible control $u(\cdot)$ is defined to be one such that every component satisfies the following

magnitude constraint,

$$u_{min} \leq u_i(t) \leq u_{max} \qquad i = 1, \ldots, 4 \tag{3.3}$$

or written more compactly

$$u(t) \in \Omega \qquad \text{for all } t \in [t_0, t_f] \tag{3.4}$$

t_f in equation (3.2) is free, and is part of the optimal solution.

In addition, $F(x(t))$ and $B(x(t))$ are assumed to posssess the follosing properties:

1. $f_i(x)$ and $b_{ij}(x)$ are continuous in x, and
2. $\partial f_i(x)/\partial x_i, \partial b_{ij}(x)/\partial x_k$ are continuous in x,

where $f_i(x), b_{ij}(x), x_k$ are components of $F(x), B(x)$, and x respectively.

3.2 Application of the Minimum Principle

Pontryagin's Minimum Principle (Athans & Falb[3]) furnishes us with necessary conditions which the time-optimal control $u^*(t)$ must satisfy. Any control $u_e(t)$ that satisfies all the necessary conditions is known as an extremal condition, and is a candidate for the optimal control. If a time-optimal control exists, and if there are more than one extremal control, then the one with the smallest cost given by equation (3.2) is optimal.

In order to apply the Minimum Principle, we will define the Hamiltonian:

$$H(x(t), p(t), u(t)) = 1 + p^T(t)[F(x(t)) + B(x(t))u(t)] \tag{3.5}$$

where $p(t)$ is a 4-dimensional costate vector.

Let $u^*(t)$ be an admissible control which transfers the system from x_0 to x_f, and let $x^*(t)$ be the corresponding trajectory. In order for $u^*(t)$ to be optimal, it is necessary that there exist a function $p^*(t)$ such that:

(a) $p^*(t)$ and $x^*(t)$ are a solution of the canonical system:

$$\dot{x}^*(t) = \frac{\partial H}{\partial p}\big(x^*(t), p^*(t), u^*(t)\big) \tag{3.6}$$

$$\dot{p}^*(t) = -\frac{\partial H}{\partial x}\big(x^*(t), p^*(t), u^*(t)\big) \tag{3.7}$$

satisfying the boundary conditions

$$\begin{aligned} x^*(t_0) &= x_0 \\ x^*(t_f) &= x_f \end{aligned} \tag{3.8}$$

(b) For all $t \in [t_0, t_f]$,

$$H\big(x^*(t), p^*(t), u^*(t)\big) \leq H\big(x^*(t), p^*(t), u\big) \qquad \text{for all } u \in \Omega \tag{3.9}$$

(c) For all $t \in [t_0, t_f]$,

$$H\big(x^*(t), p^*(t), u^*(t)\big) = 0 \tag{3.10}$$

This is a consequence of free terminal time and time invariance of the system.

Athans & Falb[3] presents a heuristic proof of the Minimum Principle, whereas a formal proof can be found in Pontryagin *et al*[4].

3.3 Bang-Bang Control

Substituting equation (3.5) into (3.9), necessary condition (b) reduces to

$$p^{*T}(t)B\big(x^*(t)\big)u^*(t) \leq p^{*T}(t)B\big(x^*(t)\big)u \qquad \text{for all } u \in \Omega \tag{3.11}$$

or written in component form,

$$\sum_{j=1}^{4} u_j^*(t)\Big(\sum_{i=1}^{4} b_{ij}\big(x^*(t)\big)p_i^*(t)\Big) \leq \sum_{j=1}^{4} u_j\Big(\sum_{i=1}^{4} b_{ij}\big(x^*(t)\big)p_i^*(t)\Big) \tag{3.12}$$

for all u_j satisfying equation (3.3).

If we define

$$q_j^*(t) = \sum_{i=1}^{4} b_{ij}(x^*(t))p_i^*(t) \qquad j = 1, \ldots, 4 \tag{3.13}$$

Equation (3.12) then becomes

$$\sum_{j=1}^{4} u_j^*(t)q_j^*(t) \leq \sum_{j=1}^{4} u_j q_j^*(t) \tag{3.14}$$

The control $u^*(t)$ which satisfies the above inequality and subject to the constraint of equation (3.3) is given by

$$\begin{aligned} u_j^*(t) &= u_{max} && \text{if } q_j^*(t) < 0 \\ u_j^*(t) &= u_{min} && \text{if } q_j^*(t) > 0 \qquad j = 1, \ldots, 4 \\ u_j^*(t) &\quad \text{indeterminate} && \text{if } q_j^*(t) = 0 \end{aligned} \tag{3.15}$$

We see that $u^*(t)$ is well-defined by equation (3.15) if there is only a countable set of times $t_{ij} \in [t_0, t_f]$ such that

$$q_j^*(t_{ij}) = 0$$

Under this condition, every component $u_j^*(t)$ of the optimal control $u^*(t)$ is a piecewise constant function of time, $u^*(t)$ is then known as a bang-bang control, and we say that the problem is Normal.

If, on the other hand, there is one (or more) subinterval $[t_m, t_n]$ within $[t_0, t_f]$ such that

$$q_j^*(t) = 0 \qquad \text{for some } j \text{ and all } t \in [t_m, t_n]$$

then $u_j^*(t)$ is not defined by equation (3.15) for $t \in [t_m, t_n]$, and we say that we have a singular time-optimal problem; the time interval $[t_m, t_n]$is called the singularity interval.

Hence we see that if the problem is normal, the time-optimal control is bang-bang. For linear time-invariant system, we can derive necessary and sufficient conditions for the time-optimal problem to

be normal (see *e.g.* Athans & Falb[3]) or singular, but for general nonlinear systems, there is no such conditions, hence it is very difficult to rule out the existence of singularity intervals before solving the problem.

3.4 Time-Optimal Control of the Tendon Arm System

For the tendon arm system, the equations corresponding to equation (3.1) are given by equations (2.60)–(2.62) which describes the reduced-order model.

Since the tendons can only pull but not push on the arm, there is a non-negativity constraint on the control, and equation (3.3) will now be replaced by

$$0 \leq u_i(t) \leq u_{max} \qquad i = 1, \ldots, 4 \tag{3.16}$$

The expression for $B(x(t))$ can be obtained from equations (2.62) and (2.59):

If we represent N^{-1} in equation (2.59) by

$$N^{-1} = \begin{bmatrix} h_{11} & h_{12} \\ h_{21} & h_{22} \end{bmatrix} \tag{3.17}$$

Then

$$\begin{aligned} \begin{bmatrix} b_3(x(t)) \\ \hdashline b_4(x(t)) \end{bmatrix} &= \begin{bmatrix} b_{31} & b_{32} & b_{33} & b_{34} \\ b_{41} & b_{42} & b_{42} & b_{44} \end{bmatrix} \\ &= \begin{bmatrix} h_{11} & h_{12} \\ h_{21} & h_{22} \end{bmatrix} \begin{bmatrix} -Kr/l_1 & Kr/l_2 & eKr/l_3 & -eKr/l_4 \\ 0 & 0 & -Kr/l_3 & Kr/l_4 \end{bmatrix} \\ &= Kr \begin{bmatrix} -h_{11}/l_1 & h_{11}/l_2 & -(h_{12} - eh_{11})/l_3 & (h_{12} - eh_{11})/l_4 \\ -h_{21}/l_1 & h_{21}/l_2 & -(h_{22} - eh_{21})/l_3 & (h_{22} - eh_{21})/l_4 \end{bmatrix} \end{aligned} \tag{3.18}$$

and from equation (2.62),

$$b_{ij} = 0 \qquad \text{for } i = 1, 2, \quad j = 1, \ldots, 4 \tag{3.19}$$

Substituting equations (3.18) and (3.19) into (3.13), we obtain the following expressions for $q_j^*(t)$:

$$\begin{aligned}
q_1^*(t) &= -Kr\frac{h_{11}p_3^*(t) + h_{21}p_4^*(t)}{l_1} \\
q_2^*(t) &= Kr\frac{h_{11}p_3^*(t) + h_{21}p_4^*(t)}{l_2} \\
q_3^*(t) &= -Kr\frac{(h_{12} - eh_{11})p_3^*(t) + (h_{22} - eh_{21})p_4^*(t)}{l_3} \\
q_4^*(t) &= Kr\frac{(h_{12} - eh_{11})p_3^*(t) + (h_{22} - eh_{21})p_4^*(t)}{l_4}
\end{aligned} \tag{3.20}$$

The $q_j^*(t)$'s will be used in equation (3.15) to determine the value of $u^*(t)$. Since the sign and not the magnitude of $q_j^*(t)$ is important, and since $K, r, l_i, i = 1, \ldots, 4$ are all positive, we will define a new set of $\bar{q}_j^*(t)$ that can also be used in equation (3.15):

$$\begin{aligned}
\bar{q}_1^*(t) &= -(h_{11}p_3^*(t) + h_{21}p_4^*(t)) \\
\bar{q}_2^*(t) &= h_{11}p_3^*(t) + h_{21}p_4^*(t) \\
\bar{q}_3^*(t) &= -((h_{12} - eh_{11})p_3^*(t) + (h_{22} - eh_{21})p_4^*(t)) \\
\bar{q}_4^*(t) &= (h_{12} - eh_{11})p_3^*(t) + (h_{22} - eh_{21})p_4^*(t)
\end{aligned} \tag{3.21}$$

and the optimal control $u^*(t)$ is given by

$$\begin{aligned}
u_j^*(t) &= u_{max} && \text{if } \bar{q}_j^*(t) < 0 \\
u_j^*(t) &= 0 && \text{if } \bar{q}_j^*(t) > 0 \qquad j = 1, \ldots, 4 \\
u_j^*(t) &\quad \text{indeterminate} && \text{if } \bar{q}_j^*(t) = 0
\end{aligned} \tag{3.22}$$

where $\bar{q}_j^*(t)$ is given by equation (3.21).

Note that in equations (3.21),

$$\begin{aligned}
\bar{q}_1^*(t) &= -\bar{q}_2^*(t) \\
\bar{q}_3^*(t) &= -\bar{q}_4^*(t)
\end{aligned}$$

If we define new variables $q_{12}^*(t)$, $q_{34}^*(t)$ given by

$$\begin{aligned}
q_{12}^*(t) &= \bar{q}_1^*(t) = -(h_{11}p_3^*(t) + h_{21}p_4^*(t)) \\
q_{34}^*(t) &= \bar{q}_3^*(t) = -((h_{12} - eh_{11})p_3^*(t) + (h_{22} - eh_{21})p_4^*(t))
\end{aligned} \tag{3.23}$$

Then equations (3.22) can be rewritten as

$$\begin{aligned} &\text{if } q_{12}^*(t) < 0, && u_1^*(t) = u_{max}, && u_2^*(t) = 0 \\ &\text{if } q_{12}^*(t) > 0, && u_1^*(t) = 0, && u_2^*(t) = u_{max} \\ &\text{if } q_{12}^*(t) = 0, && u_1^*(t),\ u_2^*(t) && \text{indeterminate} \end{aligned} \tag{3.24}$$

and

$$\begin{aligned} &\text{if } q_{34}^*(t) < 0, && u_3^*(t) = u_{max}, && u_4^*(t) = 0 \\ &\text{if } q_{34}^*(t) > 0, && u_3^*(t) = 0, && u_4^*(t) = u_{max} \\ &\text{if } q_{34}^*(t) = 0, && u_3^*(t),\ u_4^*(t) && \text{indeterminate} \end{aligned} \tag{3.25}$$

From equations (3.24) and (3.25), we see that there is a certain relation between $u_1^*(t)$ and $u_2^*(t)$, between $u_3^*(t)$ and $u_4^*(t)$, except in the case when $q_{12}^*(t) = 0$ or $q_{34}^*(t) = 0$. The four control components seem to work in pairs, $u_1^*(t)$ and $u_2^*(t)$ forming one pair, $u_3^*(t)$ and $u_4^*(t)$ forming the other. This agrees with the physical situation, in which tendons 1 and 2 form one pair, and tendons 3 and 4 form the other.

Necessary conditions (a) and (c) apply directly to the tendon arm system with the appropriate definition of the Hamiltonian function.

Chapter 4. Iterative Solution of the Time-Optimal Control Problem

4.1 Introduction

In Chapter 3, we have seen that the Minimum Principle provides us with necessary conditions that the optimal solution must satisfy. In particular, manipulation of necessary condition (b) yields equations (3.24) and (3.25) which express $u^*(t)$ in terms of $x^*(t)$ and $p^*(t)$. If the problem is non-singular, $u^*(t)$ is well-defined and theoretically we can solve the time-optimal control problem by eliminating $u^*(t)$ from the canonical system given by equations (3.6)–(3.8), and solving the resulting two-point boundary value problem to obtain $x^*(t)$ and $p^*(t)$, and hence $u^*(t)$. But two-point boundary value problems are very difficult to solve analytically except for some simple cases. Hence for higher order linear and nonlinear systems, we must in general resort to iterative methods to obtain solutions.

A solution obtained by any iterative method is characterized by:

1. it is only applicable to a specified initial and final position pair. To obtain solutions for other pairs, we have to repeat the entire iterative solution procedure, and
2. it is expressed as a function of time.

The first statement means that we have to precompute and store the control trajectories of every relevant initial-final position pair, the second means that the control is open-loop and hence cannot correct for any departure from the intended trajectory due to, say, external disturbances. These are disadvantages, but since the complexity of our system precludes any other solution approach, we have to employ the iterative approach and take into account the aforementioned disadvantages in the design of the overall control scheme which will be discussed in later Chapters.

Plant[5] and Mufti[6] provide a surveys of various computational methods in optimal control problems and each contains a long list of supporting references. The criteria for choosing an iterative method for our problem are that,

1. it is easy to code, and
2. it can handle singular problems.

The second point is essential because as mentioned in Chapter 3, the possibility of the presence of singularity cannot be ruled out, and in fact, from some preliminary runs using the steepest descent method, one pair of controls does not approach bang-bang, indicating that the problem might be singular.

There are some computational methods developed expressly for singular problems (see *e.g.* [7]-[10]). But the Conjugate Gradient method is chosen because

1. it is basically a first order method, hence its implementation is simple, and
2. it converges quadratically near the optimum solution, and
3. it can handle singular problems.

4.2 The Conjugate Gradient Method

The first order gradient method is easy to implement but suffers from slow convergence near the optimal solution. In 1967, the Conjugate Gradient Method was applied to optimal control problems [11], [12]. The convergence rate of this method is superior to the gradient method with very little additional computation per iteration. Pagurek & Woodside[13] and later Quintana & Davison[14] extended the method to problems having bounded control constraints.

We will first describe the Conjugate Gradient method as applied to a free end point, fixed terminal time, optimal control problem, and in the next section, we will show how it is adapted to solve our time-optimal control problem.

Problem Statement

Given the system

$$\dot{x}(t) = F(x(t)) + B(x(t))u(t), \qquad x(t_0) = x_0 \tag{4.1}$$

Find $u(t)$ over the interval $[t_0, t_f]$ to minimize the cost function given by

$$J(u(t)) = K(x_f(t)) + \int_{t_0}^{t_f} L(x(t), u(t))\, dt \tag{4.2}$$

where t_f is fixed, and $u(t)$ is assumed to be unconstrained.

Define the Hamiltonian

$$H(x(t), p(t), u(t)) = L(x(t), u(t)) + p^T(t)[F(x(t)) + B(x(t))u(t)] \tag{4.3}$$

Then the necessary conditions as given by the Minimum Principle are the same as equations (3.6)–(3.10) except for the boundary conditions (3.8) which are replaced by:

$$\begin{aligned} x^*(t_0) &= x_0 \\ p^*(t_f) &= \frac{\partial K}{\partial x}(x^*(t_f)) \end{aligned} \tag{4.4}$$

Solution Procedure

Define

$$H_u(x(t), p(t)) = \frac{\partial H}{\partial u}(x(t), p(t), u(t)) = B^T(x(t))p(t) \tag{4.5}$$

Let superscript i represent the iteration number, and assume that we start with an initial estimate of the optimal control trajectory $u^1(t)$.

At the ith iteration,

1. Using $u^i(t)$, integrate the state equation forward from time t_0 to t_f, with $x(t_0) = x_0$, to obtain $x^i(t)$.

   Then, substituting $x^i(t)$ and $u^i(t)$ into the costate equation, integrate it backward from t_f to t_0 with

$$p^i(t_f) = \frac{\partial K}{\partial x}(x^i(t_f))$$

   to obtain $p^i(t)$.

Compute

$$g^i(t) = H_u(p^i(t), x^i(t)) \tag{4.6}$$

2. Determine conjugate-gradient direction using:

$$s^i(t) = g^i(t) + \beta^{i-1} s^{i-1}(t) \tag{4.7}$$

where

$$\begin{aligned} \beta^{i-1} &= \frac{\int_{t_0}^{t_f} g^{i^T}(t) g^i(t) dt}{\int_{t_0}^{t_f} g^{i-1^T}(t) g^{i-1}(t) dt} \qquad \text{if } i > 1 \\ \beta^{i-1} &= 0 \qquad \text{if } i = 1 \end{aligned} \tag{4.8}$$

3. Compute next control by,

$$u^{i+1}(t) = u^i - \alpha^i s^i(t) \tag{4.9}$$

where α^i is chosen using a one-dimensional search to minimize $J\left(u^{i+1}(t)\right)$.

4. Repeat the whole procedure with $i = i + 1$ until $J(\cdot)$ does not improve significantly.

Control Constraints

To take into account constraints on the magnitude of the control as given in equation (3.16), the above procedure is modified as follows (due to Pagurek & Woodside[13]):

1. Assume that W_j^i is the saturation region of $u_j^i(t)$; define the scale function

$$\begin{aligned} w_j^i(t) &= 0 \qquad \text{for } t \in W_j^i, \text{ and} \\ &= 1 \qquad \text{elsewhere} \end{aligned} \tag{4.10}$$

Note: subscript j refers to individual components of the corresponding vector.

2. When computing β^{i-1}, $w^{i^T}(t) g^i(t)$ is used in place of $g^i(t)$.

3. After computing u^{i+1} according to equation (4.9), $u^{i+1}(t)$ is truncated at the upper and lower bounds before it is used in the computation of $J(u^{i+1}(t))$.

4.3 Algorithm for the Time-Optimal Problem

In order to apply the conjugate gradient method as presented in the last section, the time-optimal problem as stated in section 3.1 is modified as follows:

1. A sequence of fixed terminal time, free end point problems are solved instead of the original free terminal time problem.
2. The fixed end point constraint is handled by means of a quadratic penalty function, that is, we solve the following problem:

   Given the dynamical equation described by equation (3.1), find a control $u(t) \in \Omega$ so as to minimize the following cost function:

$$J = \frac{1}{2}(x(t_f) - x_f)^T Q(x(t_f) - x_f) \tag{4.11}$$

   subject to $x(t_0) = x_0$, with t_0, t_f and x_f given.

If t_f is too small, *i.e.*, $t_f < T_{min}$, where T_{min} is the minimum time solution, the system cannot reach x_f with the control in Ω, hence J will not be close to zero. As t_f increases and approaches T_{min}, however, the optimum J value will decrease, and the smallest t_f such that J is zero (within a certain tolerance) is the solution to the original time-optimal problem.

Choice of t_f

We can always start with a very small t_f and gradually increase the value of t_f, but this will take too long as each round (*i.e.* solving the modified problem with a given t_f) by itself takes a long time (when run on a PDP 11/34 mini-computer). Hence we will make use of the special structure of the optimal control to provide an estimate of T_{min}.

It was found from some preliminary runs that in an optimal solution, one pair of controls, either u_1 and u_2 or u_3 and u_4, always approaches bang-bang with only one switching, and the form of the other pair will depend on the relative magnitudes of θ_f and ϕ_f, which define the final position of the

arm (henceforth we will assume that $x_0 = 0$, *i.e.*, we are interested in moving the arm from an upright position to any specified final position). Although the two pairs of controls are coupled through the system equation, the coupling is not very strong, and one can clearly identify the pair u_1 and u_2 as affecting the angle θ much more strongly than u_3 and u_4, and similarly, the pair u_3, u_4 affects ϕ much more strongly. Hence the time taken for the arm to move from $\theta = 0$ to $\theta = \theta_f$ is determined mainly by u_1 and u_2, and is only slightly affected by u_3 and u_4, the same applies to ϕ with u_3, u_4 exchanging roles with u_1, u_2.

Hence to find the time taken for the arm to move from $\theta = \phi = 0$ to $\theta = \theta_f, \phi = 0$, we will keep u_3 and u_4 to be zero (thereby ensuring ϕ to stay 0 throughout) and find a bang-bang control that will take θ to θ_f, this is a much easier problem to solve because we need only to search over the switching time, which is only one-dimensional and can be easily done manually. Similarly we can find the time taken to move from $\theta = \phi = 0$ to $\theta = 0, \phi = \phi_f$. The larger of the two values found above will be taken as an estimate of T_{min}. This value was found, in general, to be greater than T_{min} by about one to three time steps (each time step is 5 msec). Hence the initial choice of t_f is taken to be three time steps smaller than the estimated T_{min}, and we need to solve at most three rounds of the modified problem to obtain our solution.

Choice of Q

Q is chosen to be diagonal and serves to weight the different components of x individually. We chose the q_{ii} that corresponds to the angle that is mainly affected by the bang-bang pair of controls to be twice the value of the rest. This is because as the iterations proceed, it becomes more and more difficult to reduce that error term, as we are trying to reduce the transition time of the bang-bang control, making q_{ii} larger helps.

Choice of Initial Guess of $u(t)$ in the Conjugate Gradient Method

The initial guess is chosen to be

$$u_i(t) \approx 0 \qquad \text{for } i = 1, \ldots, 4 \text{ and for all } t \in [t_0, t_f] \tag{4.12}$$

and we started with several iterations of steepest descent before switching over to the conjugate gradient method.

Method of finding α^i

As mentioned in the procedure for the conjugate gradient method, α^i is chosen using a one-dimensional search technique. The method we used is to fit a parabola to three points of α's, chosen so that the minimum of the parabola falls within the two extreme values of the α's, α^i is chosen to be the value of α that minimizes the parabola.

4.4 Approximation of the Optimal Solution

The results obtained using the conjugate gradient method for a particular final position is given in figure 4-1. From this figure, we can see that the pair u_3 and u_4 approaches bang-bang with one switching, but not the pair u_1 and u_2.

The optimal solution can be approximated by straight line segments as shown in figure 4-2, the stae trajectories for the optimal and the approximated control are shown in figure 4-3, and we see that the response due to the approximated control compares favorably with the optimal solution. Any deviations from the desired state at the terminal time will be handled by another closed-loop control law which will be switched in after the open-loop control is terminated.

The general form of the optimal control and its approximation will be elaborated in Chapter 6.

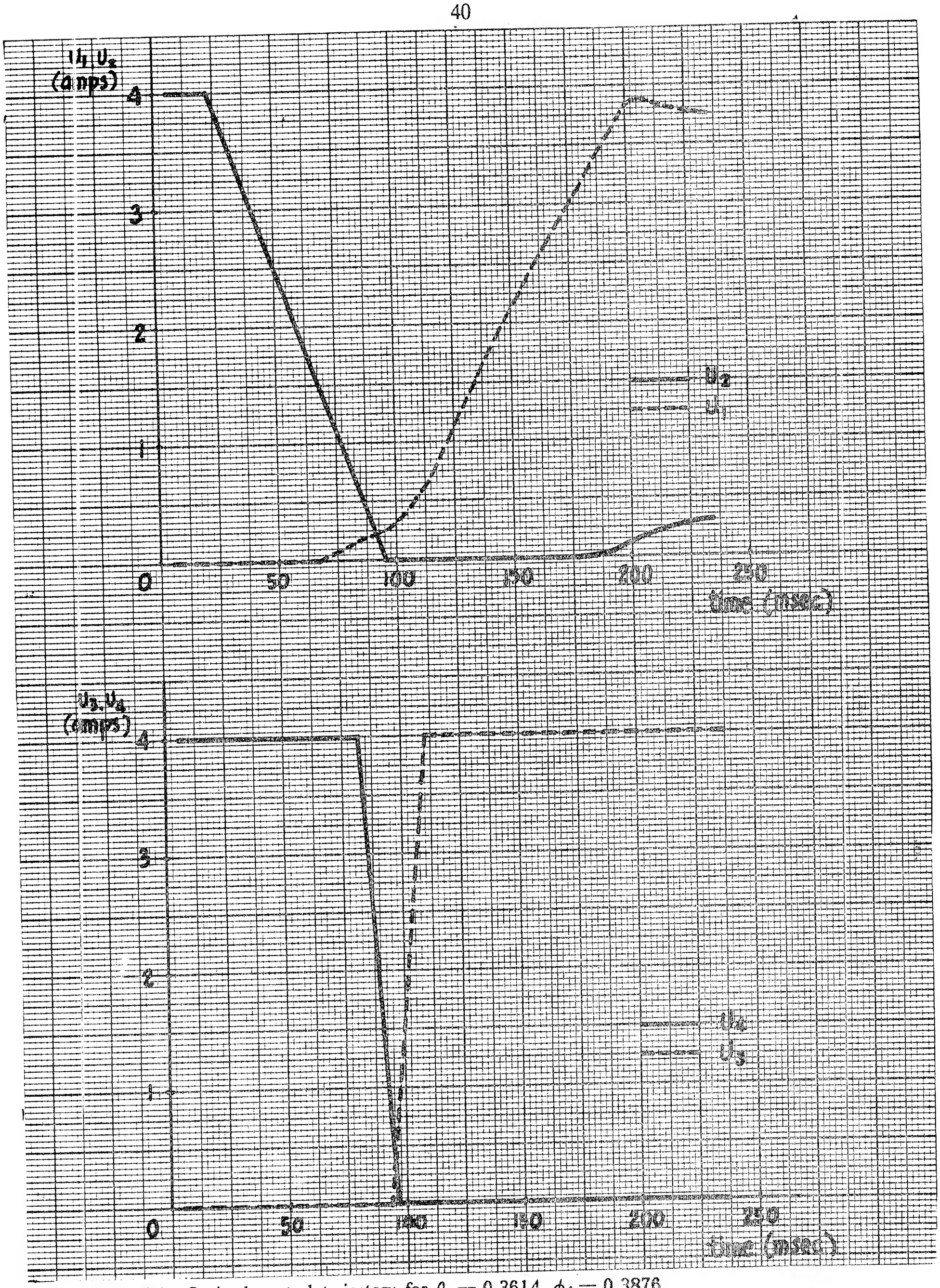

Figure 4-1. Optimal control trajectory for $\theta_f = 0.3614$, $\phi_f = 0.3876$.

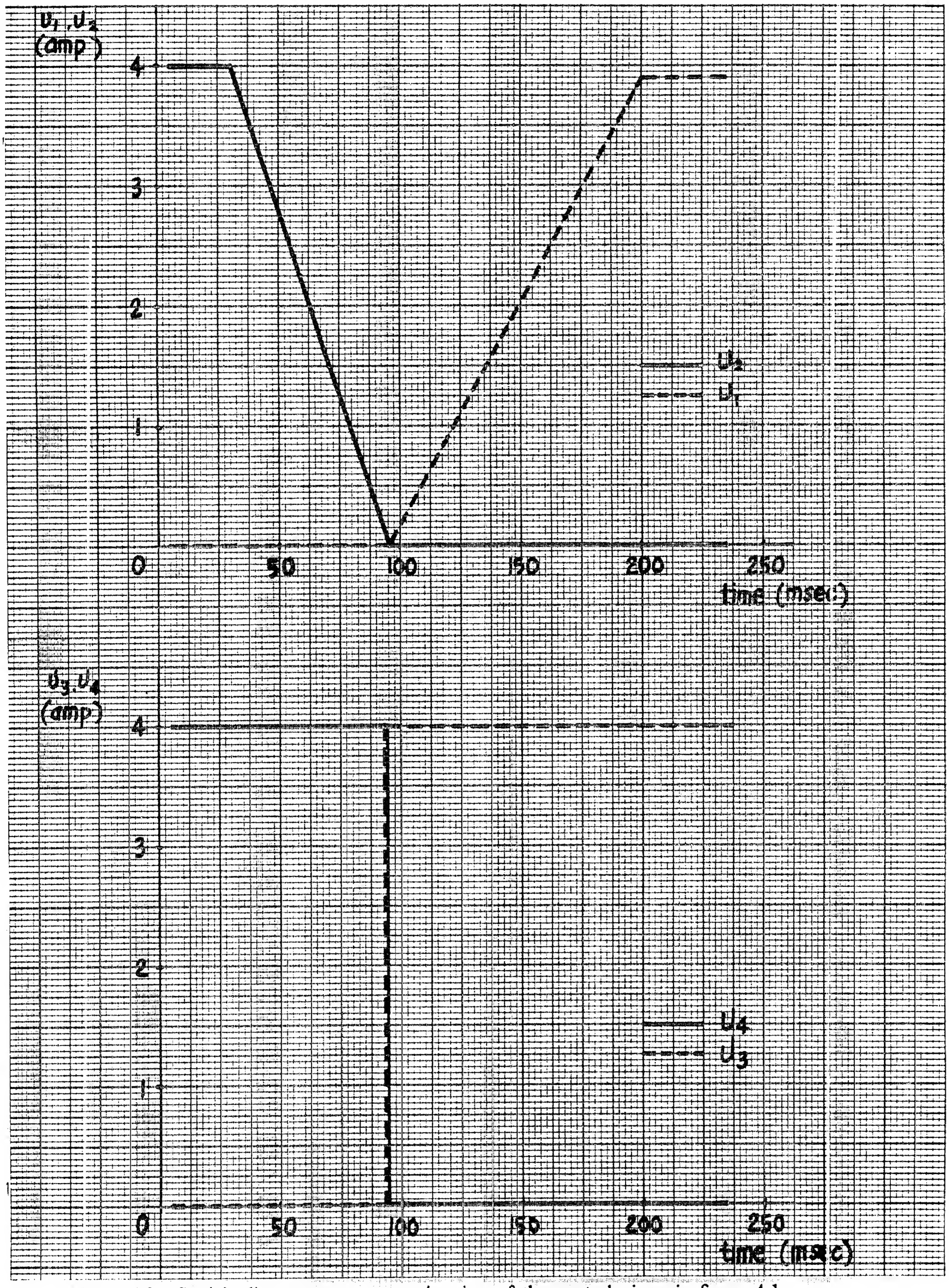

Figure 4-2. Straight line segments approximation of the control given in figure 4-1.

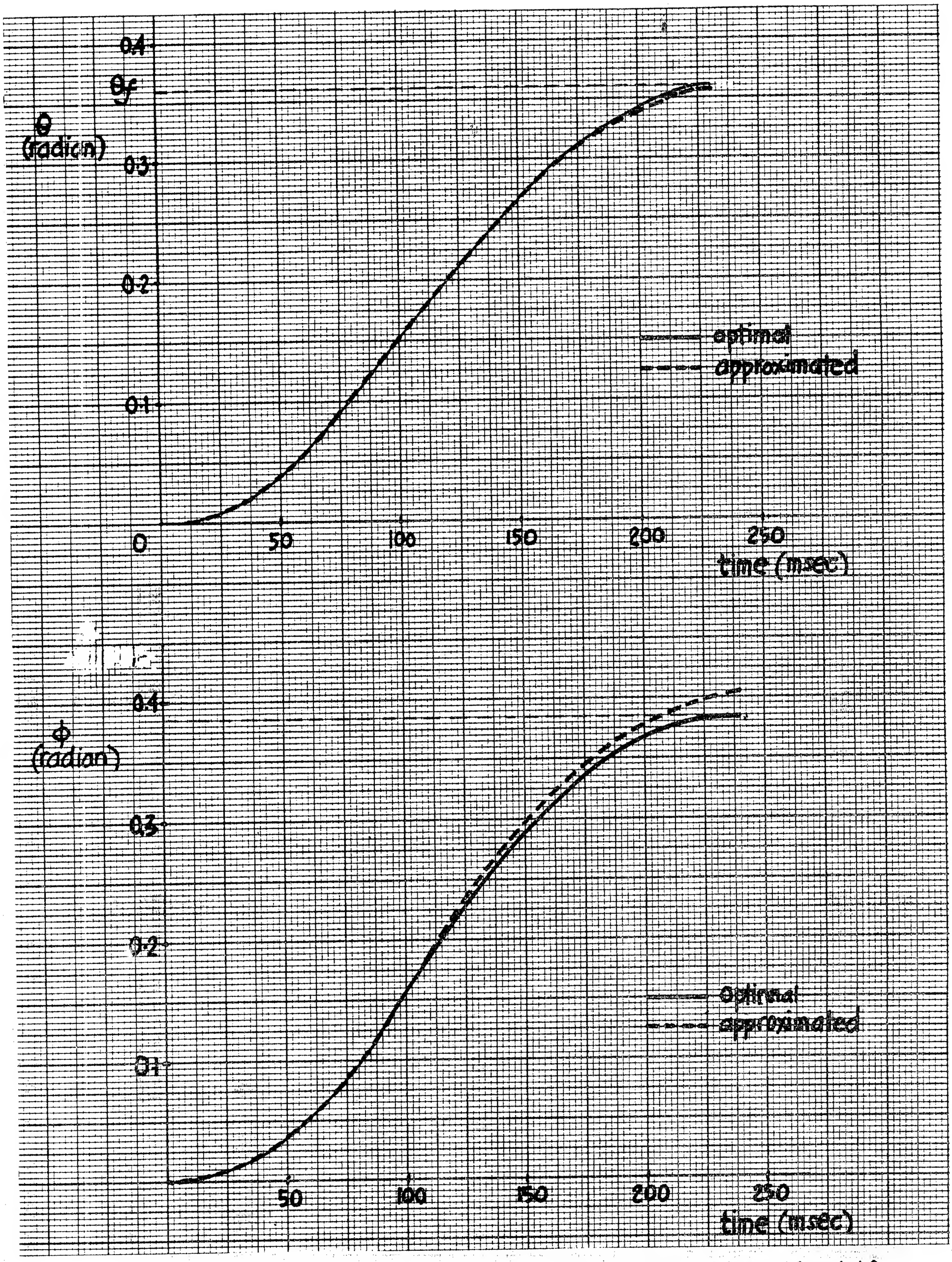

Figure 4-3. State trajectories for the optimal and approximated control of figure 4-1 and 4-2.

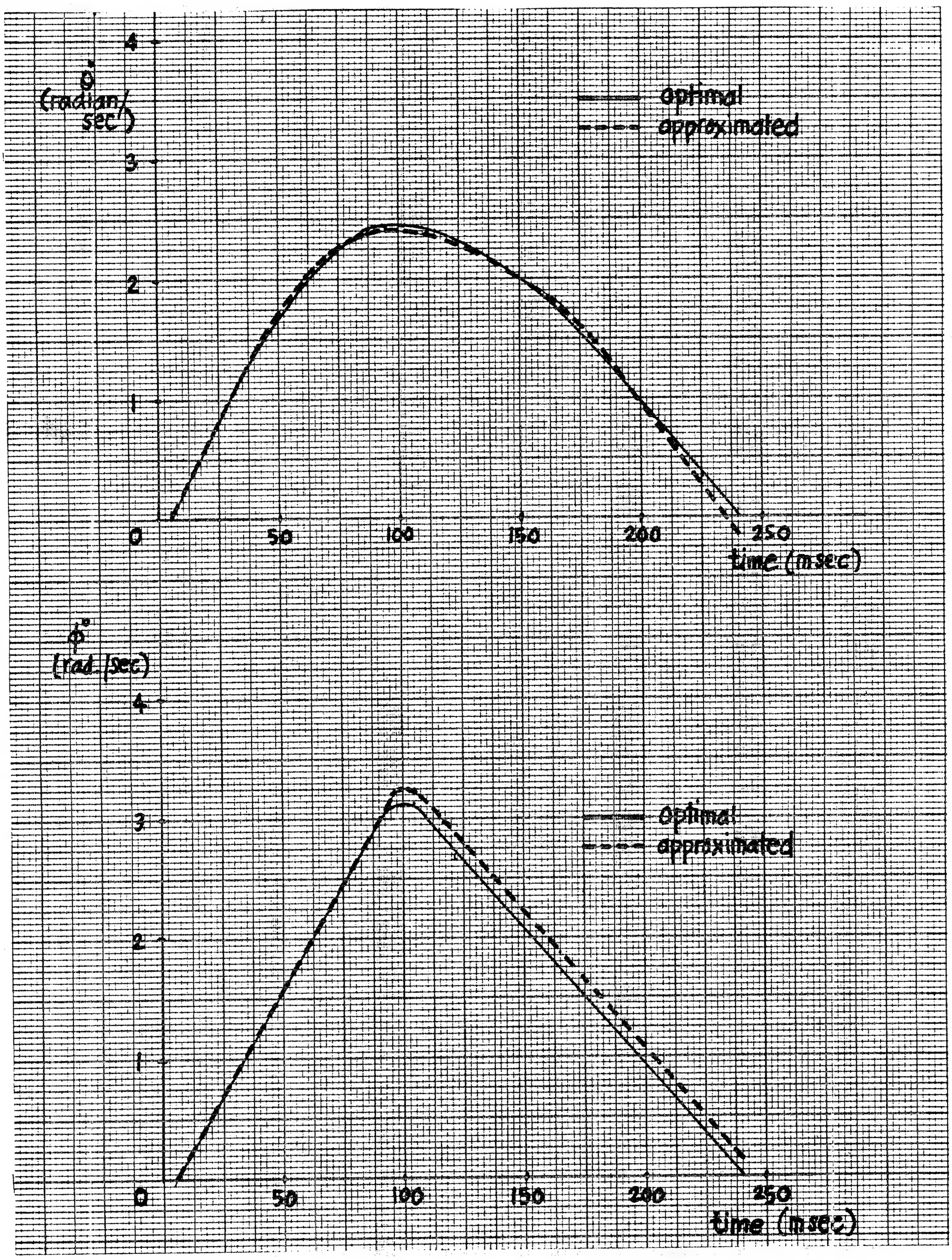

Figure 4-3. (continued)

Chapter 5. Regulation at the Final Position

5.1 Introduction

Since the arm is attached to the base plate by a three degree-of-freedom "joint", positive steady-state tensions in the tendons are required to maintain the arm at any specified final position. The required control currents can be calculated by setting

$$\dot{x}_f = f(x_f, u_f) = 0 \tag{5.1}$$

where x_f is the specified final state of the system.

A u_f that satisfies the above equation will be called a steady-state control for the set-point x_f.

If the arm is initially at the required final state x_f, then u_f will keep the arm at x_f as long as there is no external disturbance. However, any slight disturbance will cause the arm to move away from this equilibrium position because the equilibrium achieved by applying constant open-loop controls u_f is an unstable one.

Moreover, the transient phase open-loop control that brings the system from initial to final state is based on a reduced-order model of the system, and also in order to implement it, it is necessary to approximate the form of control by straight line segments. The open-loop control can only be stored at a few points and the control law at other points is derived by interpolation. Hence at the end of the transient phase during which open-loop control is applied, the final state reached by the system is not x_f, but rather somewhere in the vicinity of it.

In view of the above, closed-loop feedback control is required to

1. bring the system to the desired final state x_f,
2. maintain the system at x_f for any amount of time.

5.2 Linearized Model

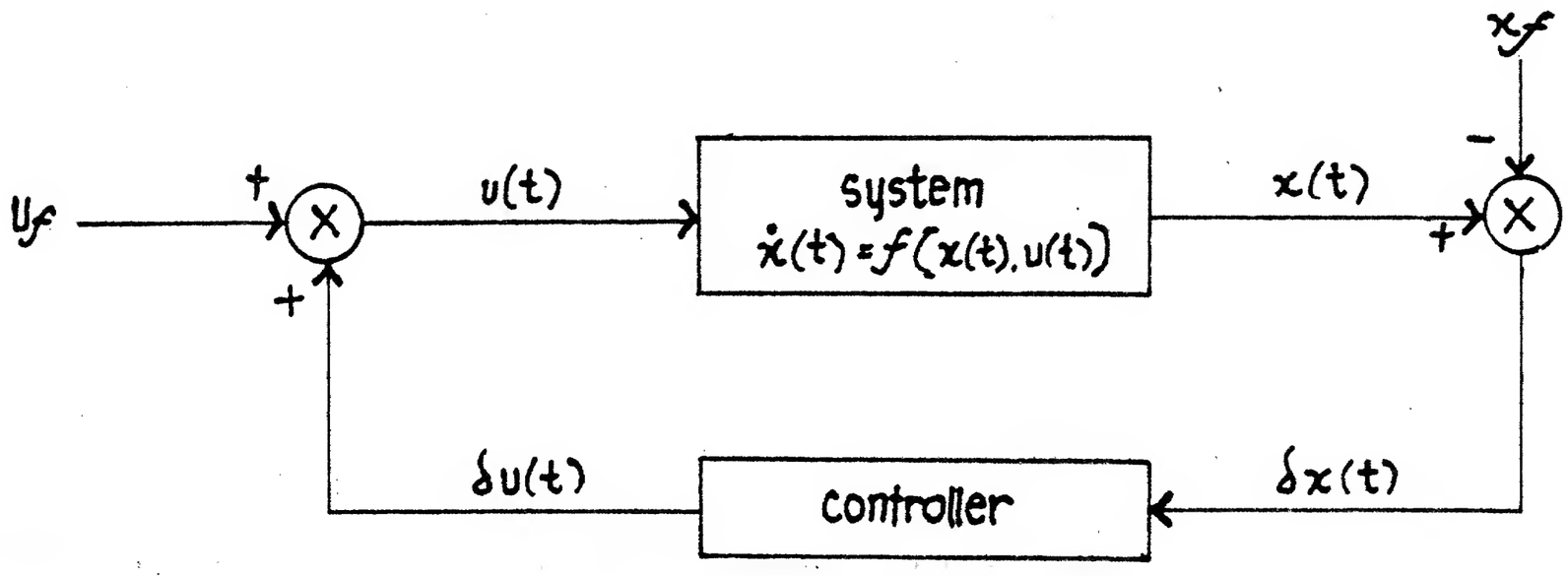

Figure 5-1. Block diagram for the closed-loop feedback control scheme.

Let x_f denote the desired final state, and u_f denote the steady-state control that satisfies equation (5.1).

Define

1. State perturbation vector $\delta x(t)$:

$$\delta x(t) = x(t) - x_f$$

2. Control correction vector $\delta u(t)$:

$$\delta u(t) = u(t) - u_f$$

Then the control objective can be stated as follows:

Given $\delta x(t)$, find $\delta u(\tau)$, $\tau \geq t$ such that future state perturbation vectors $\delta x(\tau)$ are as small as possible for all $\tau \in [t, \infty)$, or find a controller, as depicted in figure 5-1 that will accomplish this.

We will employ the linear-quadratic approach to designing the controller. Since we are trying to keep the system at a fixed set-point, this is also known as the linear regulator problem.

First we must derive the relationship between $\delta x(t)$ and $\delta u(t)$:

$x(t)$ and $u(t)$ are related by the system equation:

$$\dot{x}(t) = f(x(t), u(t)) \tag{5.2}$$

Expanding $f(x(t), u(t))$ about x_f, u_f in a Taylor series expansion,

$$f(x(t), u(t)) = f(x_f, u_f) + \frac{\partial f}{\partial x}(x_f, u_f)\delta x(t) + \frac{\partial f}{\partial u}(x_f, u_f)\delta u(t) + h.o.t. \tag{5.3}$$

where $h.o.t.$ denotes the higher order terms in the Taylor series expansion.

Since

$$\delta\dot{x}(t) = \dot{x}(t) - \dot{x}_f$$

and

$$\dot{x}_f = f(x_f, u_f) = 0,$$

we have,

$$\delta\dot{x}(t) = \frac{\partial f}{\partial x}(x_f, u_f)\delta x(t) + \frac{\partial f}{\partial u}(x_f, u_f)\delta u(t) + h.o.t \tag{5.4}$$

Define

$$\begin{aligned} A &= \frac{\partial f}{\partial x}(x_f, u_f) \\ B &= \frac{\partial f}{\partial u}(x_f, u_f) \end{aligned} \tag{5.5}$$

and assuming that the higher order terms are negligible, we obtain to first approximation that

$$\delta\dot{x}(t) = A\delta x(t) + B\delta u(t) \tag{5.6}$$

For the remainder of the Chapter, the δ-notation will be dropped for simplicity, and the linearized model will be represented as

$$\dot{x}(t) = Ax(t) + Bu(t) \tag{5.7}$$

5.3 The Linear Regulator Problem

Given the linear time-invariant system

$$\dot{x}(t) = Ax(t) + Bu(t) \tag{5.8}$$

and its initial condition x_0, find $u(t)$ such that the following quadratic cost functional is minimized

$$J = \int_0^\infty (x^T(t)Qx(t) + u^T(t)Ru(t))dt \tag{5.9}$$

where $Q = Q^T \geq 0, \quad R = R^T > 0.$

Derivation of the solution to the above problem can be found in Kwakernaak & Sivan[15]. It is shown that the optimal control $u^*(t)$ is given by

$$u^*(t) = -Gx(t) \tag{5.10}$$

where

$$G = R^{-1}B^TP \tag{5.11}$$

and P is the solution of the following Algebraic Riccati Equation (ARE):

$$0 = -PA - A^TP - Q + PBR^{-1}B^TP \tag{5.12}$$

If the original system is completely controllable, then the solution to the above ARE exists. In addition, since we are assuming that we are observing all the states, the system is completely observable, it can be shown that the feedback system is asymptotically stable (see *e.g.* Kwakernaak & Sivan[15]).

We will now consider the choice of the weighting matrices Q and R in the cost function given by equation (5.9):

In general, the selection of Q and R is not a simple matter; they are usually chosen on the basis of engineering experience coupled with simulation runs of the resultant system using different weighting values. In most practical applications, R and Q are chosen to be diagonal because in this way we can individually penalize specific components of $x(t)$ and $u(t)$. We will likewise choose R and Q to be diagonal. Since there is no reason to penalize any one component of $u(t)$ more than the others, R is chosen to be of the form ρI, where ρ is a positive scalar. Once Q is chosen, by adjusting ρ, we can vary the relative weighting between the state perturbation and control perturbation vectors.

Specifically, the effects of ρ are:

1. the smaller ρ is, the faster is the state perturbation vector $x(t)$ reduced to zero, this corresponds to the poles of the system being pushed to the left of the s-plane.
2. the smaller ρ is, the larger will be the feedback gain matrix, *i.e.* G in equation (5.10), this corresponds to large control magnitude.

Hence there will be a tradeoff between the speed of response and the amount of control to be put into the system.

When we consider the maximum allowable magnitude of control perturbation, we must bear in mind the control constraint which is given by

$$0 \leq u_i(t) \leq u_{max} \qquad \text{for } i = 1, \ldots, 4 \tag{5.13}$$

where $u_i(t)$ here is the total control input to the system.

In our case, since we are interested in reducing the position error to zero as fast as possible, we choose not to penalize the velocity terms. Hence Q is of the form,

$$Q = \begin{bmatrix} I_3 & 0_3 \\ 0_3 & 0_3 \end{bmatrix}$$

and ρ is chosen so that the slowest pair of poles is only slightly underdamped so that there will not be much overshoot.

Taking all these into consideration, and after some trial and errors and looking at the closed-loop eigenvalues and resultant runs, ρ is chosen to be 0.2. The values chosen are not optimal, but they represent a reasonable choice and yield an acceptable response. The response can of course be improved upon by further fine-tuning, but we are not putting any emphasis on it at this stage.

5.4 Determination of Steady-State Control Input

The steady-state control $u_f(t)$ required to hold the arm at any position, say θ_f, ϕ_f, ψ_f, can be obtained from equation (5.1), where $x_f = (\theta_f \quad \phi_f \quad \psi_f \quad \dot{\theta}_f \quad \dot{\phi}_f \quad \dot{\psi}_f)^T$. Since $x(t)$ is a 6-vector, we will obtain six algebraic equations from equation (5.1), but the first three do not involve $u(t)$ and only give us $x_4 = x_5 = x_6 = 0$ which corresponds to $\dot{\theta}_f = \dot{\phi}_f = \dot{\psi}_f = 0$.

Therefore from equation (5.1) and by substituting the values of $x_f = (\theta_f \quad \phi_f \quad \psi_f \quad 0 \quad 0 \quad 0)^T$ into it, we can obtain three algebraic equations involving the four scalar controls u_{fi}, $i = 1, \ldots, 4$; by solving these three equations, we can obtain u_f. However, note that we have one degree-of-freedom in choosing u_f subject to the three equations and the control constraint given by equation (5.13). By specifying any one of the u_{fi}'s, we can uniquely specify the other three.

There are two ways of taking advantage of this one degree-of-freedom:

1. we could, for each position, find the minimum values of control that will satisfy the three equations as well as the non-negativity contraint. Effectively we are setting one of the u_{fi}'s to be zero and solving the three equations for the other three u_{fi}'s. The one to be set to zero is chosen such that all u_{fi}'s are non-negative.
2. we could introduce another algebraic equation involving the u_{fi}'s, and by solving these four simultaneous equations we can get unique values for the u_{fi}'s. Specifically, the equation introduced is

$$\sum_{i=1}^{4} u_{fi} = k \tag{5.14}$$

Since all the u_{fi}'s are non-negative, the larger the value of k, the larger are the u_{fi}'s. In this context, this degree-of-freedom is thought of as providing us with the freedom of choosing the overall control level.

The first method is attractive in that it provides us with a way of specifying minimum control to keep the arm at any desired position, since we do not want to expend unnecessary energy holding the arm at a fixed position. However, since one of the components will be zero, or very near zero, the non-negativity control constraint is easily violated when we apply the feedback control law as given by equation (5.10).

On the other hand, the second method provides us with a way of specifying u_f at any position such that $\sum u_{fi}$ at all positions within the working space is the same. This is attractive because it was found that if this is so, then the "main" components of the feedback gain G as given in equation (5.11) do not vary significantly for all the positions. This point will be elaborated further in Chapter 6.

Hence the second approach is used. k is chosen such that for any position within the working space, the u_{fi}'s obtained by solving the four simultaneous equations are all non-negative.

The value of k found and used is 7, and the most critical position (with one of the u_{fi}'s nearest to zero) occurs approximately at $\alpha = 45°, \beta = 10°, \psi = 45°$.

Chapter 6. Implementation and Simulation of the Overall Control Structure

6.1 Introduction

As stated in Chapter 1, we are interested in moving the arm from an upright position to any specified final position. The overall control scheme for this movement is divided into two phases. In the first phase, open-loop time-optimal control approximation is applied to bring the arm to the vicinity of the specified final position. In the second phase, a closed-loop linear feedback control law will be switched in to bring the system to the desired final position and to maintain it there.

In order to implement this control scheme, we must have available the open-loop control and the feedback gain for every final position that can be specified. Since the computation time of the former is too long and the memory requirement for the latter is too large for them to be calculated on-line using the PDP 11/45 which is used for the control of the tendon arm, they must somehow be precalculated and stored. Since it is impossible to store the values for every possible final position, which are infinite in number, we need to partition the entire state space into regions and precompute the open-loop control trajectory and the feedback gain of a representative point of each region and store them in tables of some sort. As for the other points in the region, we can either interpolate or use the same value throughout a region. The latter approach is employed due to:

1. the feedback gain does not change significantly within a region, and
2. there is no satisfactory way of interpolating the open-loop control, and since feedback control is employed in the second phase, we rely on it to bring the system to the desired state, and
3. it is simple.

The next two sections describe means of representing and storing the open-loop control trajectories and the feedback gains. The last section describes briefly the program written for the implementation of the overall control scheme.

6.2 Representation and Storing of Open-Loop Time-Optimal Trajectories

Symmetry of the Control Trajectories

The design and construction of the tendon arm is such that it restricts the range of movement of the arm. In this thesis, this range will be taken as

$$\begin{aligned} 0 \leq \alpha &\leq \frac{\pi}{4} \\ 0 \leq \beta &\leq 2\pi \\ -\frac{\pi}{4} \leq \psi &\leq \frac{\pi}{4} \end{aligned} \tag{6.1}$$

where α, β, ψ are as defined by figure 2-4.

We will divide this space into four quadrants with the following correspondence:

$0 < \beta < \frac{\pi}{2}$	1st quadrant
$\frac{\pi}{2} < \beta < \pi$	2nd quadrant
$\pi < \beta < \frac{3\pi}{2}$	3rd quadrant
$\frac{3\pi}{2} < \beta < 2\pi$	4th quadrant

For the time-optimal trajectories, there is a symmetry among the four quadrants such that only those of the first quadrant need to be stored and those of the other three quadrants can be obtained from the corresponding trajectory in the first quadrant.

Let $u_i(t)$, $i = 1, \ldots, 4$ be the control trajectory that will bring the system from the initial position to a final position defined by $\theta = \theta_f$, $\phi = \phi_f$, where (θ_f, ϕ_f) is in the first quadrant (recall that the time-optimal control is obtained using the reduced-order model and hence ψ is not relevant).

Then, to obtain the control trajectory for

1. $\theta = -\theta_f, \phi = -\phi_f$; exchange $u_1(t)$ and $u_2(t)$, exchange $u_3(t)$ and $u_4(t)$.
2. $\theta = -\theta_f, \phi = \phi_f$; exchange $u_1(t)$ and $u_2(t)$, do not exchange $u_3(t)$ and $u_4(t)$
3. $\theta = \theta_f, \phi = -\phi_f$; do not exchange $u_1(t)$ and $u_2(t)$, exchange $u_3(t)$ and $u_4(t)$.

Hence in all the discussion that follows, we will take the final position to be in the first quadrant.

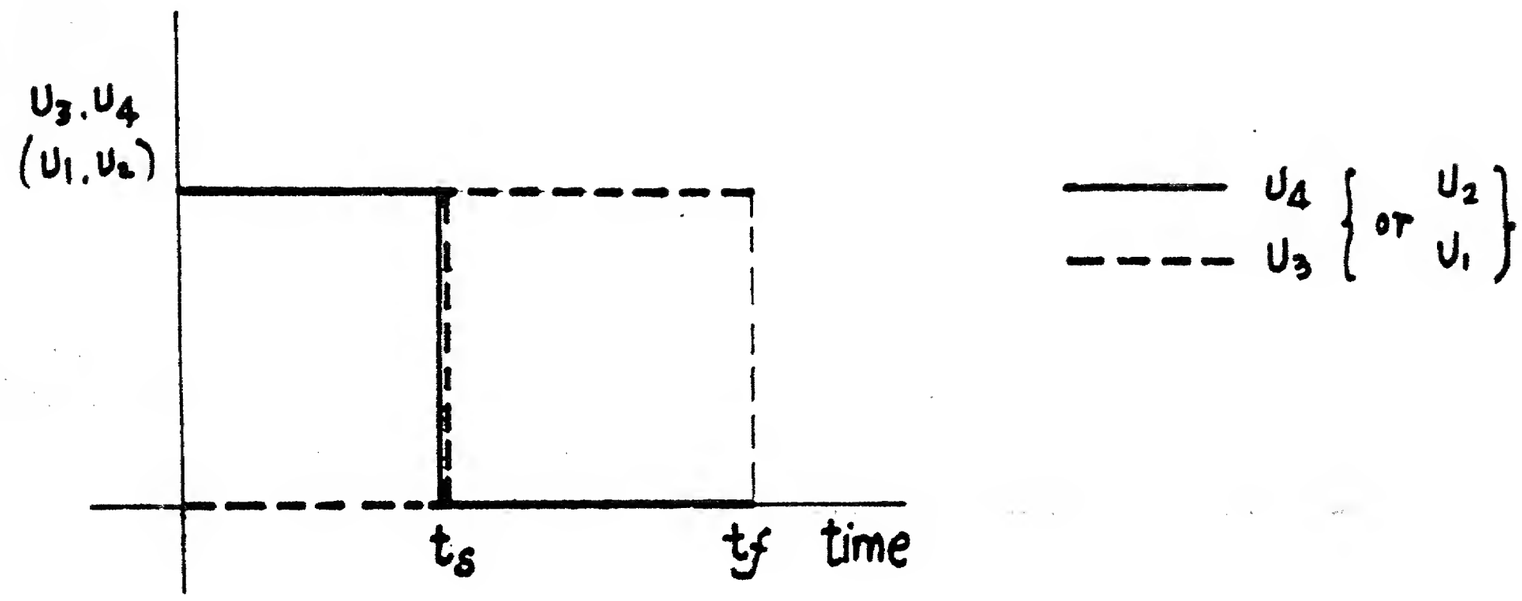

Figure 6-2. Form of the bang-bang pair of controls

Form of time-optimal control

As stated in section 4.3, it was found that, in general, one pair of controls is bang-bang and the other pair is not (both pair of controls could be bang-bang for certain values of θ_f and ϕ_f). Which pair it is that is bang-bang depends on the relative magnitude of θ_f and ϕ_f.

In general, the pair that is not bang-bang can be well-approximated by straight line segments, and they can be of any form as shown in figure 6-1. The pair that is bang-bang is of the form that is shown in figure 6-2. Hence any pair of controls can be represented by the numbers h_1, h_2, t_1, t_2, t_3, t_f as shown in figure 6-3.

There are two ways of representing the open-loop control trajectory for any final position:

1. Represent both pairs by the general form shown in figure 6-3. By choosing appropriate values for h_{1i}, h_{2i}, t_{1i}, t_{2i}, t_{3i}, t_f, $i = 1, 2$, we can represent any of the forms given by figure 6-1 and the bang-bang control of figure 6-2. ($i = 1$ represents u_1 and u_2, $i = 2$ represents u_3 and u_4). Since in implementing the control scheme with a digital computer, the time axis is discrete, hence the t_{ij}s are integer numbers. Using this scheme, we need a total of 4 real numbers and 7 integer numbers to

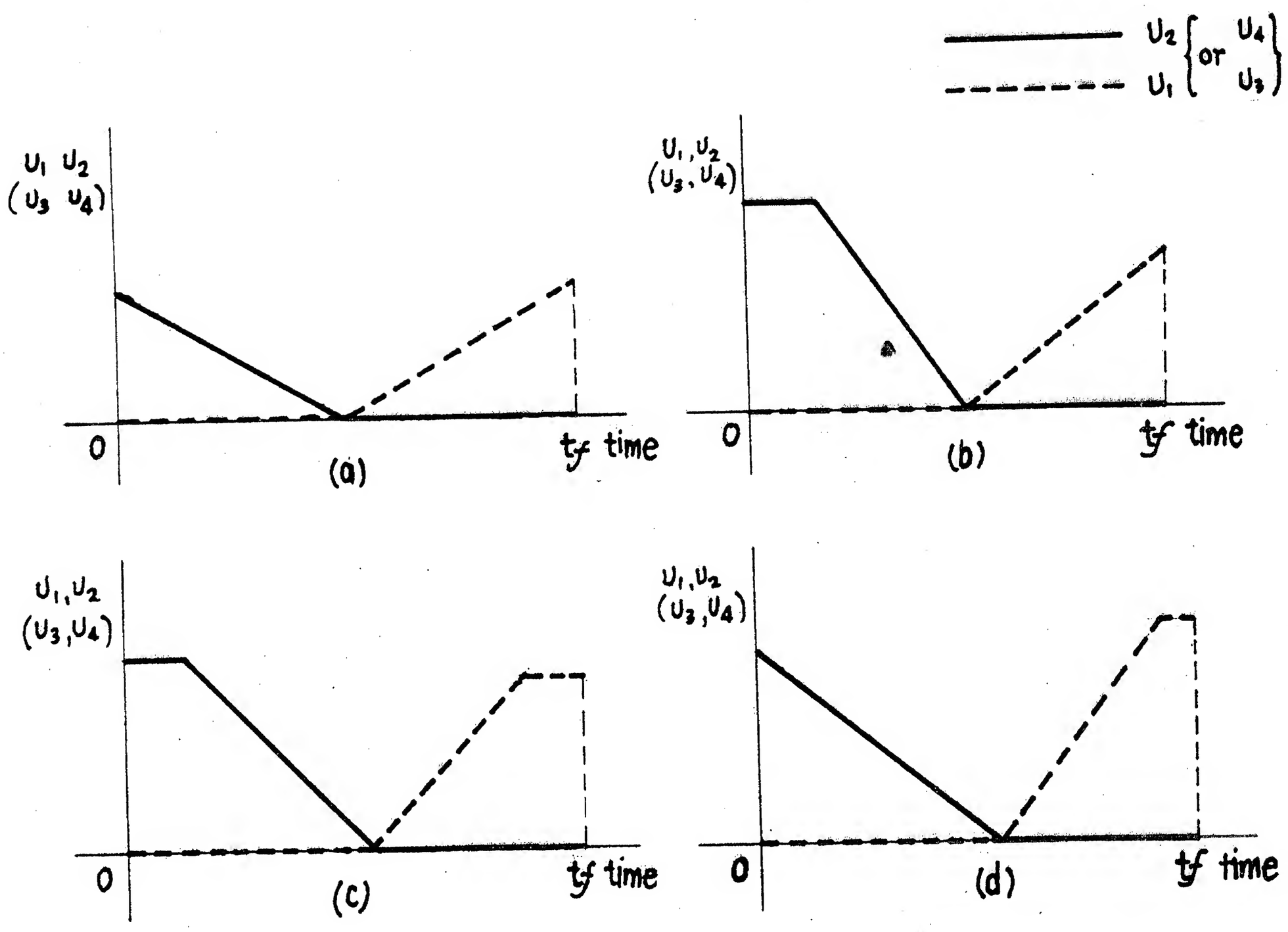

Figure 6-1. Various forms of the non-bang-bang pair of controls

represent the control trajectory of each final position.

2. Represent the non-bang-bang pair by the general form, and represent the bang-bang pair by one number, that of the switching time. Hence in this scheme, we need 2 real numbers, 5 integers and 1 bit to indicate which pair is bang-bang.

The first method is chosen because it is straightforward to code and at this stage we are only trying out the overall control scheme using simulation and hence the partitioning into regions is very coarse and is as shown in figure 6-4. We are not too concerned yet with conserving storage.

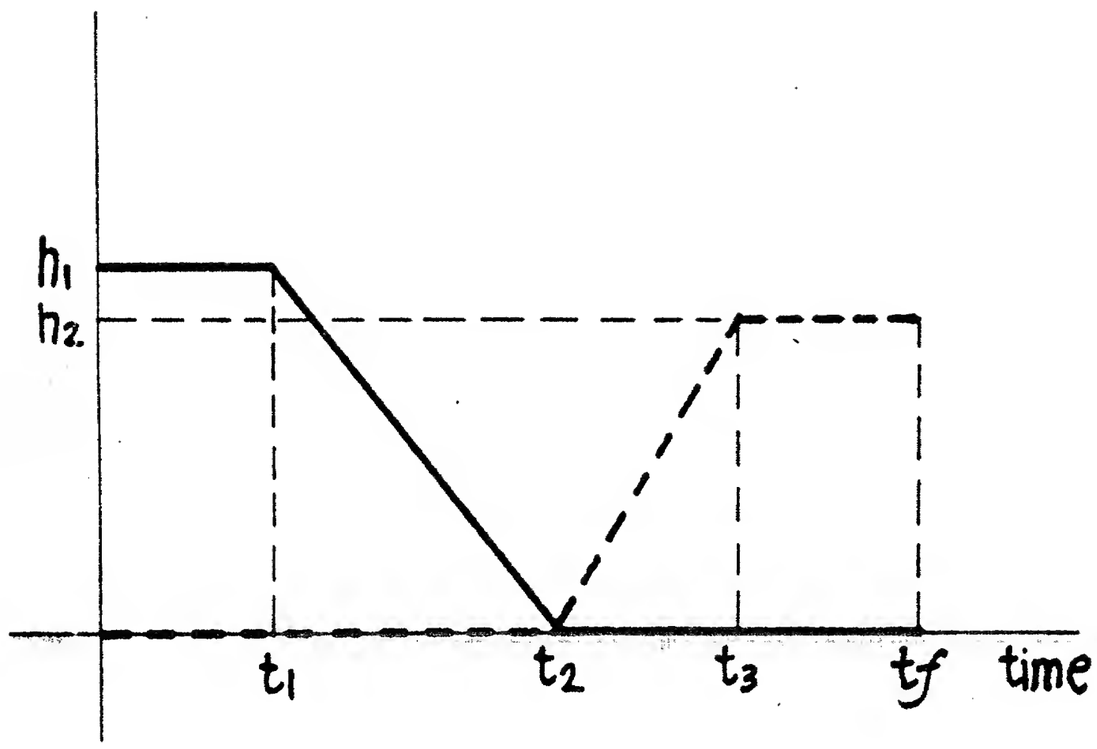

Figure 6-3. General representation of any pair of controls

In practical implementation, we need of course to partition the state-space into a finer grid, hence reducing the storage requirement per point will be one of the prime concerns. We can then consider the following two ways of saving storage:

1. With the sampling rate (5 msec) used, the maximum time step corresponding to t_f is less than 100, hence we can pack two time values (*e.g.* t_1 and t_2) into one word.

2. In actual system implementation, the control will be applied to the motors via digital-to-analog converters which takes integer value as input, hence the control values can be stored as scaled integers instead of real numbers.

If these two modifications are implemented, only 8 words for the first method and 5 words for the second method are required per point.

6.3 Representation and Storing of Feedback Gains

The feedback gain G of the linear regulator design is a 4×6 matrix. If g_{ij}, $i = 1, \ldots, 4$, $j = 1, \ldots, 6$, represents the component of G, then g_{ij} is the contribution of x_j to u_i, *i.e.*,

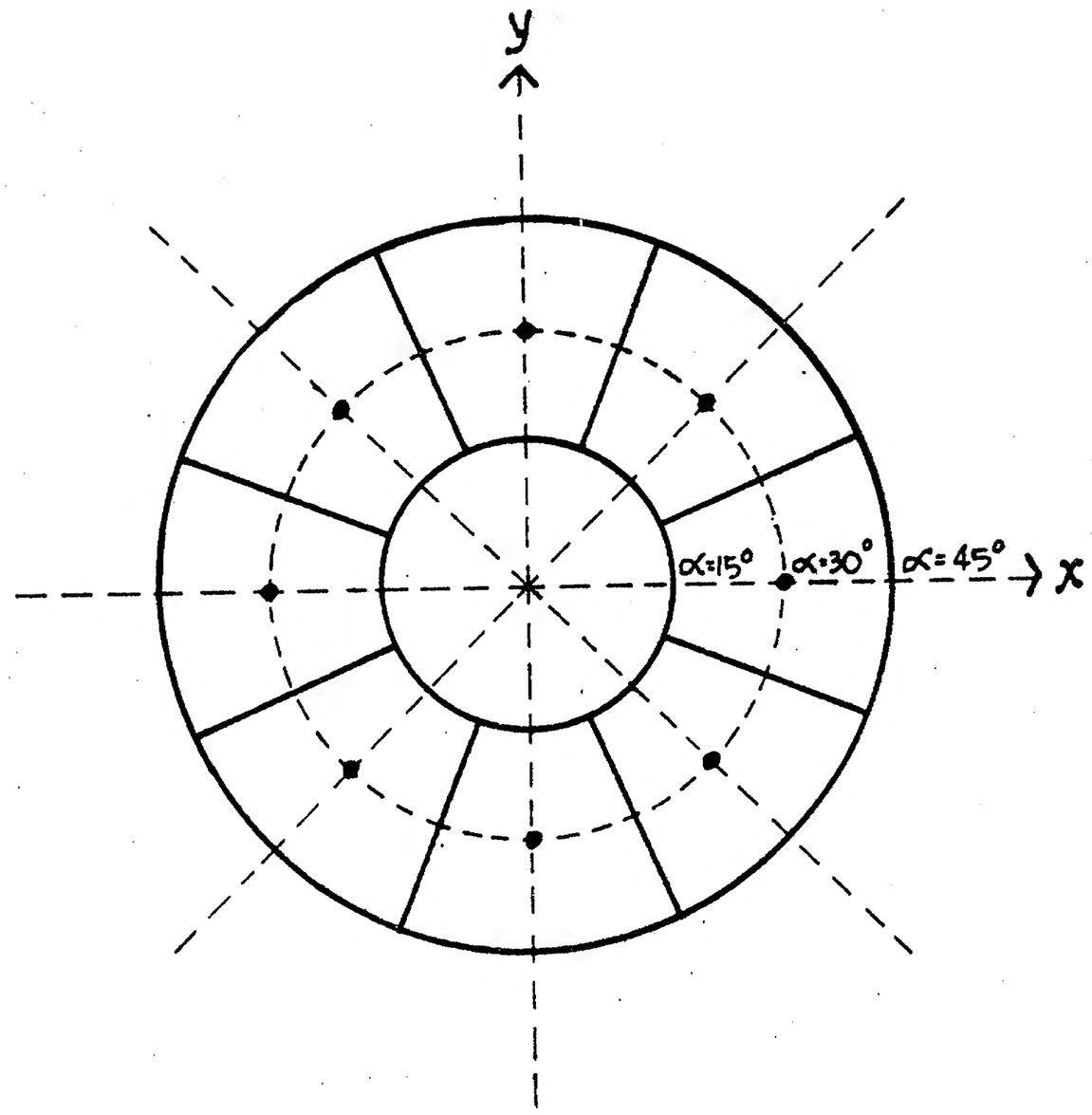

Figure 6-4. Partitioning used in the simulation run

$$u_i = \bar{u}_i - \sum_{j=1} g_{ij} x_j \tag{6.2}$$

where $\bar{u}_i$ is the steady-state control.

Hence we can partition the matrix G into main components and cross-coupled components:

For u_1 and u_2, since they directly affect θ and $\dot{\theta}$, and only indirectly ϕ and $\dot{\phi}$, we will treat g_{11}, g_{21}, g_{14}, g_{24} as main components.

Similarly for u_3 and u_4, since they directly affect ϕ and $\dot{\phi}$, we will group g_{32}, g_{42}, g_{35}, g_{45} as main components.

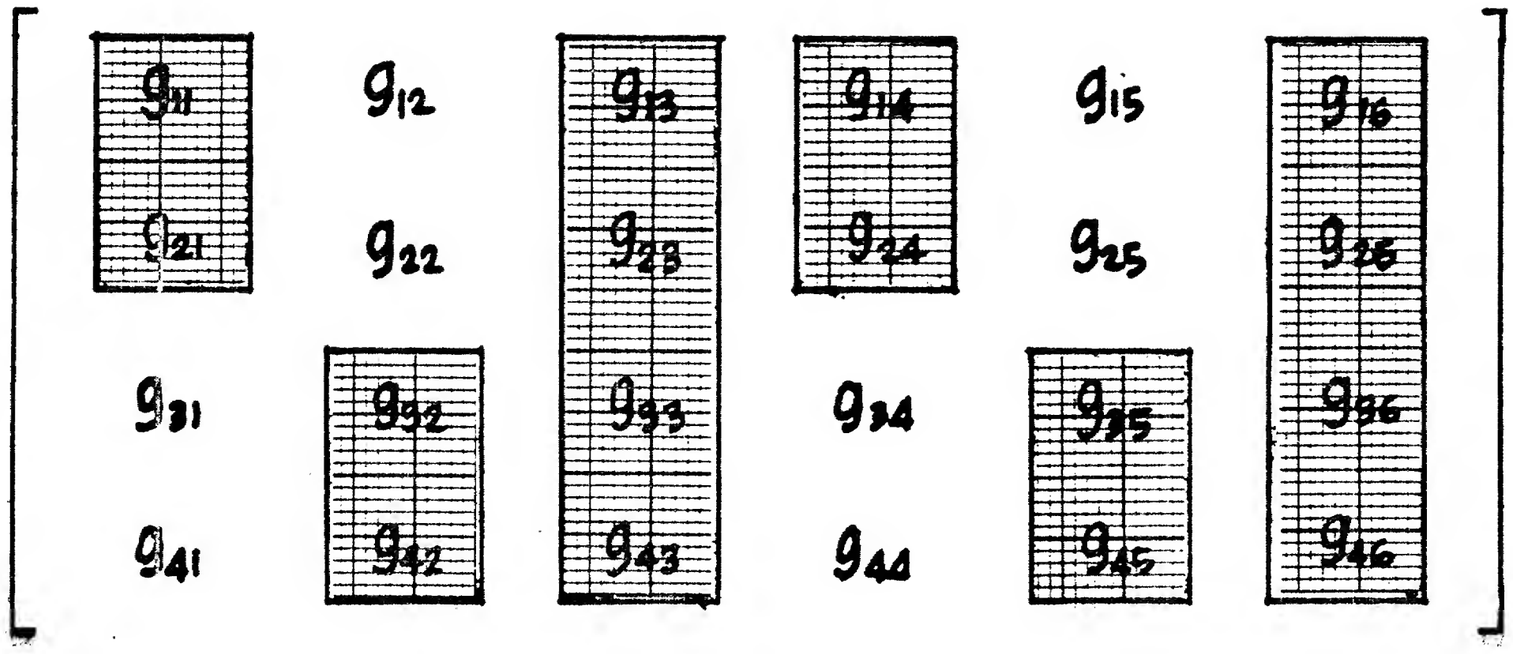

Figure 6-5. Cross-hatched area showing the main elements of matrix G

Since all four controls directly affect ψ and $\dot{\psi}$, we will treat g_{i3}, g_{i6}, $i = 1, \ldots, 4$, as main components. Hence as indicated in figure 6-5, the cross-hatched elements are the main components.

Table 6-1 shows the feedback gains for the various positions indicated in figure 6-6 and for $\psi = 0$. From this table, we can see that the values of the main components do not vary much for different positions, and it is only the cross-coupled terms that change significantly, for example, compare g_{21}, g_{22} of points 5 and 6, there is as much as an order of magnitude of difference.

Table 6-2 shows the feedback gains for position 3 ($\alpha = \pi/6$, $\beta = \pi/4$) but with different values of ψ. It can be seen that all components of G do not vary significantly for different ψ, hence we will take them as the same and equal to those at $\psi = 0$.

Table 6-3 shows the feedback gains for position 3 and its corresponding positions in the other three quadrants. To a first approximation, we can obtain G of the third quadrant from the first quadrant, and of the fourth from the second as follows:

exchange row 1 and 2, row 3 and 4, and

change the signs of all the elements except those of columns 3 and 6.

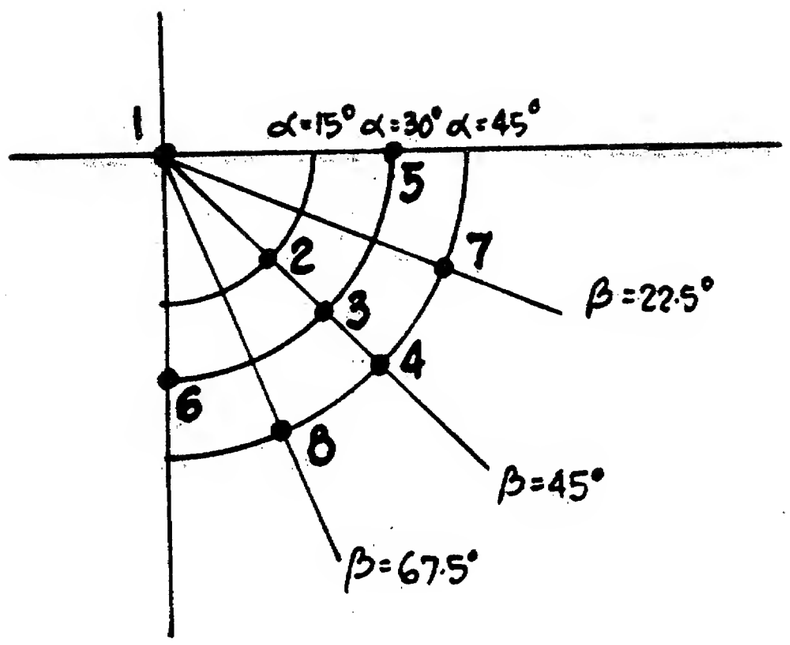

Figure 6-6. Figure showing various final positions used in Table 6-1

For implementation purposes, we will treat the main components of G to be the same for all positions in the four quadrants, using those of the upright position, and store the non-main components for position 1, 3, 5 and 6 and their corresponding positions in quadrant 2, *i.e.*, the partitioning into regions is the same as for the open-loop control.

6.4 Structure of Overall Control Program and its Implementation

The working space of the arm is defined by equation (6.1) and is partitioned into regions as shown in figure 6-4. The open-loop control and feedback gain of the representative point, called the center, of each region are stored as described in the last two sections.

When a set-point command is issued, the program will first determine which region the final position is in, after which the entire open-loop control trajectory and the feedback gain G for its center are determined, these will be used for the final position specified. At the same time, the steady-state current at the final position is calculated.

The open-loop control is then applied to the system: at each time step, generated by an interrupt

from the real-time clock, a control vector is output to the system. At the end of the first phase, determined by the final time of the open-loop control, the closed-loop linear feedback law will be used: at the occurrence of each interrupt, the state of the system is read via the A to D, from which the state perturbation vector δx is calculated, and the control correction vector is calculated by

$$u = u_f - G\delta x \tag{6.3}$$

where u_f is the steady-state control vector.

This u is then output to the system.

Because the physical tendon arm system is not ready, the overall control scheme will be simulated on the PDP 11/45 computer. But the program is written as if it is a real time system except that a software subroutine is being substituted for the arm, and the time scale is expanded due to the length of time required for the subroutine. The block diagram for the program is given in figure 6-7.

Figure 6-8 shows the state trajectories for three different final positions.

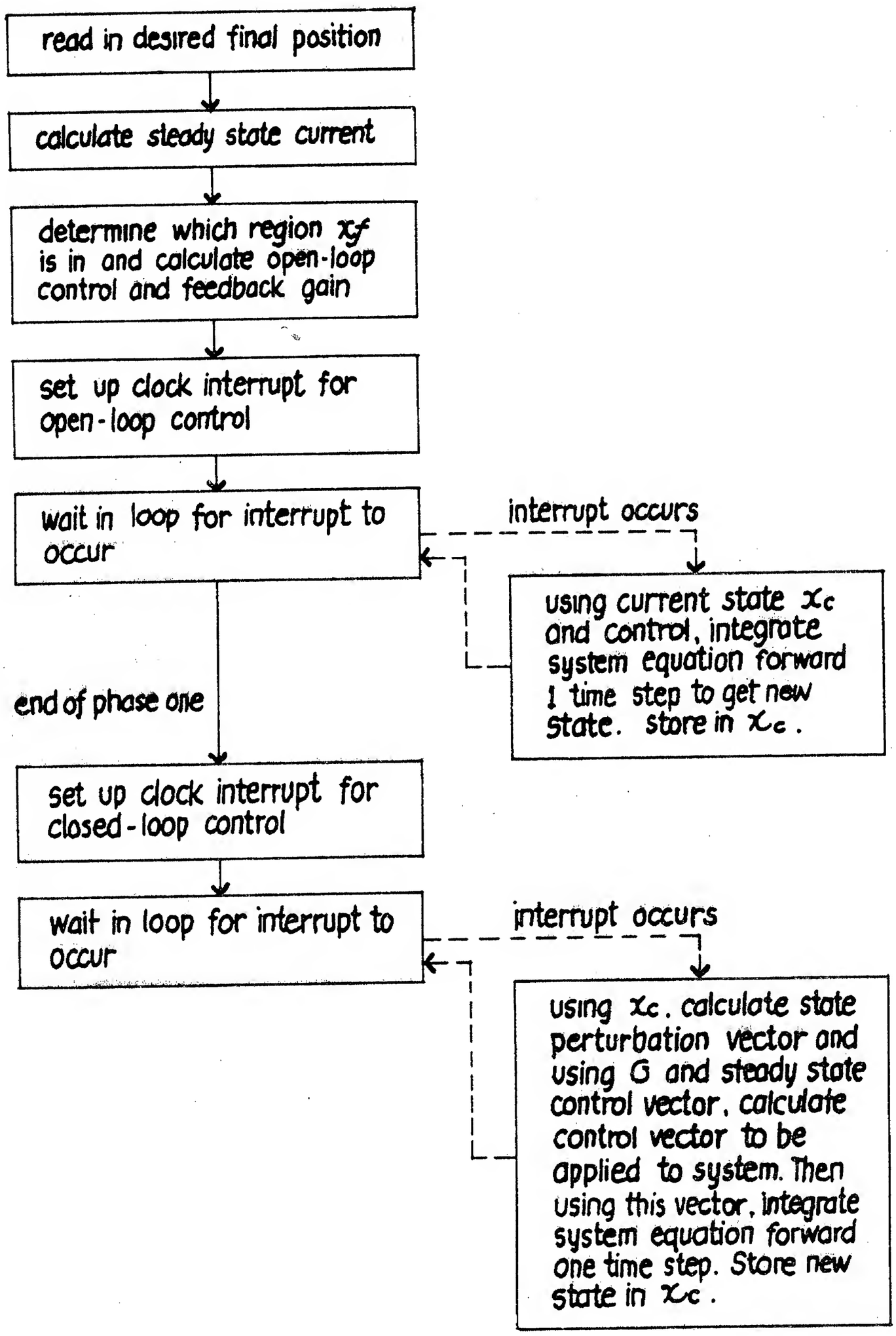

Figure 6-7. Block diagram for the overall control program

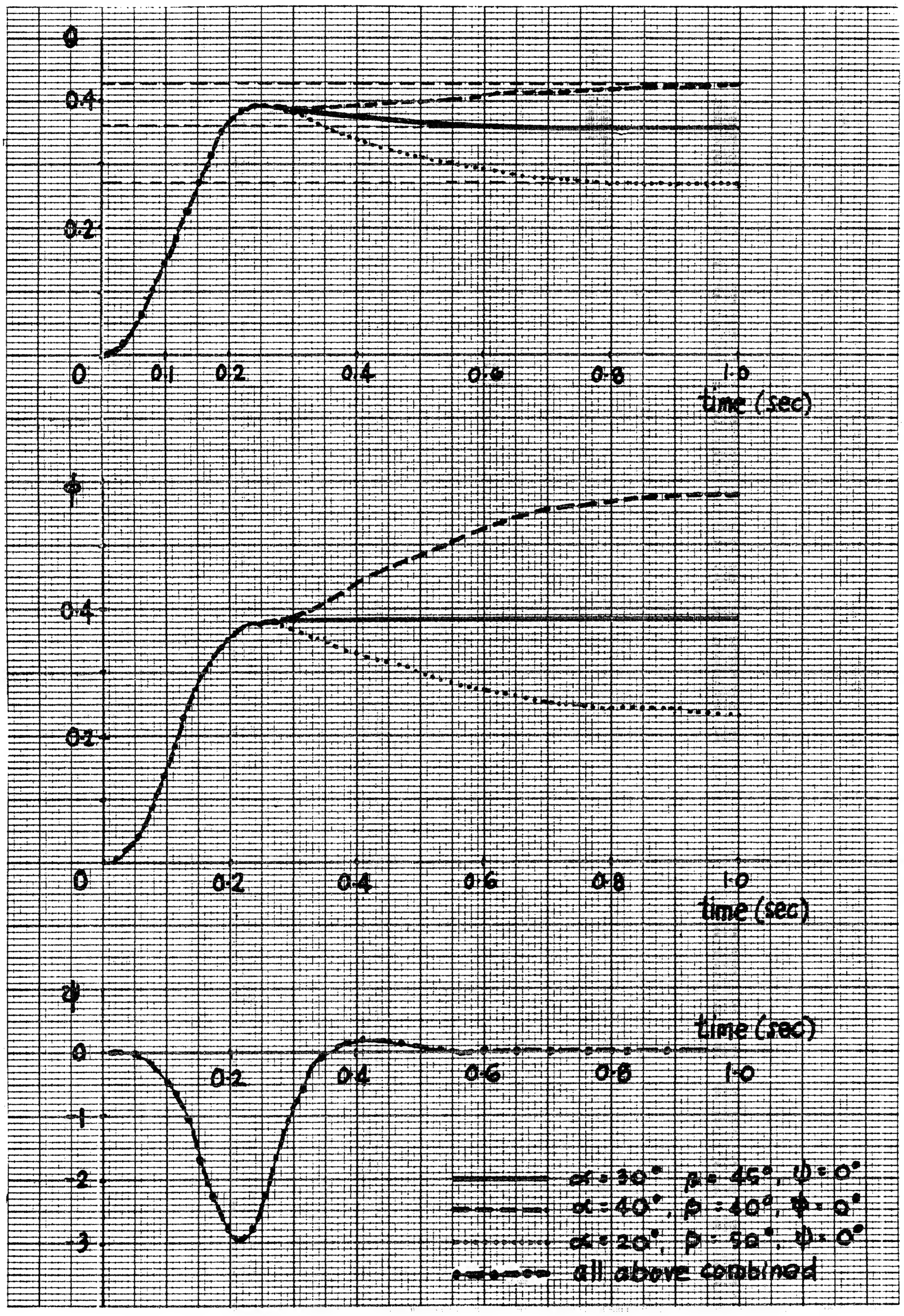

Figure 6-8. Trajectories for three different final positions

Table 6-1 Feedback gains for the various positions shown in Figure 6-6

1 $\alpha = 0^\circ$, $\beta = 0^\circ$, $\psi = 0^\circ$

-4.0294D+00 -2.1103D-01 1.5044D+00 -6.0678D-01 -2.2333D-02 8.3086D-02
4.0294D+00 2.1103D-01 1.5044D+00 6.0678D-01 2.2333D-02 8.3086D-02
-2.8960D-01 -4.8319D+00 -1.5363D+00 -1.8081D-02 -7.5378D-01 -8.4850D-02
2.8960D-01 4.8319D+00 -1.5363D+00 1.8081D-02 7.5378D-01 -8.4850D-02

2 $\alpha = 15^\circ$, $\beta = 45^\circ$

-3.4940D+00 3.6891D-01 1.0416D+00 -5.3920D-01 4.2670D-02 6.9065D-02
3.5889D+00 7.4437D-01 1.0492D+00 5.9555D-01 8.7205D-02 6.9174D-02
1.7086D-01 -4.3907D+00 -1.0396D+00 2.6577D-02 -6.8781D-01 -6.9136D-02
5.5215D-01 4.3678D+00 -1.0971D+00 4.1720D-02 7.3414D-01 -7.2071D-02

3 $\alpha = 30^\circ$, $\beta = 45^\circ$

-3.6866D+00 1.0323D+00 1.0381D+00 -5.2884D-01 1.1098D-01 6.9476D-02
3.7028D+00 1.1766D+00 1.0480D+00 6.3000D-01 1.4153D-01 6.9113D-02
9.2702D-01 -4.4483D+00 -1.0131D+00 9.9182D-02 -6.5223D-01 -6.8077D-02
5.6905D-01 4.4091D+00 -1.1180D+00 3.3458D-02 7.4456D-01 -7.3297D-02

4 $\alpha = 45^\circ$, $\beta = 45^\circ$

-4.2914D+00 1.6954D+00 1.0417D+00 -5.4604D-01 1.7014D-01 7.0824D-02
3.8881D+00 1.6345D+00 1.0409D+00 6.7243D-01 2.0166D-01 6.8619D-02
2.0307D+00 -4.5805D+00 -9.9308D-01 1.9637D-01 -6.1743D-01 -6.7677D-02
3.8914D-01 4.6025D+00 -1.1267D+00 -5.8456D-03 7.6107D-01 -7.3971D-02

5 $\alpha = 30°$, $\beta = 0°$

-3.3416D+00	1.3973D+00	1.0603D+00	-5.5295D-01	1.6731D-01	7.0848D-02
3.6233D+00	1.8534D+00	1.0966D+00	5.7216D-01	2.1213D-01	7.3349D-02
-2.5594D-01	-4.9148D+00	-9.0654D-01	-7.6211D-03	-7.1483D-01	-6.2195D-02
3.9595D-01	4.7432D+00	-1.1362D+00	3.6699D-02	8.0938D-01	-7.3063D-02

6 $\alpha = 30°$, $\beta = 90°$

-3.7638D+00	-1.3065D-02	9.7825D-01	-5.1258D-01	-9.6656D-04	6.5543D-02
4.0262D+00	3.5434D-01	1.0033D+00	6.7718D-01	3.6848D-02	6.5561D-02
8.2385D-01	-3.8834D+00	-1.1523D+00	8.1149D-02	-6.0983D-01	-7.5613D-02
1.3934D+00	4.1661D+00	-1.0909D+00	1.1188D-01	6.6908D-01	-7.3458D-02

7 $\alpha = 45°$, $\beta = 22.5°$

-3.9004D+00	2.6739D+00	1.1103D+00	-5.5416D-01	2.8682D-01	7.5540D-02
3.4575D+00	2.5295D+00	1.0946D+00	6.0214D-01	2.9411D-01	7.3503D-02
1.0434D+00	-5.0584D+00	-8.3655D-01	1.0865D-01	-6.7251D-01	-5.8113D-02
1.2179D-01	5.2718D+00	-1.1241D+00	-1.2945D-02	8.7344D-01	-7.2237D-02

8 $\alpha = 45°$, $\beta = 67.5°$

-4.1608D+00	7.1318D-01	9.2594D-01	-5.0827D-01	6.6269D-02	6.2946D-02
4.5281D+00	9.1009D-01	9.9979D-01	7.4559D-01	1.1204D-01	6.4784D-02
2.3693D+00	-3.8769D+00	-1.1557D+00	2.2660D-01	-5.3739D-01	-7.7228D-02
1.2249D+00	4.0157D+00	-1.1283D+00	7.1972D-02	5.4459D-01	-7.5914D-02

Table 6-2 Feedback gain for positions with $\alpha = 30°$, $\beta = 45°$ and different values of ψ

1 $\psi = -30°$

-3.7123D+00 1.0024D+00 1.0572D+00 -5.3019D-01 1.0528D-01 7.0897D-02
3.7314D+00 1.1506D+00 1.0610D+00 6.3314D-01 1.3728D-01 6.9960D-02
9.2553D-01 -4.3568D+00 -9.8331D-01 1.0010D-01 -6.4103D-01 -6.6190D-02
5.7194D-01 4.2893D+00 -1.1016D+00 3.4235D-02 7.2766D-01 -7.2309D-02

2 $\psi = 0°$

-3.6866D+00 1.0323D+00 1.0381D+00 -5.2884D-01 1.1098D-01 6.9478D-02
3.7028D+00 1.1766D+00 1.0480D+00 6.3000D-01 1.4153D-01 6.9113D-02
9.2702D-01 -4.4483D+00 -1.0131D+00 9.9182D-02 -6.5223D-01 -6.8077D-02
5.6905D-01 4.4091D+00 -1.1180D+00 3.3458D-02 7.4456D-01 -7.3297D-02

3 $\psi = +30°$

-3.6557D+00 1.0644D+00 1.0193D+00 -5.2694D-01 1.1692D-01 6.8126D-02
3.6706D+00 1.2022D+00 1.0350D+00 6.2642D-01 1.4577D-01 6.8266D-02
9.2745D-01 -4.5415D+00 -1.0411D+00 9.8231D-02 -6.6371D-01 -6.9876D-02
5.6379D-01 4.5372D+00 -1.1322D+00 3.2531D-02 7.6248D-01 -7.4158D-02

Table 6-3 Feedback gains for $\alpha = 30°$, $\beta = 45°$ and its corresponding positions in the other 3 quadrants

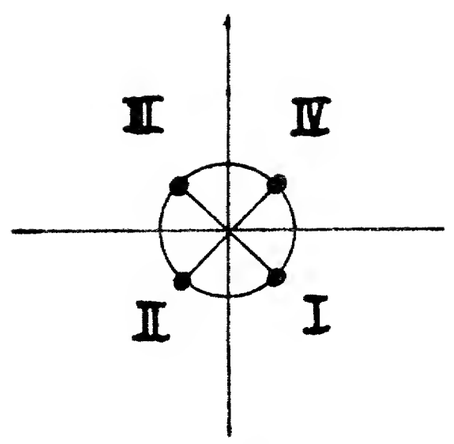

I

-3.6866D+00 1.0323D+00 1.0381D+00 -5.2884D-01 1.1098D-01 6.9478D-02

3.7028D+00 1.1766D+00 1.0480D+00 6.3000D-01 1.4153D-01 6.9113D-02

9.2702D-01 -4.4483D+00 -1.0131D+00 9.9182D-02 -6.5223D-01 -6.8077D-02

5.6905D-01 4.4091D+00 -1.1180D+00 3.3458D-02 7.4456D-01 -7.3297D-02

II

-3.8908D+00 -1.1524D+00 1.0507D+00 -5.4407D-01 -1.2512D-01 7.0484D-02

3.6138D+00 -4.7289D-01 1.0091D+00 6.2405D-01 -7.0878D-02 6.6632D-02

-1.2574D-01 -4.1834D+00 -1.1682D+00 -2.1993D-02 -7.0808D-01 -7.5408D-02

1.4616D+00 4.6588D+00 -9.9154D-01 1.1871D-01 7.0842D-01 -6.7917D-02

III

-3.7028D+00 -1.1766D+00 1.0480D+00 -6.3000D-01 -1.4153D-01 6.9113D-02

3.6866D+00 -1.0323D+00 1.0381D+00 5.2884D-01 -1.1098D-01 6.9478D-02

-5.6906D-01 -4.4091D+00 -1.1180D+00 -3.3459D-02 -7.4455D-01 -7.3297D-02

-9.2701D-01 4.4483D+00 -1.0131D+00 -9.9182D-02 6.5223D-01 -6.8077D-02

IV

-3.6238D+00 4.7528D-01 1.0084D+00 -6.2393D-01 7.1127D-02 6.6653D-02

3.8721D+00 1.1504D+00 1.0512D+00 5.4358D-01 1.2490D-01 7.0466D-02

-1.4444D+00 -4.6586D+00 -9.9158D-01 -1.1830D-01 -7.0842D-01 -6.7914D-02

1.3926D-01 4.1838D+00 -1.1683D+00 2.2027D-02 7.0814D-01 -7.5407D-02

Chapter 7. Conclusions

7.1 Summary

In this thesis, a mathematical model describing the dynamics of the tendon arm system has been developed. From this, we obtained a reduced-order model of the system and applied the Minimum Principle and the conjugate gradient method to obtain the time-optimal solution. It was found that the optimal solution is not bang-bang but that it contains singular arcs. But it was also found that these singular arcs can be approximated very well by straight line segments, this approximated control is then utilized to form part of the overall control scheme.

The open-loop tendon arm system was found to be unstable, and hence to maintain the system at any state, closed-loop feedback control is required. The feedback law was designed using the linear regulator design procedure, linearizing the nonlinear dynamics about the final state and the nominal control required to keep the system there.

The two control schemes are combined with the first phase being open-loop time-optimal control, bringing the system from its initial state to a waypoint in the vicinity of the final state, the second phase then employs the closed-loop control law to bring the system to the final state and to maintain it there.

It was intended initially to implement the overall control scheme on the actual physical system, but due to unforeseen circumstances, this was not possible, instead, digital simulations of the system with the control scheme implemented were done.

7.2 Areas for further work

There are a few directions that we can go from here:

1. Implement the control scheme on the actual physical system — this is the most natural extension to the present work. However, before this can be done, there are a few problems to be taken care of:

a. The control vector of our problem is formulated in terms of input currents to the motors. The drivers for the tendon arm motors, however, are voltage amplifiers, hence we have to reformulate and solve our problem in terms of voltage inputs. This can be easily done however, and the way to do it is shown in Appendix F.

b. The linear regulator design assumes full state feedback. For the tendon arm , we have only angle measurements but not velocity measurements, we need to find some means of constructing the full state (the simplest way, of course, is to use backward differencing of the angles to approximate the velocity terms).

c. In the simulation of the control scheme, a very coarse grid is utilized to partition the state space. In actual implementation, a finer grid has to be used, and the problems of how many grid points to use and where to place them have to be considered.

2. Investigate other means of simplifying the model — the biggest disadvantage of the present control scheme is that the third degree-of-freedom , namely, ψ, is not being controlled during the first phase of movement, this is due to the approach employed in simplifying the system equation. It was found that the coupling between θ and ϕ is not very strong, thus it may be possible to simplify the system equations while retaining the full order dynamics.

3. The motivation of using time-optimal control initially is because of its bang-bang solution nature (*i.e.* in the absence of singularity). It would be interesting to formulate the time-optimal control problem as one having a discrete control set constraint, *i.e.*,

$$u_i(t) \in \{0, u_{max}\}$$

and find out what the form of the optimal solution is. It should also be interesting to formulate the time-optimal problem based on the full order model and solve it, if possible, to see whether it is bang- bang.

4. In our control scheme, we have utilized the measurements of the angles θ, ϕ, and ψ but not the four

motor shaft angles. Investigate other control strategies that will take advantage of the availability of all seven angles.

References

[1] Kahn M.E., "The Near-Minimum-Time Control of Open-Loop Articulated Kinematic Chains", Stanford Artificial Intelligence Project Memo AIM-106, December 1969

[2] Riemenschneider P.R.H., Johnson T.L., Lim K.H., "Final-Position Control of a Single Degree-of-Freedom Tendom Arm", **Proc. IEEE conf. on Decision and Control**, Albuquerque, December 1980

[3] Athans M., Falb P.L., **Optimal Control**–An Introduction to the Theory and Its Application, McGraw-Hill, 1966

[4] Pontryagin L.S., Boltyanskii V., Gamkrelidze R., Mishchenko E., **The Mathematical Theory of Optimal Processes**, Interscience Publishers, 1962

[5] Plant J.B., **Some Iterative Solutions in Optimal Control**, MIT Press, 1968

[6] Mufti I.H., **Computational Methods in Optimal Control Problems**, Springer-Verlag, 1970

[7] Jacobson D.H., Gershwin S.B., Lele M.M., "Computation of Optimal Singular Controls", **IEEE Trans Aut Control**, AC-15 no.1, February 1970

[8] Soliman M.A., Ray W.H., "A Computational Technique for Optimal Control Problems having Singular Arcs", **Int J Control**, vol-16 no.2, 1972

[9] Maurer H., "Numerical Solution of Singular Control Problems using Multiple Shooting Techniques", **J Opt Th App**. vol-18 no.2, 1976

[10] Edge E.R., Powers W.F., "Function-space Quasi-Newton Algorithms for Optimal Control Problems with Bounded Controls and Singular Arcs", **J Opt Th App**, vol-20 no.4, December 1976

[11] Lasdon L.S., Mitter S.K., Warren A.D., "The Conjugate Gradient Method for Optimal Control Problems", **IEEE Trans Aut Control**, AC-12 no.2, April 1967

[12] Sinnott J.F., Luenburger D.G., "Solution of Optimal Control Problems by the method of Conjugate Gradients", **Joint Aut Control Conf**, 1967

[13] Pagurek B., Woodside C.M., "The Conjugate Gradient Method for Optimal Control Problems with Bounded Control Variables", **Automatica**, vol-4, 1968

[14] Quintana V.H., Davison E.J., "Clipping off Gradient Algorithm to Compute Optimal Controls with Constrained Magnitude", **Int J Control**, vol-20 no.2, 1974

[15] Kwakernaak H., Sivan R., **Linear Optimal Control Systems**, John Wiley, 1972

Appendix A. Deriving the equations of motion of the system when either pair of tendons is completely unwrapped from the arm

Due to the way the four tendons are wrapped around the arm, at any one time it is possible for only one pair to be completely unwrapped. Hence there are three different sets of equations describing the motion of the system depending on the values of $\omega + \lambda$ and $\omega' + \lambda'$ (refer to figures 2-7(a) and 2-8(a) for the definitions of ω, λ, ω', λ', where R_i is now the point at which a tangent from P_i touches the arm, all projected onto the $x' - y'$ plane).

The three cases correspond to:

1. $\omega + \lambda < 3\pi/4$ and $\omega' + \lambda' < 3\pi/4$, both pair of tendons are properly wrapped on the arm, this is the normal mode of operation.
2. $\omega + \lambda \geq 3\pi/4$ and $\omega' + \lambda' < 3\pi/4$, the first pair, corresponding to tendons 1 and 2, is completely unwrapped, whereas the second pair remains wrapped.
3. $\omega + \lambda < 3\pi/4$ and $\omega' + \lambda' \geq 3\pi/4$, the first pair remains wrapped, whereas the second pair is completely unwrapped.

The equations of motion corresponding to case 1. have been developed in Chapter 2; those of the last two cases will be developed in this Appendix.

A.1 Tendons 1 and 2 are completely unwrapped

When $\omega + \lambda \geq 3\pi/4$, where ω and λ are still being defined by equations (2.7) and (2.8), tendons 1 and 2 are completely unwrapped, the situation is shown in figure A-1.

The directions of F_1 and F_2 (the tensions in tendons 1 & 2) are now given by $\vec{Q_1P_1}$ and $\vec{Q_2P_2}$ respectively, and equations (2.12)–(2.13), (2.17)–(2.18) are modified to

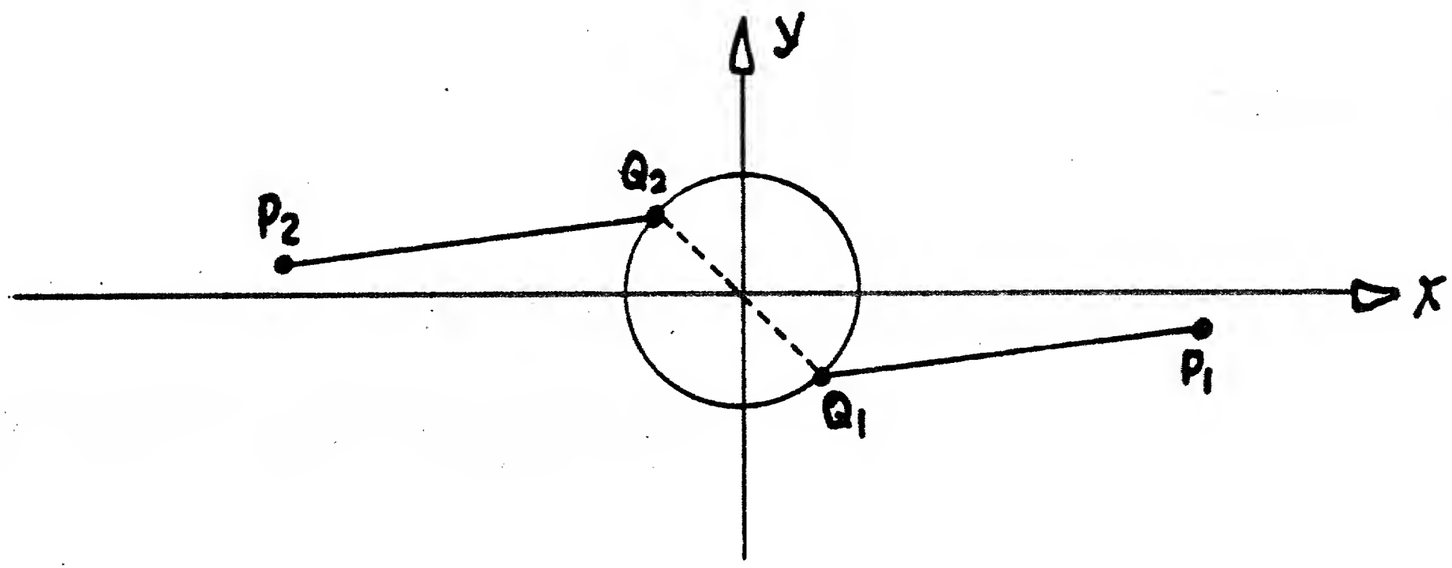

Figure A-1. Schematic diagram showing the arm and tendons 1 & 2(projected onto the $x' - y'$ plane) when $\omega + \lambda \geq 3\pi/4$.

$$L_1 = l_1 = Q_1P_1 = \left[(a\cos\theta\sin\psi - \frac{1}{\sqrt{2}}\rho)^2 + (a\cos\theta\cos\psi + \frac{1}{\sqrt{2}}\rho)^2 + (b + a\sin\theta)^2\right]^{\frac{1}{2}}$$

$$= \left[2ab\sin\theta + a^2 + b^2 + \rho^2 + \sqrt{2}\rho a\cos\theta(\cos\psi - \sin\psi)\right]^{\frac{1}{2}} \qquad (A.1)$$

$$L_2 = l_2 = Q_2P_2 = \left[(-a\cos\theta\sin\psi + \frac{1}{\sqrt{2}}\rho)^2 + (-a\cos\theta\cos\psi - \frac{1}{\sqrt{2}}\rho)^2 + (a\sin\theta - b)^2\right]^{\frac{1}{2}}$$

$$= \left[-2ab\sin\theta + a^2 + b^2 + \rho^2 + \sqrt{2}\rho a\cos\theta(\cos\psi - \sin\psi)\right]^{\frac{1}{2}} \qquad (A.2)$$

Equation (2.35) now becomes:

Resultant torque acting on the arm about point O

$$= \vec{OQ_1} \times \vec{F_1} + \vec{OQ_2} \times \vec{F_2} + \vec{OR_3} \times \vec{F_3} + \vec{OR_4} \times \vec{F_4} + \vec{OG} \times \vec{mg}$$

$$= \frac{F_1}{|Q_1P_1|}\vec{OQ_1} \times \vec{Q_1P_1} + \frac{F_2}{|Q_2P_2|}\vec{OQ_2} \times \vec{Q_2P_2} + \frac{F_3}{|R_3P_3|}\vec{OR_3} \times \vec{R_3P_3}$$

$$+ \frac{F_4}{|R_4P_4|}\vec{OR_4} \times \vec{R_4P_4} + mg\,\vec{OG} \times \vec{GD}$$

$$= iT_1 + jT_2 + kT_3 \qquad (A.3)$$

where

$$T_1 = \frac{F_1}{L_1}\left[\frac{1}{\sqrt{2}}\rho a \sin\theta - ab\cos\theta\cos\psi\right] + \frac{F_2}{L_2}\left[\frac{1}{\sqrt{2}}\rho a\sin\theta + ab\cos\theta\cos\psi\right]$$
$$+ \frac{F_3}{L_3}[\rho s\sin\phi\cos\theta\sin(\omega' + \lambda') - z_3 s(\cos\phi\sin\psi - \sin\theta\sin\phi\cos\psi)]$$
$$+ \frac{F_4}{L_4}[\rho s\sin\phi\cos\theta\sin(\omega' + \lambda') + z_4 s(\cos\phi\sin\psi - \sin\theta\sin\phi\cos\psi)]$$
$$+ mgd(\sin\phi\sin\psi + \cos\phi\sin\theta\cos\psi) \qquad (A.4)$$

$$T_2 = \frac{F_1}{L_1}\left[\frac{1}{\sqrt{2}}\rho a\sin\theta + ab\cos\theta\sin\psi\right] + \frac{F_2}{L_2}\left[\frac{1}{\sqrt{2}}\rho a\sin\theta - ab\cos\theta\sin\psi\right]$$
$$+ \frac{F_3}{L_3}[-\rho s\sin\phi\cos\theta\cos(\omega' + \lambda') - z_3 s(\cos\phi\cos\psi + \sin\theta\sin\phi\sin\psi)]$$
$$+ \frac{F_4}{L_4}[-\rho s\sin\phi\cos\theta\cos(\omega' + \lambda') + z_4 s(\cos\phi\cos\psi + \sin\theta\sin\phi\sin\psi)]$$
$$+ mgd(\sin\phi\cos\psi - \cos\phi\sin\theta\sin\psi) \qquad (A.5)$$

$$T_3 = \left(\frac{F_1}{L_1} + \frac{F_2}{L_2}\right)\frac{1}{\sqrt{2}}\rho a\cos\theta(\cos\psi + \sin\psi)$$
$$+ \left(\frac{F_3}{L_3} + \frac{F_4}{L_4}\right)\rho s[\sin\phi\sin\theta\cos(\lambda' + \mu') - \cos\phi\sin(\lambda' + \mu')] \qquad (A.6)$$

In equations (A.4)–(A.6), L_1 and L_2 are as defined in equations (A.1) –(A.2), the others are defined as in equations (2.19)–(2.32).

A.2 Tendons 2 and 4 are completely unwrapped

Following the same procedure as in section A.1, when $\omega' + \lambda' > 3\pi/4$, the directions of F_3 and F_4 will be given by $\hat{Q_3P_3}$ and $\hat{Q_4P_4}$ respectively, and

$$L_3 = l_3 = Q_3\vec{P}_3 = [(-s\cos\phi\cos\psi - s\sin\phi\sin\theta\sin\psi - \frac{1}{\sqrt{2}}\rho)^2 + (s\cos\phi\sin\psi - s\sin\phi\sin\theta\cos\psi + \frac{1}{\sqrt{2}}\rho)^2 + (-s\sin\phi\cos\theta - t)^2]^{\frac{1}{2}}$$

$$= [s^2 + t^2 + \rho^2 + \sqrt{2}\rho s\cos\phi(\cos\psi + \sin\psi) + \sqrt{2}\rho s\sin\phi\sin\theta(\sin\psi - \cos\psi) + 2st\sin\phi\cos\theta]^{\frac{1}{2}} \qquad (A.7)$$

$$L_4 = l_4 = Q_4\vec{P}_4 = [(s\cos\phi\cos\psi + s\sin\phi\sin\theta\sin\psi + \frac{1}{\sqrt{2}}\rho)^2 + (-s\cos\phi\sin\psi + s\sin\phi\sin\theta\cos\psi - \frac{1}{\sqrt{2}}\rho)^2 + (s\sin\phi\cos\theta - t)^2]^{\frac{1}{2}}$$

$$= [s^2 + t^2 + \rho^2 + \sqrt{2}\rho s\cos\phi(\cos\psi + \sin\psi) + \sqrt{2}\rho s\sin\phi\sin\theta(\sin\psi - \cos\psi) - 2st\sin\phi\cos\theta]^{\frac{1}{2}} \qquad (A.8)$$

$$T_1 = \frac{F_1}{L_1}[-\rho a\sin\theta\cos(\omega + \lambda) - z_1 a\cos\theta\cos\psi] + \frac{F_2}{L_2}[-\rho a\sin\theta\cos(\omega + \lambda) + z_2 a\cos\theta\cos\psi] + \frac{F_3}{L_3}[\frac{1}{\sqrt{2}}\rho s\sin\phi\cos\theta - ts(\cos\phi\sin\psi - \sin\phi\sin\theta\cos\psi)] + \frac{F_4}{L_4}[\frac{1}{\sqrt{2}}\rho s\sin\phi\cos\theta + ts(\cos\phi\sin\psi - \sin\phi\sin\theta\cos\psi)] + mgd(\sin\phi\sin\psi + \cos\phi\sin\theta\cos\psi) \qquad (A.9)$$

$$T_2 = \frac{F_1}{L_1}[\rho a\sin\theta\sin(\omega + \lambda) + z_1 a\cos\theta\sin\psi] + \frac{F_2}{L_2}[\rho a\sin\theta\sin(\omega + \lambda) - z_2 a\cos\theta\sin\psi] + \frac{F_3}{L_3}[\frac{1}{\sqrt{2}}\rho s\sin\phi\cos\theta - ts(\cos\phi\cos\psi + \sin\phi\sin\theta\sin\psi)] + \frac{F_4}{L_4}[\frac{1}{\sqrt{2}}\rho s\sin\phi\cos\theta + ts(\cos\phi\cos\psi + \sin\phi\sin\theta\sin\psi)] + mgd(\sin\phi\cos\psi - \cos\phi\sin\theta\sin\psi) \qquad (A.10)$$

$$T_3 = (\frac{F_1}{L_1} + \frac{F_2}{L_2})\rho a\cos\theta\sin\lambda + (\frac{F_3}{L_3} + \frac{F_4}{L_4})\frac{1}{\sqrt{2}}\rho s[\cos\phi(\sin\psi - \cos\psi) - \sin\phi\sin\theta(\cos\psi + \sin\psi)] \qquad (A.11)$$

Note: In equations (A.9)–(A.11), L_3 and L_4 are as defined in equations (A.7) and (A.8), the others are as defined in equations (2.7)–(2.18).

A.3 Equations of Motion

The equations of motion for the two cases of unwrapped tendons can be derived following the procedure in subsection 2.2.4, and instead of using equations (2.36)–(2.38) for the expressions for T_1, T_2, and T_3, equations (A.4)–(A.6) or equations (A.9)–(A.11) are used depending on which pair of tendons are unwrapped. The full detail of the equations corresponding to equation (2.48) is given in Appendix B.

Appendix B. Equations of motion for the full order model

By substituting expressions for T_1, T_2, T_3 and equations (2.40)–(2.45) into equations (2.39), the three equations become,

$$
\begin{aligned}
&\ddot{\theta}\left[J\cos\psi - \frac{J_m}{r^2}(c_{11}\frac{\partial l_1}{\partial\theta} + c_{12}\frac{\partial l_2}{\partial\theta} + c_{13}\frac{\partial l_3}{\partial\theta} + c_{14}\frac{\partial l_4}{\partial\theta})\right] \\
&\quad + \ddot{\phi}\left[J\cos\theta\sin\psi - \frac{J_m}{r^2}(c_{11}\frac{\partial l_1}{\partial\phi} + c_{12}\frac{\partial l_2}{\partial\phi} + c_{13}\frac{\partial l_3}{\partial\phi} + c_{14}\frac{\partial l_4}{\partial\phi})\right] \\
&\quad + \ddot{\psi}\left[-\frac{J_m}{r^2}(c_{11}\frac{\partial l_1}{\partial\psi} + c_{12}\frac{\partial l_2}{\partial\psi} + c_{13}\frac{\partial l_3}{\partial\psi} + c_{14}\frac{\partial l_4}{\partial\psi})\right] \\
&\quad = \frac{K}{r}[c_{11}I_1 + c_{12}I_2 + c_{13}I_3 + c_{14}I_4] + c_{15} + \dot{\theta}\frac{B_m}{r^2}\left[c_{11}\frac{\partial l_1}{\partial\theta} + c_{12}\frac{\partial l_2}{\partial\theta} + c_{13}\frac{\partial l_3}{\partial\theta} + c_{14}\frac{\partial l_4}{\partial\theta}\right] \\
&\qquad + \dot{\phi}\frac{B_m}{r^2}\left[c_{11}\frac{\partial l_1}{\partial\phi} + c_{12}\frac{\partial l_2}{\partial\phi} + c_{13}\frac{\partial l_3}{\partial\phi} + c_{14}\frac{\partial l_4}{\partial\phi}\right] \\
&\qquad + \dot{\psi}\frac{B_m}{r^2}\left[c_{11}\frac{\partial l_1}{\partial\psi} + c_{12}\frac{\partial l_2}{\partial\psi} + c_{13}\frac{\partial l_3}{\partial\psi} + c_{14}\frac{\partial l_4}{\partial\psi}\right] \\
&\qquad + \dot{\theta}^2\frac{J_m}{r^2}\left[c_{11}\frac{\partial^2 l_1}{\partial\theta^2} + c_{12}\frac{\partial^2 l_2}{\partial\theta^2} + c_{13}\frac{\partial^2 l_3}{\partial\theta^2} + c_{14}\frac{\partial^2 l_4}{\partial\theta^2}\right] \\
&\qquad + \dot{\phi}^2\left[(-J + J_3)\sin\theta\cos\theta\cos\psi + \frac{J_m}{r^2}(c_{11}\frac{\partial^2 l_1}{\partial\phi^2} + c_{12}\frac{\partial^2 l_2}{\partial\phi^2} + c_{13}\frac{\partial^2 l_3}{\partial\phi^2} + c_{14}\frac{\partial^2 l_4}{\partial\phi^2})\right] \\
&\qquad + \dot{\psi}^2\frac{J_m}{r^2}\left[c_{11}\frac{\partial^2 l_1}{\partial\psi^2} + c_{12}\frac{\partial^2 l_2}{\partial\psi^2} + c_{13}\frac{\partial^2 l_3}{\partial\psi^2} + c_{14}\frac{\partial^2 l_4}{\partial\psi^2}\right] \\
&\qquad + 2\dot{\theta}\dot{\phi}\left[(J - \frac{1}{2}J_3)\sin\theta\sin\psi + \frac{J_m}{r^2}(c_{11}\frac{\partial^2 l_1}{\partial\theta\partial\phi} + c_{12}\frac{\partial^2 l_2}{\partial\theta\partial\phi} + c_{13}\frac{\partial^2 l_3}{\partial\theta\partial\phi} + c_{14}\frac{\partial^2 l_4}{\partial\theta\partial\phi})\right] \\
&\qquad + 2\dot{\phi}\dot{\psi}\left[-\frac{J_3}{2}\cos\psi\cos\theta + \frac{J_m}{r^2}(c_{11}\frac{\partial^2 l_1}{\partial\phi\partial\psi} + c_{12}\frac{\partial^2 l_2}{\partial\phi\partial\psi} + c_{13}\frac{\partial^2 l_3}{\partial\phi\partial\psi} + c_{14}\frac{\partial^2 l_4}{\partial\phi\partial\psi})\right] \\
&\qquad + 2\dot{\psi}\dot{\theta}\left[\frac{1}{2}J_3\sin\psi + \frac{J_m}{r^2}(c_{11}\frac{\partial^2 l_1}{\partial\psi\partial\theta} + c_{12}\frac{\partial^2 l_2}{\partial\psi\partial\theta} + c_{13}\frac{\partial^2 l_3}{\partial\psi\partial\theta} + c_{14}\frac{\partial^2 l_4}{\partial\psi\partial\theta})\right] \qquad (B.1)
\end{aligned}
$$

$$
\begin{aligned}
&\ddot{\theta}\left[-J\sin\psi-\frac{J_m}{r^2}\left(c_{21}\frac{\partial l_1}{\partial\theta}+c_{22}\frac{\partial l_2}{\partial\theta}+c_{23}\frac{\partial l_3}{\partial\theta}+c_{24}\frac{\partial l_4}{\partial\theta}\right)\right]\\
&+\ddot{\phi}\left[J\cos\theta\cos\psi-\frac{J_m}{r^2}\left(c_{21}\frac{\partial l_1}{\partial\phi}+c_{22}\frac{\partial l_2}{\partial\phi}+c_{23}\frac{\partial l_3}{\partial\phi}+c_{24}\frac{\partial l_4}{\partial\phi}\right)\right]\\
&+\ddot{\psi}\left[-\frac{J_m}{r^2}\left(c_{21}\frac{\partial l_1}{\partial\psi}+c_{22}\frac{\partial l_2}{\partial\psi}+c_{23}\frac{\partial l_3}{\partial\psi}+c_{24}\frac{\partial l_4}{\partial\psi}\right)\right]\\
&=\frac{K}{r}\left[c_{21}I_1+c_{22}I_2+c_{23}I_3+c_{24}I_4\right]+c_{25}+\dot{\theta}\frac{B_m}{r^2}\left[c_{21}\frac{\partial l_1}{\partial\theta}+c_{22}\frac{\partial l_2}{\partial\theta}+c_{23}\frac{\partial l_3}{\partial\theta}+c_{24}\frac{\partial l_4}{\partial\theta}\right]\\
&\quad+\dot{\phi}\frac{B_m}{r^2}\left[c_{21}\frac{\partial l_1}{\partial\phi}+c_{22}\frac{\partial l_2}{\partial\phi}+c_{23}\frac{\partial l_3}{\partial\phi}+c_{24}\frac{\partial l_4}{\partial\phi}\right]\\
&\quad+\dot{\psi}\frac{B_m}{r^2}\left[c_{21}\frac{\partial l_1}{\partial\psi}+c_{22}\frac{\partial l_2}{\partial\psi}+c_{23}\frac{\partial l_3}{\partial\psi}+c_{24}\frac{\partial l_4}{\partial\psi}\right]\\
&\quad+\dot{\theta}^2\frac{J_m}{r^2}\left[c_{21}\frac{\partial^2 l_1}{\partial\theta^2}+c_{22}\frac{\partial^2 l_2}{\partial\theta^2}+c_{23}\frac{\partial^2 l_3}{\partial\theta^2}+c_{24}\frac{\partial^2 l_4}{\partial\theta^2}\right]\\
&\quad+\dot{\phi}^2\left[(J-J_3)\sin\theta\cos\theta\sin\psi+\frac{J_m}{r^2}\left(c_{21}\frac{\partial^2 l_1}{\partial\phi^2}+c_{22}\frac{\partial^2 l_2}{\partial\phi^2}+c_{23}\frac{\partial^2 l_3}{\partial\phi^2}+c_{24}\frac{\partial^2 l_4}{\partial\phi^2}\right)\right]\\
&\quad+\dot{\psi}^2\frac{J_m}{r^2}\left[c_{21}\frac{\partial^2 l_1}{\partial\psi^2}+c_{22}\frac{\partial^2 l_2}{\partial\psi^2}+c_{23}\frac{\partial^2 l_3}{\partial\psi^2}+c_{24}\frac{\partial^2 l_4}{\partial\psi^2}\right]\\
&\quad+2\dot{\theta}\dot{\phi}\left[(J-\frac{1}{2}J_3)\sin\theta\cos\psi+\frac{J_m}{r^2}\left(c_{21}\frac{\partial^2 l_1}{\partial\theta\partial\phi}+c_{22}\frac{\partial^2 l_2}{\partial\theta\partial\phi}+c_{23}\frac{\partial^2 l_3}{\partial\theta\partial\phi}+c_{24}\frac{\partial^2 l_4}{\partial\theta\partial\phi}\right)\right]\\
&\quad+2\dot{\phi}\dot{\psi}\left[\frac{1}{2}J_3\cos\theta\sin\psi+\frac{J_m}{r^2}\left(c_{21}\frac{\partial^2 l_1}{\partial\phi\partial\psi}+c_{22}\frac{\partial^2 l_2}{\partial\phi\partial\psi}+c_{23}\frac{\partial^2 l_3}{\partial\phi\partial\psi}+c_{24}\frac{\partial^2 l_4}{\partial\phi\partial\psi}\right)\right]\\
&\quad+2\dot{\psi}\dot{\theta}\left[\frac{1}{2}J_3\cos\psi+\frac{J_m}{r^2}\left(c_{21}\frac{\partial^2 l_1}{\partial\psi\partial\theta}+c_{22}\frac{\partial^2 l_2}{\partial\psi\partial\theta}+c_{23}\frac{\partial^2 l_3}{\partial\psi\partial\theta}+c_{24}\frac{\partial^2 l_4}{\partial\psi\partial\theta}\right)\right] \qquad (B.2)
\end{aligned}
$$

$$
\begin{aligned}
&-\ddot{\theta}\frac{J_m}{r^2}\left[c_{31}\frac{\partial l_1}{\partial\theta}+c_{32}\frac{\partial l_2}{\partial\theta}+c_{33}\frac{\partial l_3}{\partial\theta}+c_{34}\frac{\partial l_4}{\partial\theta}\right]\\
&+\ddot{\phi}\left[-J_3\sin\theta-\frac{J_m}{r^2}(c_{31}\frac{\partial l_1}{\partial\phi}+c_{32}\frac{\partial l_2}{\partial\phi}+c_{33}\frac{\partial l_3}{\partial\phi}+c_{34}\frac{\partial l_4}{\partial\phi})\right]\\
&+\ddot{\psi}\left[J_3-\frac{J_m}{r^2}(c_{31}\frac{\partial l_1}{\partial\psi}+c_{32}\frac{\partial l_2}{\partial\psi}+c_{33}\frac{\partial l_3}{\partial\psi}+c_{34}\frac{\partial l_4}{\partial\psi})\right]\\
&=\frac{K}{r}[c_{31}I_1+c_{32}I_2+c_{33}I_3+c_{34}I_4]+\dot{\theta}\frac{B_m}{r^2}\left[c_{31}\frac{\partial l_1}{\partial\theta}+c_{32}\frac{\partial l_2}{\partial\theta}+c_{33}\frac{\partial l_3}{\partial\theta}+c_{34}\frac{\partial l_4}{\partial\theta}\right]\\
&\quad+\dot{\phi}\frac{B_m}{r^2}\left[c_{31}\frac{\partial l_1}{\partial\phi}+c_{32}\frac{\partial l_2}{\partial\phi}+c_{33}\frac{\partial l_3}{\partial\phi}+c_{34}\frac{\partial l_4}{\partial\phi}\right]\\
&+\dot{\psi}\frac{B_m}{r^2}\left[c_{31}\frac{\partial l_1}{\partial\psi}+c_{32}\frac{\partial l_2}{\partial\psi}+c_{33}\frac{\partial l_3}{\partial\psi}+c_{34}\frac{\partial l_4}{\partial\psi}\right]\\
&+\dot{\theta}^2\frac{J_m}{r^2}\left[c_{31}\frac{\partial^2 l_1}{\partial\theta^2}+c_{32}\frac{\partial^2 l_2}{\partial\theta^2}+c_{33}\frac{\partial^2 l_3}{\partial\theta^2}+c_{34}\frac{\partial^2 l_4}{\partial\theta^2}\right]\\
&+\dot{\phi}^2\frac{J_m}{r^2}\left[c_{31}\frac{\partial^2 l_1}{\partial\phi^2}+c_{32}\frac{\partial^2 l_2}{\partial\phi^2}+c_{33}\frac{\partial^2 l_3}{\partial\phi^2}+c_{34}\frac{\partial^2 l_4}{\partial\phi^2}\right]\\
&+\dot{\psi}^2\frac{J_m}{r^2}\left[c_{31}\frac{\partial^2 l_1}{\partial\psi^2}+c_{32}\frac{\partial^2 l_2}{\partial\psi^2}+c_{33}\frac{\partial^2 l_3}{\partial\psi^2}+c_{34}\frac{\partial^2 l_4}{\partial\psi^2}\right]\\
&+2\dot{\theta}\dot{\phi}\left[\frac{1}{2}J_3\cos\theta+\frac{J_m}{r^2}(c_{31}\frac{\partial^2 l_1}{\partial\theta\partial\phi}+c_{32}\frac{\partial^2 l_2}{\partial\theta\partial\phi}+c_{33}\frac{\partial^2 l_3}{\partial\theta\partial\phi}+c_{34}\frac{\partial^2 l_4}{\partial\theta\partial\phi})\right]\\
&+2\dot{\phi}\dot{\psi}\frac{J_m}{r^2}\left[c_{31}\frac{\partial^2 l_1}{\partial\phi\partial\psi}+c_{32}\frac{\partial^2 l_2}{\partial\phi\partial\psi}+c_{33}\frac{\partial^2 l_3}{\partial\phi\partial\psi}+c_{34}\frac{\partial^2 l_4}{\partial\phi\partial\psi}\right]\\
&+2\dot{\psi}\dot{\theta}\frac{J_m}{r^2}\left[c_{31}\frac{\partial^2 l_1}{\partial\psi\partial\theta}+c_{32}\frac{\partial^2 l_2}{\partial\psi\partial\theta}+c_{33}\frac{\partial^2 l_3}{\partial\psi\partial\theta}+c_{34}\frac{\partial^2 l_4}{\partial\psi\partial\theta}\right]
\end{aligned}
\tag{B.3}
$$

In the above three equations, the values of c_{ij}, L_j, l_j, $i = 1, 2, 3$, $j = 1, \ldots, 4$, will depend on the values of $\omega + \lambda$ and $\omega' + \lambda'$ as defined by equations (2.7)–(2.8) and (2.19)–(2.22).

For $\omega + \lambda < 3\pi/4$,

$$
\begin{aligned}
c_{11} &= [-\rho a\sin\theta\cos(\omega+\lambda)-z_1 a\cos\theta\cos\psi]/L_1\\
c_{12} &= [-\rho a\sin\theta\cos(\omega+\lambda)+z_2 a\cos\theta\cos\psi]/L_2\\
c_{21} &= [\rho a\sin\theta\sin(\omega+\lambda)+z_1 a\cos\theta\sin\psi]/L_1\\
c_{22} &= [\rho a\sin\theta\sin(\omega+\lambda)-z_2 a\cos\theta\sin\psi]/L_2\\
c_{31} &= \rho a\cos\theta\sin\lambda/L_1\\
c_{32} &= \rho a\cos\theta\sin\lambda/L_2
\end{aligned}
$$

$z_1, L_1, l_1, z_2, L_2, l_2$ are as given by equations (2.11) –(2.13) and (2.16)–(2.18).

For $\omega + \lambda \geq 3\pi/4$,

$$c_{11} = [\frac{1}{\sqrt{2}}\rho a \sin\theta - ab\cos\theta\cos\psi]/L_1$$
$$c_{12} = [\frac{1}{\sqrt{2}}\rho a \sin\theta + ab\cos\theta\cos\psi]/L_2$$
$$c_{21} = [\frac{1}{\sqrt{2}}\rho a \sin\theta + ab\cos\theta\sin\psi]/L_1$$
$$c_{22} = [\frac{1}{\sqrt{2}}\rho a \sin\theta - ab\cos\theta\sin\psi]/L_2$$
$$c_{31} = \frac{1}{\sqrt{2}}\rho a\cos\theta(\cos\psi + \sin\psi)/L_1$$
$$c_{32} = \frac{1}{\sqrt{2}}\rho a\cos\theta(\cos\psi + \sin\psi)/L_2$$

L_1, l_1, L_2, l_2 are as given by equations (A.1) and (A.2).

For $\omega' + \lambda' < 3\pi/4$,

$$c_{13} = [\rho s\sin\phi\cos\theta\sin(\omega' + \lambda') - z_3 s(\cos\phi\sin\psi - \sin\theta\sin\phi\cos\psi)]/L_3$$
$$c_{14} = [\rho s\sin\phi\cos\theta\sin(\omega' + \lambda') + z_4 s(\cos\phi\sin\psi - \sin\theta\sin\phi\cos\psi)]/L_4$$
$$c_{23} = [-\rho s\sin\phi\cos\theta\cos(\omega' + \lambda') - z_3 s(\cos\phi\cos\psi + \sin\theta\sin\phi\sin\psi)]/L_3$$
$$c_{24} = [-\rho s\sin\phi\cos\theta\cos(\omega' + \lambda') + z_4 s(\cos\phi\cos\psi + \sin\theta\sin\phi\sin\psi)]/L_4$$
$$c_{33} = \rho s[\sin\phi\sin\theta\cos(\lambda' + \mu') - \cos\phi\sin(\lambda' + \mu')]/L_3$$
$$c_{34} = \rho s[\sin\phi\sin\theta\cos(\lambda' + \mu') - \cos\phi\sin(\lambda' + \mu')]/L_4$$

$z_3, L_3, l_3, z_4, L_4, l_4$ are as defined in equations (2.25)–(2.27) and (2.30)–(2.32).

For $\omega' + \lambda' \geq 3\pi/4$,

$$c_{13} = [\frac{1}{\sqrt{2}}\rho s \sin\phi\cos\theta - st(\cos\phi\sin\psi - \sin\theta\sin\phi\cos\psi)]/L_3$$

$$c_{14} = [\frac{1}{\sqrt{2}}\rho s \sin\phi\cos\theta + st(\cos\phi\sin\psi - \sin\theta\sin\phi\cos\psi)]/L_4$$

$$c_{23} = [\frac{1}{\sqrt{2}}\rho s \sin\phi\cos\theta - st(\cos\phi\cos\psi + \sin\theta\sin\phi\sin\psi)]/L_3$$

$$c_{24} = [\frac{1}{\sqrt{2}}\rho s \sin\phi\cos\theta + st(\cos\phi\cos\psi + \sin\theta\sin\phi\sin\psi)]/L_4$$

$$c_{33} = \frac{1}{\sqrt{2}}\rho s[\cos\phi(\sin\psi - \cos\psi) - \sin\phi\sin\theta(\cos\psi + \sin\psi)]/L_3$$

$$c_{34} = \frac{1}{\sqrt{2}}\rho s[\cos\phi(\sin\psi - \cos\psi) - \sin\phi\sin\theta(\cos\psi + \sin\psi)]/L_4$$

L_3, l_3, L_4, l_4 are as defined in equations (A.7) and (A.8).

For all cases,

$$c_{15} = mgd(\sin\phi\sin\psi + \cos\phi\sin\theta\cos\psi)$$
$$c_{25} = mgd(\sin\phi\cos\psi - \cos\phi\sin\theta\sin\psi)$$

Equations (B.1)–(B.3) are of the form,

$$h_{i1}\ddot{\theta} + h_{i2}\ddot{\phi} + h_{i3}\ddot{\psi} = g_i(\theta, \phi, \psi, \dot{\theta}, \dot{\phi}, \dot{\psi}) + \sum_{j=1}^{4} q_{ij}I_j \qquad i = 1, 2, 3 \qquad (B.4)$$

where the h_{ij}'s, and q_{ij}'s are functions of θ, ϕ, ψ.

Written in component form,

$$\begin{bmatrix} h_{11} & h_{12} & h_{13} \\ h_{21} & h_{22} & h_{23} \\ h_{31} & h_{32} & h_{33} \end{bmatrix} \begin{bmatrix} \ddot{\theta} \\ \ddot{\phi} \\ \ddot{\psi} \end{bmatrix} = \begin{bmatrix} g_1(\theta, \phi, \psi, \dot{\theta}, \dot{\phi}, \dot{\psi}) \\ g_2(\theta, \phi, \psi, \dot{\theta}, \dot{\phi}, \dot{\psi}) \\ g_3(\theta, \phi, \psi, \dot{\theta}, \dot{\phi}, \dot{\psi}) \end{bmatrix} + \begin{bmatrix} q_{11} & q_{12} & q_{13} & q_{14} \\ q_{21} & q_{22} & q_{23} & q_{24} \\ q_{31} & q_{32} & q_{33} & q_{34} \end{bmatrix} \begin{bmatrix} I_1 \\ I_2 \\ I_3 \\ I_4 \end{bmatrix} \qquad (B.5)$$

Define

$$H = \begin{bmatrix} h_{11} & h_{12} & h_{13} \\ h_{21} & h_{22} & h_{23} \\ h_{31} & h_{32} & h_{33} \end{bmatrix}$$

Then from equation (B.5),

$$\begin{bmatrix}\ddot{\theta}\\ \ddot{\phi}\\ \ddot{\psi}\end{bmatrix} = H^{-1}\begin{bmatrix}g_1\\ g_2\\ g_3\end{bmatrix} + H^{-1}\begin{bmatrix}q_{11} & q_{12} & q_{13} & q_{14}\\ q_{21} & q_{22} & q_{23} & q_{24}\\ q_{31} & q_{32} & q_{33} & q_{34}\end{bmatrix}\begin{bmatrix}I_1\\ I_2\\ I_3\\ I_4\end{bmatrix}$$

$$= \begin{bmatrix}f_4\\ f_5\\ f_6\end{bmatrix} + \left[\begin{array}{c}b_4\\ \hdashline b_5\\ \hdashline b_6\end{array}\right]\begin{bmatrix}I_1\\ I_2\\ I_3\\ I_4\end{bmatrix} \qquad (B.6)$$

Define

$$x = [\theta \quad \phi \quad \psi \quad \dot{\theta} \quad \dot{\phi} \quad \dot{\psi}]^T$$
$$u = [I_1 \quad I_2 \quad I_3 \quad I_4]^T$$

$$F_0(x(t)) = \begin{bmatrix}x_4\\ x_5\\ x_6\\ f_4\\ f_5\\ f_6\end{bmatrix} \qquad \text{a 6-vector}$$

$$B_0(x(t)) = \left[\begin{array}{c}0\\ \hdashline 0\\ \hdashline 0\\ \hdashline b_4\\ \hdashline b_5\\ \hdashline b_6\end{array}\right] \qquad \text{a } 6 \times 4 \text{ matrix}$$

Then equation (B.6) can be written as

$$\dot{x} = F_0(x) + B_0(x)u$$

which is equation (2.48).

Appendices C-E have been excluded from the Memo version of this thesis.

Appendix F. Using voltage instead of current inputs

The electrical equation of motor i is given by,

$$V_i = L_a \frac{dI_i}{dt} + RI_i + K_E \dot{\gamma}_i \qquad (F.1)$$

where L_a, R, K_E are the motor's inductance, resistance and EMF constant respectively, and $\dot{\gamma}_i$ is the angular speed of the motor.

For the pancake type of motor that we are using,

$$L_a \approx 0$$

and since in $S.I.$ units, the EMF constant and the torque constant are equal, we will use the symbol K for both of them.

Hence equation (F.1) can be written as

$$V_i = RI_i + K\dot{\gamma}_i$$

or

$$I_i = \frac{1}{R} V_i - \frac{K}{R} \dot{\gamma}_i \qquad (F.2)$$

From equation (2.42), the dynamic equation of motor i is given by,

$$J_m \ddot{\gamma}_i + B_m \dot{\gamma}_i + F_i r = KI_i \qquad (F.3)$$

Substituting equation (F.2) into (F.3), we obtain,

$$J_m \ddot{\gamma}_i + (B_m + \frac{K^2}{R}) \dot{\gamma}_i + F_i r = \frac{K}{R} V \qquad (F.4)$$

which is of the same structure as equation (F.3) except that $(B_m + K^2/R)$ is substituted for B_m and K/R is substituted for K.

Hence all the equations and programs that have been developed for current inputs can be applied to the case of voltage inputs by changing the values of the damping constant B_m and torque constant K of the motor.

Appendix G. Values of the parameters used in the simulation runs

G.1 Arm Parameters

a	$0.4064\,m$	refer to figure 2-6
b	$0.4064\,m$	refer to figure 2-6
d	$0.117\,m$	refer to figure 2-6
s	$0.2032\,m$	refer to figure 2-6
t	$0.2032\,m$	refer to figure 2-6
ρ	$0.02223\,m$	radius of the cylindrical rod
m	$1.581\,kg$	mass of arm
J	$0.0906\,kg\,m^2$	momemt of inertia of am about $X-X$ and $Y-Y$ axes
J_3	$0.000407\,kg\,m^2$	moment of inertia of arm about $Z-Z$ axis

G.2 Motor Parameters (PMI motor type U12M4)

r	$0.016\,m$	radius of motor shaft
K	$0.11\,N\,m/A$	torque constant
J_m	$0.00016\ kg\,m^2$	moment of inertia of motor shaft
B_m	$0.000135\,N\,m/rad\,s^{-1}$	damping constant

The rated current of the motor is $4.4\,A$.